Effect of Installation Practices on Galvanic Corrosion in Service Lines, Low Flow Rate Sampling for Detecting Water-Lead Hazards, and Trace Metals on Drinking Water Pipeline Corrosion: Lessons in Unintended Consequences

Brandi Nicole Clark

Dissertation submitted to the faculty of the Virginia Polytechnic Institute and State University in partial fulfillment of the requirements for the degree of

Doctor of Philosophy
In
Civil Engineering

Marc Edwards, Chair
Emily Sarver
Sunil Sinha
Peter Vikesland

March 19, 2015
Blacksburg, Virginia

Keywords: drinking water, plumbing, lead, pipeline corrosion, crevice corrosion, galvanic corrosion, deposition corrosion

Effect of Installation Practices on Galvanic Corrosion in Service Lines, Low Flow Rate Sampling for Detecting Water-Lead Hazards, and Trace Metals on Drinking Water Pipeline Corrosion: Lessons in Unintended Consequences

Brandi Nicole Clark

ABSTRACT

Corrosion of drinking water distribution systems can cost water utilities and homeowners tens of billions of dollars each year in infrastructure damage, adversely impacting public health and causing water loss through leaks. Often, seemingly innocuous choices made by utilities, plumbers, and consumers can have a dramatic impacts on corrosion and pipeline longevity.

This work demonstrated that brass pipe connectors used in partial lead service line replacements (PLSLR) can significantly influence galvanic corrosion between lead and copper pipes. Galvanic crevice corrosion was implicated in a fourfold increase in lead compared to a traditional direct connection, which was previously assumed to be a worst-case connection method.

In field sampling conducted in two cities, a new sampling method designed to detect particulate lead risks demonstrated that the choice of flow rate has a substantial impact on lead-in-water hazards. On average, lead concentrations detected in water at high flow without stagnation were at least 3X-4X higher than in traditional regulatory samples with stagnation, demonstrating a new "worst case" lead release scenario due to detachment of lead particulates.

Although galvanized steel was previously considered a minor lead source, it can contain up to 2% lead on the surface, and elevated lead-in-water samples from several cities were traced to galvanized pipe, including the home of a child with elevated blood lead.

Furthermore, if both galvanized and copper pipe are present, as occurs in large buildings, deposition corrosion is possible, leading to both increased lead exposure and pipe failures in as little as two years. Systematic laboratory studies of deposition corrosion identified key factors that increase or decrease its likelihood; soluble copper concentration and flow pattern were identified as controlling factors. Because of the high copper concentrations and continuous flow associated with mixed-metal hot water recirculating systems, these systems were identified as a worst-case scenario for galvanic corrosion.

Deposition corrosion was also confirmed as a contributing mechanism to increased lead release, if copper pipe is placed before a lead pipe as occurs in partial service line replacements. Dump-and-fill tests confirmed copper solubility as a key factor in deposition corrosion impacts, and a detailed analysis of lead pipes from both laboratory studies and field tests was consistent with pure metallic copper deposits on the pipe surface, especially near the galvanic junction with copper.

Finally, preliminary experiments were conducted to determine whether nanoparticles from novel water treatment techniques could have a negative impact on downstream drinking water pipeline infrastructure. Although increases in the corrosion of iron, copper, and stainless steel pipes in the presence of silver and carbon nanomaterials were generally small or non-existent, in one case the presence of silver nanoparticles increased iron release from stainless steel by more than 30X via a localized corrosion mechanism, with pitting rates as high as 1.2 mm/y, implying serious corrosion consequences are possible for stainless steel pipes if nanoparticles are present.

AUTHOR'S PREFACE

The five chapters of this dissertation are presented according to the specifications of Virginia Tech's manuscript format. All chapters were produced as collaborations between student and advisor and in many cases also include contributions from other co-authors, which are outlined below. The student is the primary contributor (and author) for all chapters.

Chapter 1 describes a systematic investigation of the effect of historical and existing pipe connection practices on lead release to drinking water after a lead service line is partially replaced with copper (known as a partial lead service line replacement, or PLSLR). While PLSLR is performed with the intent of reducing consumer exposure to lead in water, it has recently been acknowledged that this practice can increase lead release in both the short and long term. The study found that small crevices created around the outside of the lead pipe by modern brass connectors significantly worsened lead corrosion, releasing four times more lead than the historical practice of direct connection achieved by melting lead into copper. By identifying the connector design factors that influence lead release, this work is intended to assist utilities in selecting connectors for use in PLSLR. The study was a collaboration between two universities and included several coauthors. Clément Cartier and his research advisor Michèle Prévost were responsible for the design and execution of the experiments carried out in Montreal. Justin St. Clair performed part of the laboratory work at Virginia Tech, and Simoni Triantafyllidou developed the proposal on which this work was based. Chapter 1 was published in *Journal American Water Works Association (Journal AWWA)* in 2013 and is available at http://dx.doi.org/10.5942/jawwa.2013.105.0113.

Chapter 2 continues to investigate consumer lead exposure associated with lead service lines, but focuses on another unintended consequence: by designing regulatory lead sampling protocols to detect one type of lead hazard (soluble lead), they have become less effective at detecting another type of lead hazard (particulate lead). This work defines four conceptual lead exposure risk categories for homes with lead service lines, depending on the relative contributions of soluble and particulate lead. The work also describes a new sequential sampling protocol for lead in drinking water designed to identify a range of particulate lead in water risks. These approaches can provide health officials, utilities, and regulators informed guidance based on the risk category of individual homes to help avoid these risks. Coauthor Sheldon Masters helped organize and carry out the extensive field sampling effort described in this work. Chapter 2 was published in *Environmental Science and Technology (ES&T)* in 2014 and is available at http://dx.doi.org/10.1021/es501342j.

Chapter 3 shifted the focus from lead service lines to an alternative material, galvanized (zinc coated) steel, which was the dominant pipe material for most of the 20th century and is still installed in buildings today. Historically, the level of lead in the zinc coating of galvanized pipe was thought to be a minor source of lead, but increasing concern over the health risks associated with lead in drinking water has prompted new interest in lead sources once considered relatively unimportant. This work re-examines the role of galvanized pipe as a lead source in modern homes, schools, and large buildings using a combination of surface analysis of harvested pipe, bench-scale tests, and field sampling from four U.S. cities. The study revealed relatively high levels of lead (≈ 2%) in the surface coatings of both service lines and premise plumbing,

demonstrating that lead release from these coatings is a concern for both utilities and homeowners. Furthermore, the presence of galvanized pipe was linked to levels of lead in drinking water several times higher than the EPA lead action level, including in a home where a child was diagnosed with elevated blood lead, implicating the lead in galvanized coatings as a potential public health risk. Coauthor Sheldon Masters conducted all experiments associated with the Florida utility, including both a bench-scale study and field sampling. Chapter 3 has been submitted to *Environmental Engineering Science (EES)* and is currently under review.

Chapter 4 continues the investigation of galvanized steel infrastructure by exploring another unintended consequence: the effect of copper ions on iron plumbing infrastructure. This work describes an in-depth investigation of deposition corrosion, a specific corrosion mechanism responsible for dramatic increases in corrosion rate of iron and galvanized steel pipes in the presence of dissolved copper. The study combines systematic electrochemical studies, head-to-head bench scale experiments, and surface analysis of both field and laboratory pipes to draw conclusions about the key factors that control this phenomenon. A key practical conclusion of this experiment was that mixed-metal hot water recirculating systems may represent a worst-case scenario for deposition corrosion, which is concerning, given that hot water recirculating systems are becoming more common to improve water conservation and pathogen control. Chapter 4 has been submitted to *CORROSION* and is currently under review.

Chapter 5 applies the insights into deposition corrosion gained in Chapter 4 to the practice of PLSLR explored in Chapter 1. Because a PLSLR places copper upstream of lead, the lead portion of the service line is susceptible to deposition corrosion effects. This study describes a combination of bench-scale testing in two waters and surface analysis of lead pipes from bench scale experiments, pilot scale experiments, and the field. This work was the first to successfully identify discrete "islands" of copper deposited on the lead pipe surface, providing strong support for the deposition corrosion mechanism. Coauthor Justin St. Clair was responsible for all analysis conducted of the lead-brass connection harvested in Washington, D.C. Chapter 5 has been submitted to *Journal AWWA* and is currently under review.

Chapter 6 applies the deposition corrosion mechanism to a new challenge: determining the potential consequences of proposed novel water treatment techniques on downstream drinking water pipe infrastructure. The noble nature of silver, gold, carbon, and other common nanomaterials makes a deposition corrosion mechanism possible for all common metal pipe materials, and this work describes an initial screening test conducted to determine the effect of three common nanomaterials on the corrosion rate of four different common pipe materials. Coauthor Casey Murray was responsible for most of the experimental work described in this chapter. Chapter 6 is currently being prepared for publication.

ACKNOWLEDGEMENTS

I would first like to thank my advisor, Dr. Marc Edwards, for his invaluable guidance and infectious enthusiasm. I would also like to thank my committee members, Dr. Emily Sarver, Dr. Sunil Sinha, and Dr. Peter Vikesland, for asking the right questions and providing valuable insights.

This work would not have been possible without the help of the very talented and hard-working undergraduate and master's students who helped me carry out all of these experiments, including Ana Laura Hernandez, Justin St. Clair, Brent Casteele, Jessica Hekl, Casey Murray, Samuel Ferrara, Megan Ahart, and Dian Zhang. In addition, I'd like to thank all of the past and current Edwards research group members who provided me help and advice, as well as making my Ph.D. a lot more fun! Thank you also to Betty Wingate, Beth Lucas, Julie Petruska and Jody Smiley for their administrative and lab support. I would further like to thank everyone who worked with me at the Virginia Tech ICTAS Nanoscale Characterization and Fabrication Laboratory (NCFL) for their invaluable assistance with the surface characterization of my (often uncooperative!) environmental samples.

I would also like to acknowledge the financial support of the National Science Foundation and the Robert Wood Johnson Foundation for this research, as well as the fellowships that made my Ph.D. possible, including the National Science Foundation Graduate Research Fellowship, the Via Fellowship, the Jeremy Herbstritt Memorial Internship (Sussman Foundation), and both the Holly Cornell Scholarship and Abel Wolman Fellowship from the American Water Works Association.

Finally, a very special thank you to my incredibly patient and supportive fiancé, Navarre – this Ph.D. should be at least half yours!

TABLE OF CONTENTS

LIST OF FIGURES

LIST OF TABLES

CHAPTER 1. EFFECT OF CONNECTION TYPE ON GALVANIC CORROSION BETWEEN LEAD AND COPPER PIPES

Brandi Clark,[1] Clément Cartier,[2] Justin St. Clair,[3] Simoni Triantafyllidou,[4] Michèle Prévost,[5] and Marc Edwards[1]

[1]Virginia Polytechnic Institute and State University, Blacksburg, Va.
[2]Claro Environmental Technologies and Equipment, Laval, Que.
[3]Balzer and Associates, Christiansburg, Va.
[4]US Environmental Protection Agency Office of Research and Development, Cincinnati, Ohio
[5]École Polytechnique de Montréal, Montréal, Que

ABSTRACT

Pipe connectors can significantly influence galvanic corrosion between lead and copper pipes by distancing the lead from copper pipe, introducing a third metal, and forming crevices. In this study, the effects of distance, connector material, and crevices on galvanic corrosion were examined, and bench-scale comparison testing of commercial connectors was conducted using real tap waters. Brass connectors were found to only slightly decrease (< 25%) the galvanic current that sacrifices, or corrodes, lead pipe, with higher reductions for brasses with higher zinc content. Crevices in brass connectors contained water with extremely high levels of lead (up to 9.4 × 106 μg/L); in bench-scale tests, crevices produced approximately four times more lead release to the water than did direct connections.

KEYWORDS: brass connector(s), crevice corrosion, dielectric(s), galvanic corrosion, partial lead service line replacement

The practice of partial lead service line replacement (PLSLR), which involves replacing a portion of a lead service line with new copper, has come under scrutiny due to concern over elevated lead in water in both the short and long-term (Brown et al. 2011; Triantafyllidou and Edwards 2011; US EPA 2011; Cartier et al. 2012; Giammar et al. 2012). Longer-term problems can arise from direct galvanic corrosion between lead and copper pipe or from deposition corrosion from copper onto lead (Britton and Richards 1981; Triantafyllidou and Edwards 2011; Hu et al. 2012), and it is widely accepted that the magnitude of the problems might depend on the type of connection between the pipes (Triantafyllidou and Edwards 2011; US EPA 2011; Boyd et al. 2012; Giammar et al. 2012; St. Clair et al. 2012). Recent studies (Triantafyllidou and Edwards 2011; US EPA 2011; Giammar et al. 2012) have highlighted the need for research to quantify differences in galvanic corrosion performance of available connectors in PLSLRs with copper.

BACKGROUND

Historical and existing connection practices. Historically, lead was joined to copper without a connector, by melting leaded solder and forming it around the joint (Jensen 1918). This practice is no longer used, and today a typical lead-copper connection is formed using a brass connector (Figure 1-1, #4-6). A dielectric variant of these brass connectors is also available but was not tested as part of this this study. Traditionally, a dielectric is defined as a connector that is specifically designed to block the flow of electrical current. A plastic (insulating) connector (Figure 1-1, #7) can also be used to interrupt the lead-copper electrical connection. In laboratory studies (Triantafyllidou and Edwards 2011; Cartier et al. 2012; Hu et al. 2012), these connections have been simulated using an insulating spacer and flexible plastic tubing, which can be operated with lead and copper electrically disconnected (Figure 1-1, #2) or externally connected to allow current flow (Figure 1-1, #3). The different connectors are expected to affect galvanic corrosion in at least four ways:

(1) by breaking the electrical connection between the copper cathode and the lead anode via an insulator or dielectric,
(2) by changing the distance between the lead anode and copper cathode of the galvanic cell,
(3) by introducing a third metal if a conductive connector is used, and
(4) by introducing a crevice.

The authors analyzed commercially available connectors and connectors used in previous research (Cartier et al, 2012; Hu et al, 2012; Wang et al, 2012; Triantafyllidou & Edwards, 2011) and found wide variation in connector material (brass, plastic), connector length (0 –5.5 in), and the presence or absence of a crevice or broken electrical connection (Table 1-1).

Breaking the Electrical Connection. In order to form a galvanic cell, three conditions are required: two dissimilar metals, an electrical connection, and an electrolyte through which ions can be transported. When an insulating material is installed between two dissimilar metals, the electrical connection is broken, and galvanic corrosion is no longer possible. Although this can be done deliberately by using a dielectric connector, practical experience has shown that nondielectric brass connectors can sometimes unintentionally break the lead-copper electrical connection. This occurs when significant exterior scaling is present or if lead and copper are not

completely inserted into the connector, and the insulating rubber gasket, intended to make the joint watertight, interrupts electrical contact between the pipe and the brass connector. For connectors that include pipe clamps, interruption by the rubber gasket would only occur in an improper installation, in which the clamps are not fully tightened. For the purpose of discussion in the remainder of this chapter, the definition of the term "dielectric" has been expanded to include any connector that breaks the electrical connection between lead and copper, intentionally or otherwise.

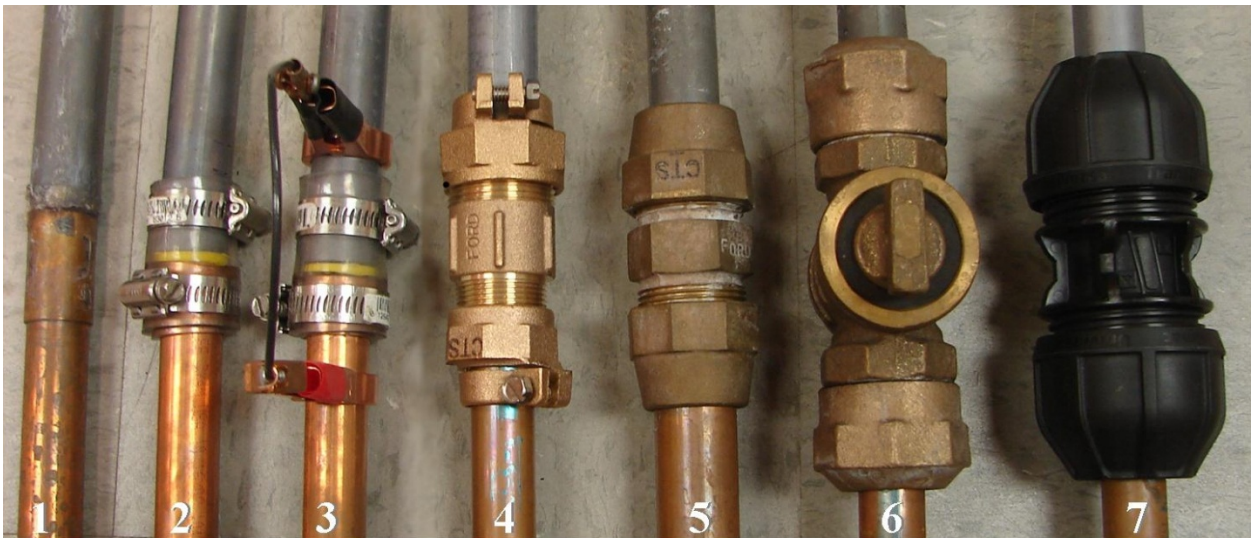

Figure 1-1. Seven examples show representative connections between lead and copper in a partial lead service line replacement: **(1)** direct connection; **(2)** flexible plastic laboratory connector with insulating spacer, disconnected and **(3)** connected; **(4)** brass union 1 (Ford Meter Box Q14-23-Q34-13); **(5)** brass union 2 (Ford Meter Box C44-44G); **(6)** brass corporation valve (Mueller H15209 1"); **(7)** plastic universal transition coupling (Philmac UTC Size B).

Figure 1-2 shows the possible effects of real connectors on galvanic corrosion. Part A of the figure shows a direction connection. Part B of the figure shows a dielectric connector without a grounding strap, and part C shows a dielectric connector with a grounding strap. In Figure 1-2, part D, use of a metal connector complicates galvanic corrosion because of interactions among the three metals.

Effect of distance. As shown in Figure 1-2, part C, increasing the spacing between the anode (lead) and the cathode (copper) while maintaining electrical contact through an external circuit is expected to decrease the galvanic current via an ohmic resistance effect (Hack and Wheatfall 1995; Bradford 2001; Frankel and Landolt 2007; St. Clair et al. 2012). The theory behind this current-distance effect has recently been discussed elsewhere (Edwards 2012; Frankel 2012; St. Clair et al. 2012). Although a lead pipe-brass connector-copper pipe electrical connection in a typical joint creates the galvanic connection internally, it remains hypothetically possible that increased distance between the strongest anode (lead) and strongest cathode (copper) when the three metals are connected might reduce galvanic corrosion (Figure 1-2, part D) compared to a direct connection (Figure 1-2, part A).

Table 1-1. Summary of key properties of real and laboratory connectors with respect to galvanic corrosion

Connector	Dielectric Properties?	Min/Max Distance Between Pb/Cu (in)	Crevice Volume
Direct Connection	NO	0 / 0	NO CREVICE
Tygon Connectors Used in Previous Lab Studies	YES if no external bridging; NO if external wire is used	0.25 / 0.25	NO CREVICE
Brass Union Fitting	Only with significant exterior scaling or incorrect installation	0 / 3	8.7 mL
Corporation Valve	Depending on installation practices, which can allow Cu and Pb to touch one another or the connector wall	2 / 4.5	3.5 mL
Universal Transition Coupling (UTC) B		0 / 2	3.7 mL
Brass Union, Dielectric Variant	YES with respect to Pb and Cu; however, Pb touches brass, creating a brass/Pb cell	1.25 / 3	5.5 mL

Effect of connector material. Galvanic corrosion is also dependent on the material used to connect lead and copper. If a dielectric connector is used, no current can flow between the two metals and direct galvanic corrosion is eliminated (Figure 1-2, Part B). If the connector is made of a conductive material, galvanic corrosion is complicated by interactions between all three materials (Figure 1-2, Part D). If a less noble metal (such as steel or iron) was used to connect lead and copper, it would be predicted based on the galvanic series (Davis 2000) that the connector might act as a sacrificial anode and protect both lead and copper from corrosion. However, brass, which is commonly used in commercially available connectors (Table 1-1), lies between copper and lead on the galvanic series (Davis 2000), and lead is still expected to act as the strongest sacrificial anode in the connection. Although the galvanic series can be used to make general predictions, these three-metal systems are complicated because of possible electrochemical reversal in the presence of chlorine, e.g. lead becomes cathodic to copper (Arnold and Edwards 2012), and other issues.

Crevice corrosion. Crevice corrosion can occur in a small gap that is sometimes created between the connector and the outside of the lead or copper pipe (Figure 1-3). The water sitting essentially stagnant in the crevice can become depleted in oxygen, pH can decrease as metal ions hydrolyze, and concentrations of lead and counter ions (potentially aggressive or passivating) can rise to very high levels (Rosenfeld 1971; Nguyen et al. 2010). The effect of a crevice on corrosion rate is highly dependent on crevice geometry (Rosenfeld 1971). In a large crevice, frequent exchange of the crevice water with the bulk water mitigates crevice corrosion by preventing pH drop and the buildup of aggressive ions. On the other hand, in a very small crevice, ion transport and oxygen diffusion are limited by the narrow opening, reducing the corrosion rate. Rosenfeld's research showed that in stainless steel crevices these two competing factors produced a peak in corrosion rate at an intermediate crevice width (Rosenfeld 1971).

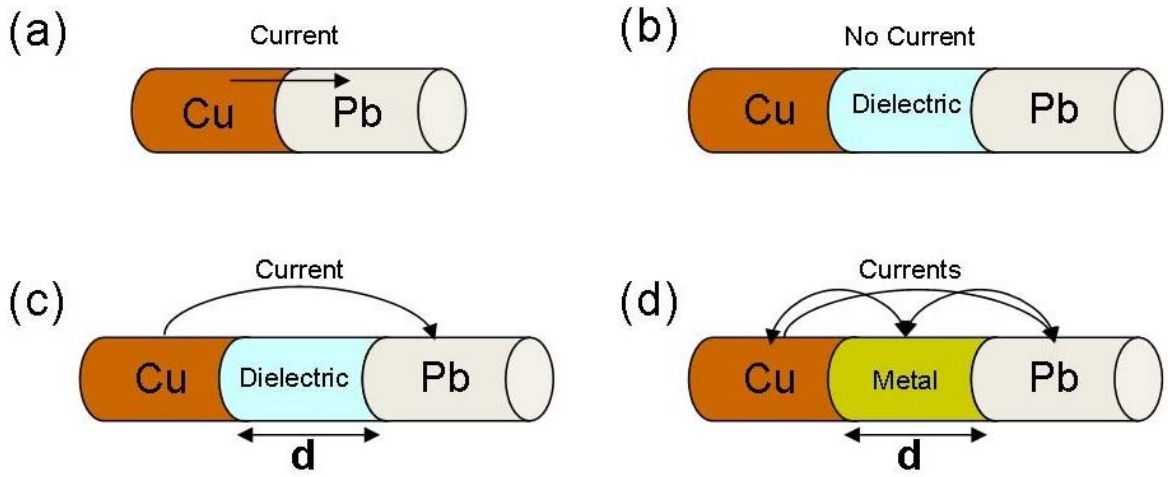

Figure 1-2. Illustration of possible effects of real connectors on galvanic corrosion: **(a)** direct connection, in which current can pass directly from copper (Cu) to lead (Pb); **(b)** dielectric connector (without grounding strap), which does not allow current to pass between these metals, eliminating galvanic corrosion; **(c)** dielectric connector (with grounding strap) still allows current to pass between Cu and Pb, which is a function of the distance "d" apart; **(d)** the use of a metal connector complicates galvanic corrosion due to three-metal interactions.

Even in passivated, single metal systems, a crevice can become anodic relative to the rest of the pipe and corrode severely (Lennox and Peterson 1971; Rosenfeld 1971; Salamat et al. 1995). In a two-metal crevice, such as that present in a PLSLR, the effect is more complicated. If the pipe material is cathodic to (i.e., more noble than) the connector material – such as a Cu pipe in a brass connector – it is expected to be protected from crevice corrosion (Lennox and Peterson 1971; Salamat et al. 1995). However, if the pipe material is anodic to (i.e., less noble than) the connector material, it will be driven to corrode even more severely because of the combination of galvanic and crevice corrosion effects (Salamat et al. 1995; Nguyen et al. 2010), resulting in high galvanic currents and possibly elevated lead levels in water. Therefore, to avoid crevice corrosion, key factors in connector selection theoretically include both the geometry of the crevice and the connector material.

Objectives. The goal of the current study was to develop a mechanistic understanding of the effects of connector length, connector material, and the presence of a crevice on galvanic corrosion arising from PLSLRs. To accomplish this, short-term bench-scale studies were designed to isolate each of these three effects. The findings of these mechanistic experiments were then used to interpret comparison studies of lead contamination of water using several commercially available connectors. In the latter studies, two research groups coordinated bench-scale simulated PLSLRs using tap waters from Blacksburg, Va. and Montreal, Que.

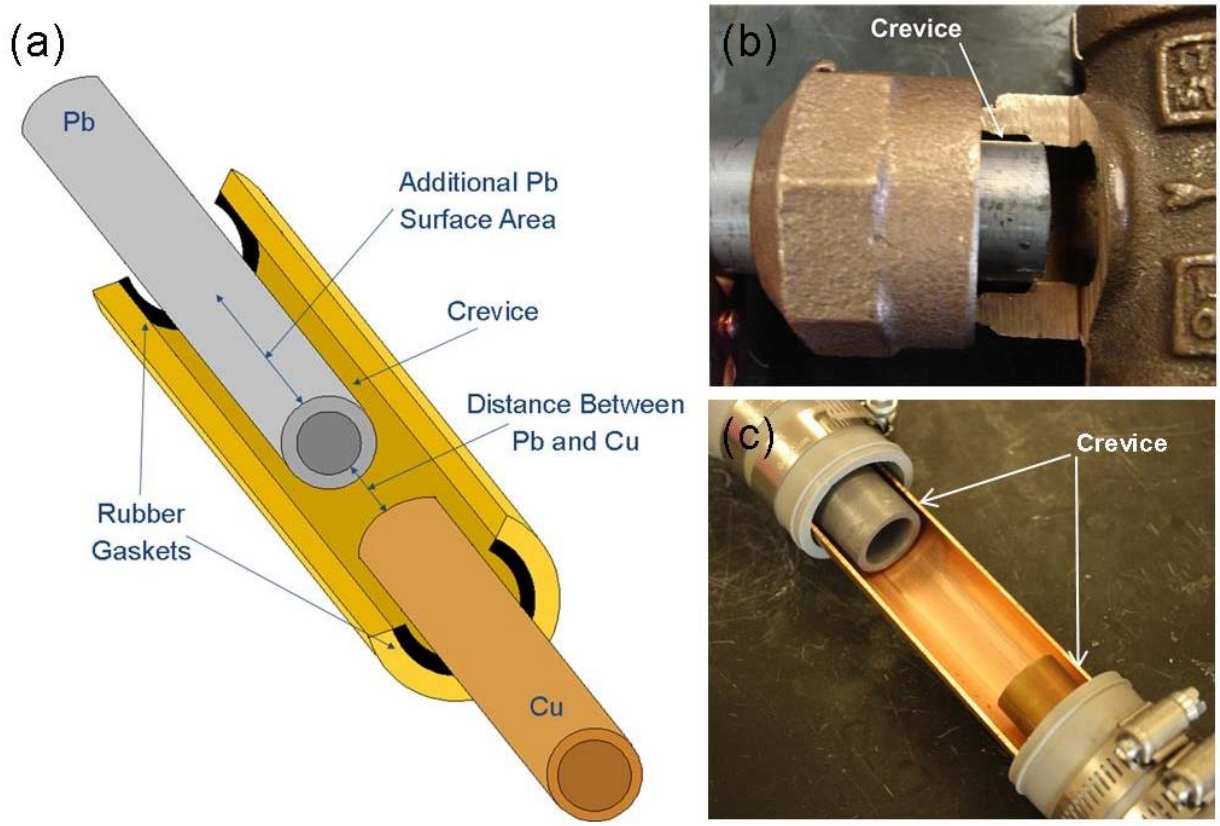

Figure 1-3. (a) Illustration of key terms in this study on a cutaway view of a brass connector. Cutaway photos showing the presence of crevices in both **(b)** a commercially available connector (Mueller H15209 1") and **(c)** the "copper sleeve" connector used in this study.

MATERIALS AND METHODS

Phase 1: effect of distance. The test rig was constructed by connecting 6 in. (15.2 cm) of copper pipe (type M), with a ¾-in inside diameter (ID) and ⅞-in outside diameter (OD) to 2.5 ft (76.2 cm) of lead pipe (¾-in ID, 1-in OD). Before testing, these pipes were aged for approximately three years in experiments using various water quality conditions (Triantafyllidou and Edwards 2011), with the last 14 weeks of exposure in Blacksburg tap water (Table 1-2). To test the effect of separation distance between lead and copper on galvanic corrosion rate, the pipes were connected with flexible plastic tubing at separation distances varying from ¼-in (0.64 cm) to 12 in (30.5 cm), as shown in Figure 1-4, part A. Galvanic currents between lead and copper were measured using a digital multimeter (RadioShack 22-811) via an external connection through a grounding strap. Testing comparing the multimeter to a zero-resistance ammeter found that current differences were less than 3%. To conduct the test, the pipe rig was assembled with the desired separation distance, and then filled with Blacksburg tap water. The current was measured immediately after filling. The rig was then drained, disassembled, and reassembled at the next separation distance to begin the next test.

Table 1-2. Key water quality parameters of Blacksburg drinking water and Montréal drinking water (after aeration)

	Blacksburg	Montréal (aerated)
pH	7.8	8.5
Disinfectant	Chloramines, 3 mg/L	Free Chlorine < 0.3 mg/L
Alkalinity (as $CaCO_3$)	40 mg/L	100 mg/L
Chloride-to-Sulfate Mass Ratio (CSMR)	3.0	0.9
Corrosion Inhibitor	Zinc Orthophosphate	None

$CaCO_3$ = calcium carbonate

Phase 2: effect of metallic connector materials. This test was conducted using the lead and copper pipes from the test rig in phase 1. In this setup, however, a 1-in (2.54-cm) brass connector was used between two ¼-in (0.64-cm) insulating spacers for a total separation distance of 1.5-in (3.8 cm), as shown in Figure 1-4, part B. Because these insulating spacers electrically isolate the three metals, metallic components can be externally connected via grounding straps in order to measure the current between each piece. Most commercial connectors are made of some type of brass, and in this phase, three different types of brass were tested: a yellow brass (61% copper, 35% zinc, 3% lead), a red brass (87% copper, 13% zinc) and a dezincified yellow brass (Figure 1-4, part C). In order to create a dezincified yellow brass in the laboratory (simulating an aged brass connector after some time in service under dezincifying conditions), the same type of yellow brass used earlier in the experiment was exposed to 1% cupric chloride at 75°C for 24 hours as specified by the ISO 6509 protocol (Sarver et al. 2011). Galvanic current was measured as in phase 1.

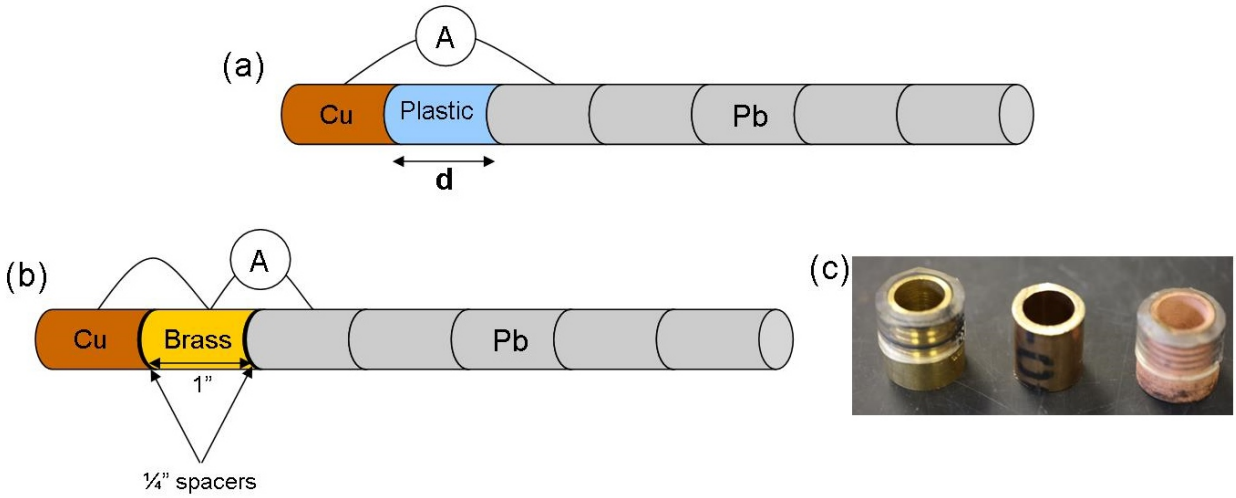

Figure 1-4. Illustration of experimental setup to study (a) the effect of distance (phase 1) and (b) the effect of different brass connectors on galvanic corrosion (phase 2). Three types of brass (c) were tested in phase 2 including (left to right) yellow brass, red brass, and dezincified yellow brass.

Phase 3: mechanistic study of crevices. This phase of the experiment was designed to explore some mechanistic impacts of the crevice formed between the connector and the lead pipe in several commercially available connectors (Figure 1-3). Commercial connectors tested included a brass union (Ford Meter Box Q14-23-Q34-13) and a brass corporation valve (Mueller H15209 1"). In order to demonstrate the mechanism of crevice attack without the complication of a third material (brass, which contains traces of lead), a "copper sleeve" connection was constructed with the same crevice geometry as the commercially available corporation valve. Finally, a "polyvinyl chloride (PVC) sleeve" connector was constructed (also with similar geometry to the corporation valve) to eliminate all galvanic effects and study the effect of a crevice alone. For the copper sleeve, the brass union, and the corporation valve, connectors were installed in such a way that they acted as dielectrics, then externally bridged in order to allow measurement of galvanic current.

To allow access to the crevice for sampling during experimentation and to enable visualization of the connections occurring within the crevice, the top half of each connector was cut away in the region surrounding the crevice (Figure 1-3, part B). Each connector was used to connect 1.5 ft (45.7 cm) of new lead pipe (¾-in ID, 1-in OD) to 1.5 ft (45.7 cm) of new copper pipe (¾-in ID, ⅞-in OD, Type M) or ¾-in PVC pipe for the "PVC sleeve" condition. For the corporation valve, which is designed for 1-in copper pipe, the length of copper pipe was reduced to allow for identical water volume for each condition. For the brass union, lead and copper pipe were placed in two different configurations – touching and not touching one another inside the connector – to represent variability in installation practices (Table 1-1). For each of the metal connectors, a control was also constructed in which the outside of the lead pipe was coated with epoxy to eliminate certain crevice effects. This resulted in a total of nine conditions for this experiment.

All pipes were filled with Blacksburg water throughout the seven-week experiment. Water was completely changed in the pipes once weekly and added as necessary throughout the week to compensate for slight evaporation occurring through the cutaway. Measurements of galvanic current and pH were taken daily (Monday through Friday). Current was measured as in phases 1 and 2. The pH was measured both in the crevice and the bulk water using a micro pH electrode (Microelectrodes, Inc. MI-406). Samples were collected from the crevice for anion and total metals analysis on Monday (both before and after the water change), Wednesday, and Friday each week. Anion analysis was conducted according to method 4110B (*Standard Methods*, 1998) using a Dionex DX-120 ion chromatograph. The analytical and guard columns used were Dionex AS9-HC and AG9-HC, respectively. An ASRS 300 suppressor was used, and the eluent was 9 mM sodium carbonate at a flow rate of 1 mL/min. Analysis for total metals was conducted by inductively coupled plasma – mass spectrometry (ICP-MS; Thermo Scientific Thermo Electron X Series) using method 3125B (*Standard Methods*, 1998) with acidification to 2% nitric acid by volume.

Phase 4: comparison testing in real tap waters. To extend the mechanistic insights to practical situations, a 26-week bench-scale study of simulated PLSLRs with copper was conducted using two different tap waters (Table 1-2). The test setups were constructed by connecting 2.5 ft (76.2 cm) of new lead pipe (¾-in ID, 1-in OD) to 2.5 ft (76.2 cm) of new copper pipe (¾-in ID, ⅞-in OD, Type M) using a variety of laboratory and commercial connectors. As in phase 3, In some

cases, a 1-in copper pipe was needed to fit the connector; in this case, the length of copper was reduced to give an equivalent total setup volume to the ¾-in conditions.

In Montreal, three connector types were tested in triplicate. The first type was an insulating spacer that has been used in several recent laboratory studies (Triantafyllidou and Edwards 2011; Cartier et al. 2012; Hu et al. 2012). This connector was tested in both externally connected and disconnected conditions. The other connectors in this study included the brass union and corporation valve from phase 3. A pure copper control was also used. Water was changed in the pipes three times weekly on a Monday-Wednesday-Friday schedule using a dump-and-fill protocol. The entire pipe volume was collected as a composite sample each week, and digested by acidification to 2% nitric acid by volume. After dilution of samples to 0.5% nitric acid by volume and addition of 0.5% hydrochloric acid by volume, analysis for total metals was conducted by ICP-MS (Agilent Technologies, Santa Clara, CA) in an ISO 179025-certified laboratory based on method 3125B (*Standard Methods*, 1998)

In Blacksburg, two brass connectors were tested. The first was the corporation valve used in phase 3 and the second was a type of brass union (Ford Meter Box C44-44G). In addition, a direct connection between lead and copper was constructed by melting the two pipes into one another (direct connections or equivalent practices were common in the past). These experimental rigs were tested alongside both a pure copper and a pure lead control. Water was changed in the pipes twice per week using a dump-and-fill protocol. As in Montreal, the entire sample volume was collected as a composite sample each week and analyzed for total metals using the same method as in phase 3.

To determine whether lead leaching from brass contributed a significant percentage of total lead released to water during comparison testing, a four-week control experiment was also conducted. The union and the corporation valve from phase 3 were connected to PVC or chlorinated PVC pipe to give an equivalent volume to that used for comparison testing. For this phase of testing, Blacksburg water was used, and water change and analysis procedures were identical to those used in Blacksburg water comparison tests.

RESULTS AND DISCUSSION

Phase 1 results: effect of distance. In short-term experiments with aged simulated PLSLRs with copper, the galvanic current decreased markedly as the distance between lead and copper increased (Figure 1-5). At the minimum separation distance tested of ¼-in (0.64 cm), the galvanic current was more than 50 μA. However, a separation of 4.3-in (10.9 cm) was sufficient to reduce the current to half this value, and a separation of 12-in (30.5 cm), the largest tested, reduced the galvanic current by 80%. This result is in agreement with expectations based on galvanic theory (Hack and Wheatfall 1995; Bradford 2001; Frankel and Landolt 2007). It also implies that commercial connectors, which can provide a separation between lead and copper of nearly 6-in (15.2 cm) as shown in Table 1-1, could be beneficial in some cases in reducing galvanic effects, even if electrical grounding concerns require bridging across dielectric connectors with a grounding strap. This benefit was proven in a recent four-month study in drinking water (St. Clair et al. 2012) and in earlier work in seawater (Hack and Wheatfall 1995).

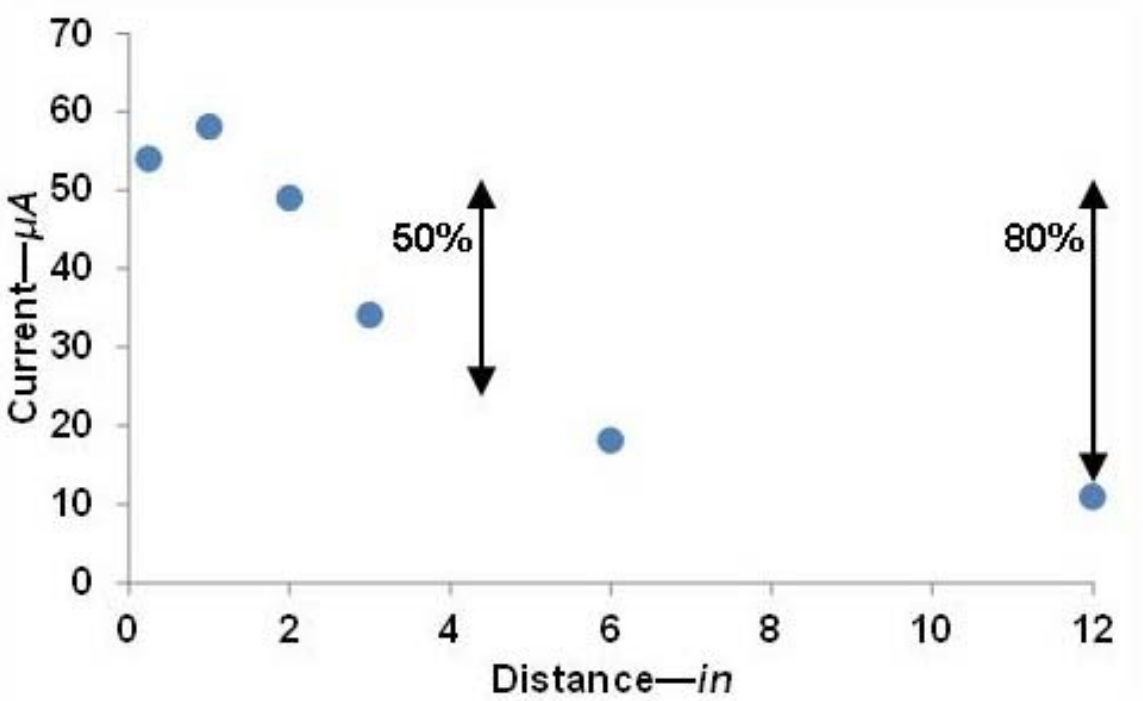

Figure 1-5. Effect of plastic connector length on galvanic current (phase 1). As the distance between lead and copper increases, the galvanic current decreases. At a separation of 4.3-in (10.9 cm), the current had dropped by 50%; at a separation of 12-in (30.5 cm), the current had dropped by 80%.

Phase 2 results: effect of metallic connector materials. When a red brass connector was substituted for the plastic connector in the previous experiment, the total galvanic current to the lead decreased by nearly 25% (Figure 1-6). With yellow brass, an even greater decrease in the current to the lead was observed; however, a dezincified connector of the same brass showed a small increase in galvanic current compared to the plastic spacer. In general, the higher the zinc content of the brass the greater the decrease in galvanic current relative to the plastic spacer, as would be expected in light of previous research (Zhang & Edwards 2011) and given that zinc is below lead on the galvanic series (Davis 2000). If the brass was dezincified, however, the current increased because the brass was effectively equivalent to an additional length of copper pipe (dezincified brass is essentially highly porous copper) at a reduced distance from the lead. In practice, because only lower-zinc-content brasses are allowed for underground connections according to AWWA standards (AWWA 2005), the use of brass itself provides no protection against galvanic corrosion, and even if higher zinc content brasses were allowed, benefits would likely decrease over time. Additionally, measurements of the relative contributions of current from copper and brass showed that even with this relatively small brass connector, 40-60% of the total galvanic current to the lead could be attributed to brass, while only a very small amount of current (on the order of 5 μA) was observed between copper and brass. This is consistent with theory based on the galvanic series (in which brass and copper have very similar potentials whereas lead is anodic to both metals) and supports the finding that brass can provide only limited, if any, protection against galvanic corrosion.

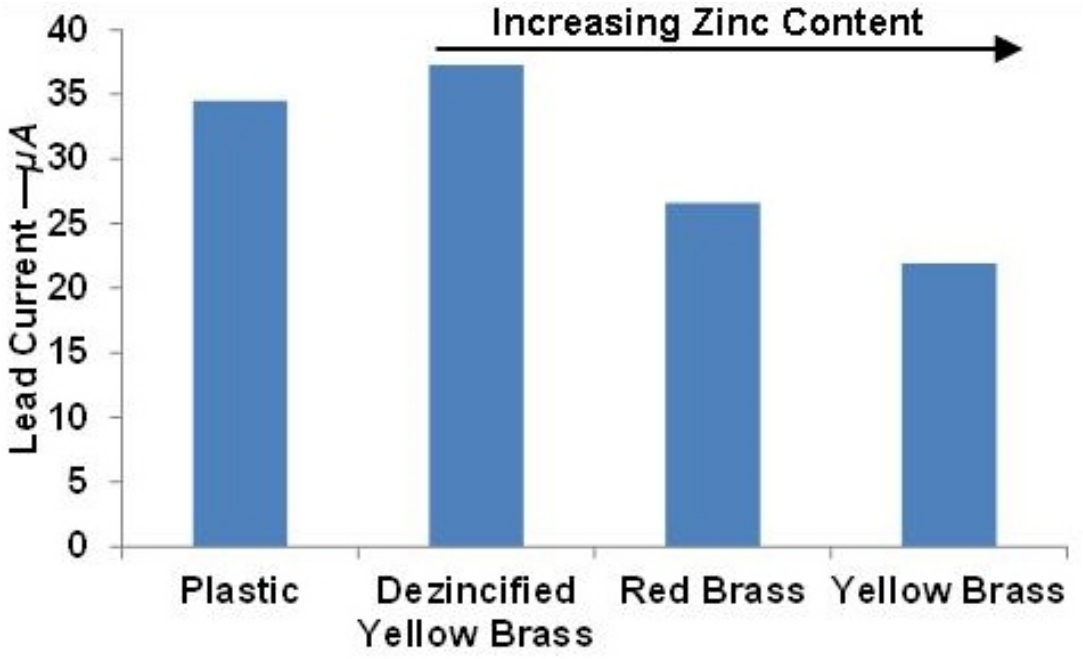

Figure 1-6. Effect of different connector materials on total galvanic current to lead pipe from both copper and brass for a fixed connector distance of 1.5 in (3.8 cm). A small decrease in current was observed when a brass connector was used relative to plastic; however, the lead current tended to increase as the zinc content of brass decreased (dezincification). Relative to the results presented in Figure 1-5, these experiments were conducted at a later date and cannot be directly compared to the values in the previous figure

Phase 3 results: presence of crevices. The simplest case tested in this mechanistic study of crevices was the PVC sleeve condition, which was not coated with epoxy and represented the effect of crevice corrosion without any galvanic corrosion. When this simple case was compared with each of the four different metal connections without epoxy (which exhibited both galvanic and crevice corrosion), the average increase in lead concentration attributable to galvanic and crevice corrosion was 20 – 700 times (data not shown). The differences between the metal connectors and the PVC control were statistically significant in all cases at the 95% confidence level (t-test paired by sampling date).

The difference in the behavior of the same connectors with and without epoxy on the outer lead pipe surface provides insight into the effect of involving the outer wall of the lead pipe in the galvanic corrosion (Figure 1-3). This can be examined from the perspective of galvanic current and possible effects on lead leaching. For the copper sleeve condition, the without-epoxy condition had a current 2.5 times higher, on average, than for the same condition with epoxy (Figure 1-7, part A). This indicates that the presence of a crevice can accelerate corrosion because of involvement of the surface on the outside of the lead pipe wall. Conversely, for other connectors, such as the brass union (Figure 1-7, part B) and the corporation valve (data not shown), the galvanic current remained roughly the same with and without epoxy on the outer pipe wall.

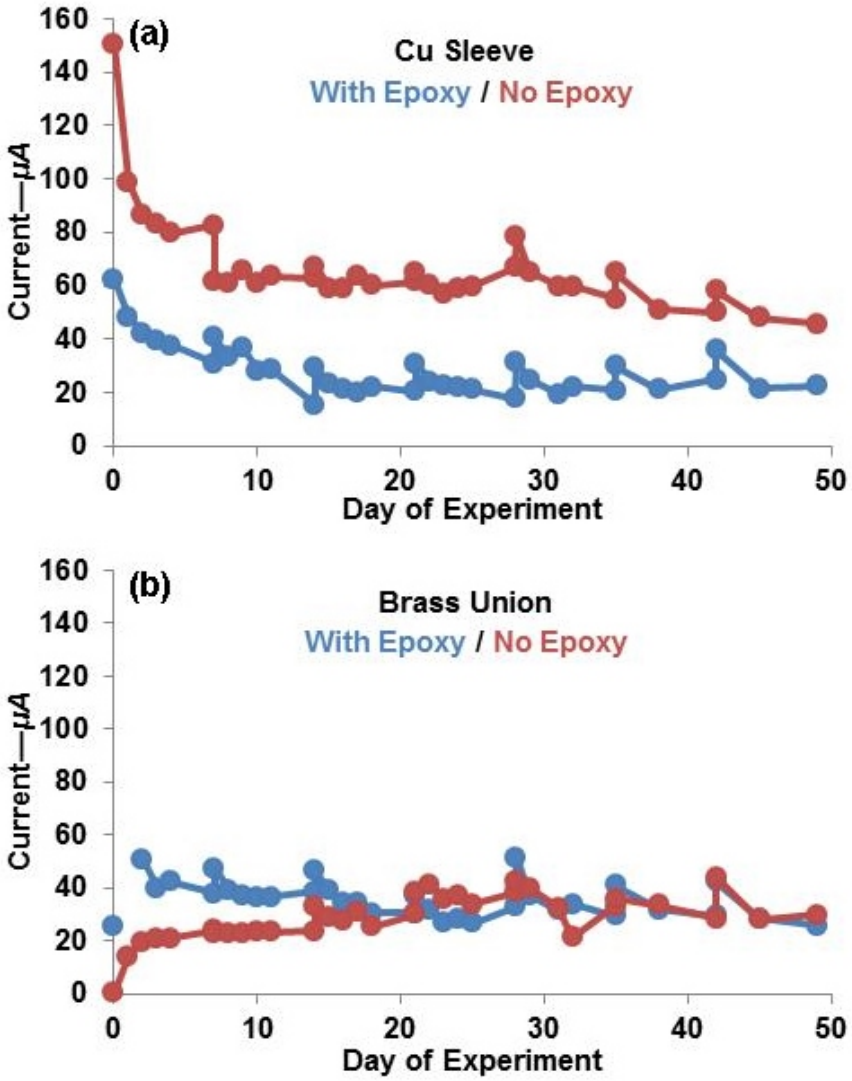

Figure 1-7. Galvanic current as a function of time over the seven weeks of the crevice experiment (phase 3) for (a) the copper sleeve connector and (b) the brass union connector (not touching). For the copper sleeve, galvanic current is an average of 2.5 times higher and a maximum of 4 times higher for the condition without epoxy than the condition with epoxy. For the brass union, the galvanic current is roughly the same for both conditions.

However, it was also discovered that the measured galvanic current was not a good predictor of total actual galvanic current in all of these cases. In the brass union, for example, the rubber ring included with the connector (Figure 1-3, part A) was discovered to be relatively conductive (resistance of only 1-5 kΩ) and would have allowed significant galvanic current to pass directly between lead and copper without passing through the ammeter. This is reflected in the results for the brass union (not touching). As shown in Figure 1-7, part B, the current was the same both with and without epoxy; however, under the same conditions as shown in Figure 1-7, part B, the lead concentration in the crevice was an average of 100 times higher without epoxy than with epoxy (Figure 1-8). This difference persisted for the first six weeks of the study and was significant at the 95% confidence level ($p = 0.01$; t-test paired by sampling date). When lead and copper pipe were inserted completely into the union, allowing the two pipes to touch, the adverse

effect of involving the outer wall of the lead pipe in galvanic corrosion was even more dramatic. Compared with when epoxy was used, the pipe without epoxy saw an average increase in crevice Pb concentration of 150 times ($p = 0.0003$; data not shown). For the corporation valve and copper sleeve, the differences between the conditions with and without epoxy were not statistically significant at 95% confidence, but the average crevice lead concentration was always higher without epoxy.

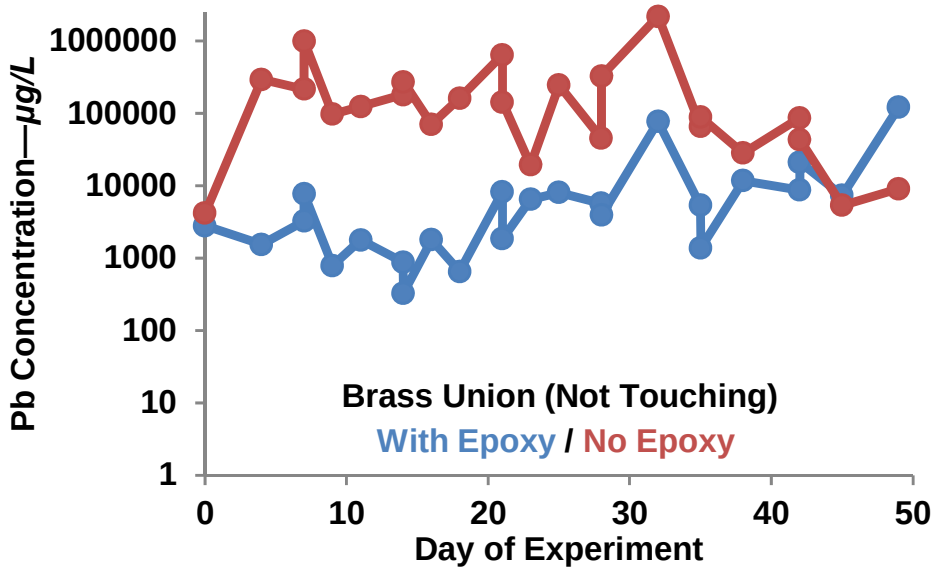

Figure 1-8. Log scale concentration of lead in the crevice as a function of time over the seven weeks of the crevice experiment (phase 3) for the brass union connector (not touching). When the crevice was not coated with epoxy, the crevice lead concentration was an average of 100 times higher. This difference is significant at the 95% confidence level ($p = 0.01$, t-test paired by sampling date).

The orders-of-magnitude higher lead in the condition without epoxy implies that "leaking" of lead from the crevice to the water at the joint could be a serious health concern in practice. This is a consequence of the extremely high lead concentration (9,400 mg/L, or 9.4 million µg/L) in some crevices. Although the sample size did not allow direct measurement of soluble lead, thermodynamic modeling predicted that only 0.0003%, or less than 30 µg/L, of this worst-case lead concentration is soluble. The predicted lead solid is mostly (99.1%) lead hydroxide; and the remaining 0.9% is pyromorphite, a lead phosphate mineral. The lowest average crevice lead concentration for a metal connector without epoxy was nearly 40,000 µg/L. Although this concentration was confined to the very small volume of the crevice that likely exchanged slowly with the bulk water, even the slightest exchange of this water with the bulk poses a potential health concern. For example, if only 0.02 to 0.4 mL of water from the crevice mixed with water passing through the joint, that would be enough to contaminate of 1-L of water to a level above the 15 µg/L action level.

Consistent with expectations based on theories of crevice corrosion (Rosenfeld 1971; Dudi 2004), given that Pb^{2+} is a relatively weak Lewis acid, extremely low pH was not observed in these crevices. On average, the pH remained in the range of 6-9 in all crevices, as measured by micro-pH electrode. Somewhat contrary to expectations based on past research (Nguyen et al. 2010), the very high lead concentrations in the crevice were not accompanied by dramatic

increases in chloride and/or sulfate concentrations. The highest chloride and sulfate concentrations observed were approximately three to four times higher than those in the influent water, but the phosphate concentration was an average of sever times higher and as much as 25 times higher than that of the influent water. The reasons for the increase in phosphate are not known, but it is possible that phosphate increased as a result of precipitation of a lead phosphate solid in the crevice. This theory is supported by chemical equilibrium modeling results, which predict that more than 99.9% of phosphate was present in the crevice as pyromorphite. Higher phosphate is concerning, because it has been associated with greater Pb release from galvanic connections for reasons that are not yet fully understood (Nguyen 2011).

The effects of crevice corrosion were also visually obvious (Figure 1-9). For all metal connectors, a white corrosion scale was clearly visible on the exterior of the lead pipe in the area exposed to the crevice. For the PVC control with a non-galvanic crevice, this surface appeared relatively unchanged. In an actual PLSLR, the effect of crevice corrosion will be complicated by pre-existing scale from long-term contact with soil. However, recent studies with harvested lead pipes have shown that large adverse galvanic effects are still possible for pipes with pre-existing interior and exterior scales (Cartier et al. 2013; Wang et al. 2012). Clearly, the increased lead pipe surface area, in proximity and in galvanic connection with copper, is likely to be a factor of concern in connections made after PLSLRs.

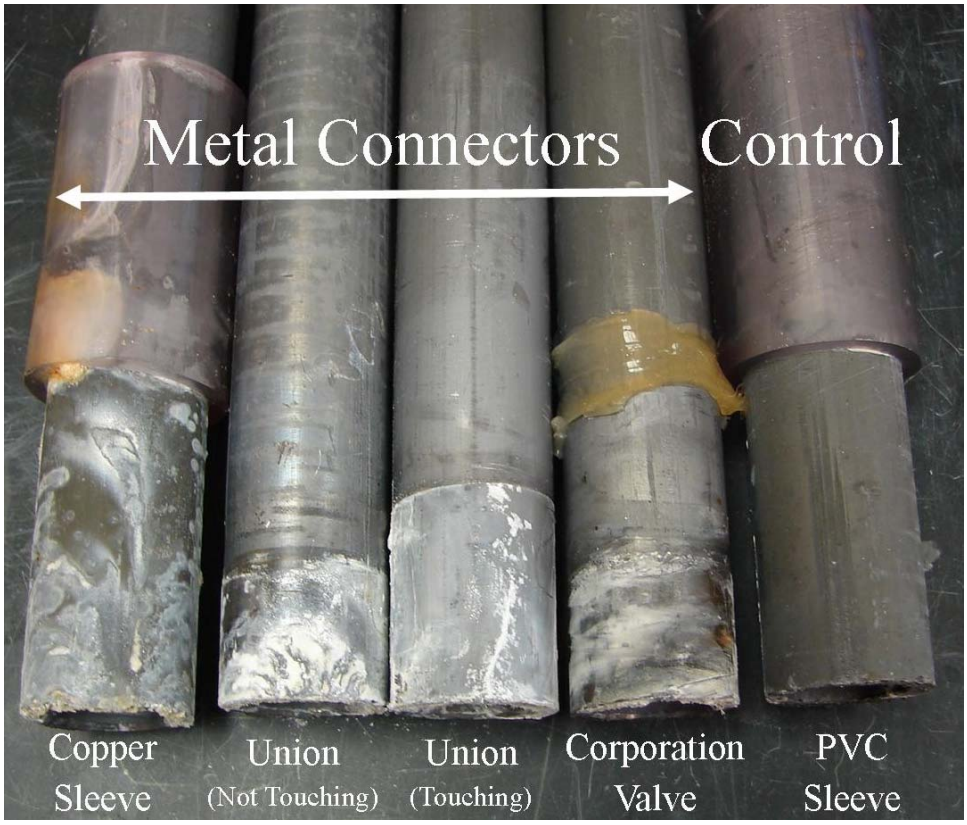

Figure 1-9. Photo of the exterior surface of the lead pipes without epoxy in the crevice corrosion experiment (phase 3) at the end of the seven week study, including, from left to right, the copper sleeve, brass union (not touching),brass union (touching, corporation valve, and PVC sleeve. In all conditions except for the PVC sleeve, white corrosion scale is visible in the area exposed to the crevice.

Phase 4 results: Comparison testing in real tap waters. Bench scale testing conducted in Blacksburg and Montreal showed similar trends although the two tap waters had very different characteristics (Table 1-2).

In Blacksburg, direct connection between lead and copper, which represents the worst case for lead and copper connections without brass (St. Clair et al. 2012), increased lead leaching during the final eight weeks of the study by a factor of five, on average, compared with leaving the lead pipe intact (Figure 1-10, part A). However, when brass connectors were used, lead leaching was increased, on average, by a factor of 19 for the union fitting and a factor of 20 for the corporation valve, compared with lead pipe alone. In contrast, at the beginning of the study, lead leaching between the brass connectors was, on average, only five to six times greater than with pure lead pipe. These differences imply that the effects of galvanic and crevice corrosion persist or even worsen in the long term. The brass leaching control experiment resulted in lead in water levels that were, on average, approximately 2.5% of those observed during comparison testing. This result is similar to reports by others (Wang et al. 2012) and effectively ruled out the leaded brass as the source of the elevated lead concentrations observed. It appears that the expected benefit of increased distance between lead and copper and the use of brass as a connector material is not enough to negate the adverse effects of both a crevice and the resultant involvement of the outside of the lead pipe in the galvanic cell.

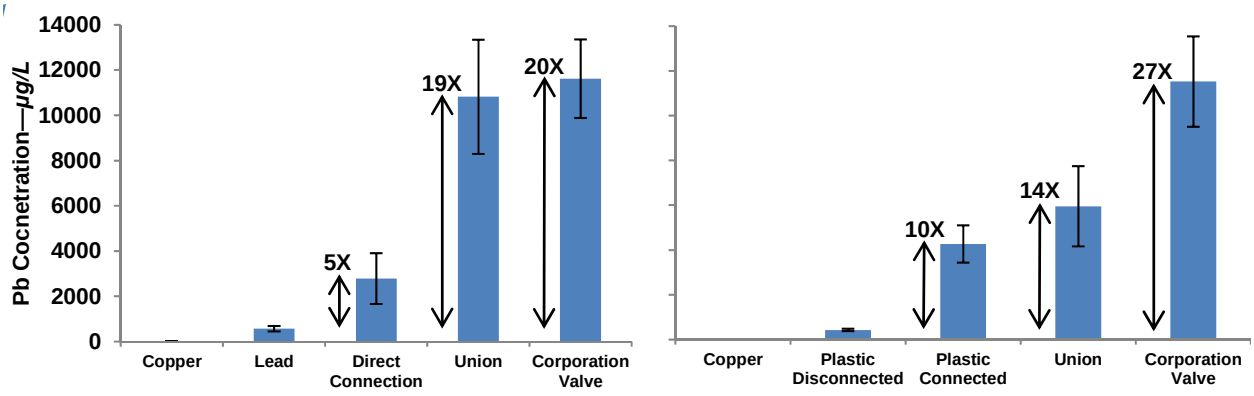

Figure 1-10. Pooled lead concentration data for the last eight weeks of the 26-week dump-and-fill studies (phase 4) in **(a)** Blacksburg and **(b)** Montreal. In Blacksburg, direct end-to-end connection, a brass union, and a corporation valve were compared to pure Pb pipe. In Montreal, an external galvanic connection, a brass union, and a corporation valve were compared to a disconnected flexible plastic laboratory connector (simulated dielectric). Error bars represent 95% confidence intervals.

Results for the Montreal tap water, which differed greatly from the Blacksburg water in that it had no corrosion inhibitor and higher alkalinity (Table 1-2), demonstrated a similar trend (Figure 1-10, part B). When pipes connected using the flexible plastic laboratory connector were externally bridged, they released, on average, 10 times more Pb in the last eight weeks of the study than when they were not bridged. Some have speculated that external bridging could lead to extremely high lead release (Boyd et al. 2012) and that commercial brass connectors would not be subject to elevated lead from galvanic corrosion; however, in this work the average lead released in the last eight weeks of the study via galvanic corrosion attributable to commercial connectors was much higher than direct or bridged connections between pipes, e.g. 14 times higher for the brass union and 27 times higher for the corporation valve, compared to the

unbridged flexible plastic connector. As in Blacksburg tap water, galvanic and crevice effects persisted or worsened throughout the study. For example, the average increases in lead leaching between the brass connectors and the control condition over the first eight weeks of the Montreal study were a factor of six for the brass union and a factor of 30 for the corporation valve.

According to the theory of galvanic corrosion, increased corrosion at the anode (lead) should be accompanied by a decrease in corrosion of the cathode (copper). In Montreal, after normalizing for dilution, both laboratory and commercial connectors were associated with a decrease in copper concentration to 30-50% of the levels released from a pure copper pipe. In Blacksburg, however, although similar decreases in copper concentration were observed for the union fitting and direct connection, the corporation valve showed no decrease in copper concentration compared with the pure copper pipe. One possible reason for this is the increased distance between lead and copper with this connector, decreasing the extent to which lead can protect copper from corrosion.

Effects of stagnation. In phases 3 and 4, a dump-and-fill protocol was used to study the effect of crevice corrosion and compare different connector types. This method, which allows water to stagnate in the pipes for extended periods of time (up to one week in this research), is believed to represent a worst-case scenario for galvanic corrosion (Triantafyllidou 2011). However, higher galvanic currents have been observed under flowing conditions (Cartier 2012), likely as a result of improved mass transport of oxidants, implying that more frequent water changes could cause an overall increase in the corrosion rate. Additionally, for crevice corrosion, more frequent water changes are likely to result in greater exchange between the highly contaminated crevice water and the bulk water. Therefore, for galvanic connections involving crevice corrosion, the net effect on lead release of decreasing the stagnation time to more realistic levels cannot be determined without further study.

CONCLUSIONS

Mechanistic studies and short-term bench-scale studies of simulated PLSLRs with copper in two real tap waters yielded the following conclusions.

- As distance between lead and copper increases, galvanic current tends to decrease. In this study, at a separation distance of 12 in (30.5 cm), 80% reduction in current was achieved.
- As a connector material, new brass may have slight benefits over direct connection to copper in terms of decreasing galvanic corrosion. These benefits are greatest when the zinc content of the brass is high and may dissipate with time as brass dezincifies.
- Creation of a crevice involves the outer wall of the lead pipe in galvanic corrosion, and also creates a small volume of water with extremely high lead levels (as high as 9.4 million μg/L) and elevated anion concentrations (as much as 8.5 times higher chloride, 6.5 times higher sulfate, and 25 times higher phosphate than in the bulk water). In some cases, when the outermost lead pipe wall was coated with epoxy, lead concentrations in the crevice dropped by a factor as high as 150. Connectors with crevices can markedly worsen lead release to water, compared with direct connections or brass connectors without crevices.

- Some rubber materials present in brass connectors do not function as a true dielectric because their resistance is on the order of 1-5 kΩ.
- In both Blacksburg and Montreal tap water during the 26-week dump-and-fill study, all commercial brass connectors used in partial pipe replacements exhibited higher lead release than both externally bridged connectors used in previous laboratory studies and direct connection between lead and copper. This is believed to be a result of crevice corrosion. Although dielectrics are the best connector choice in terms of lead release, in Montreal, some of the brass connectors released only one third of the lead released by other brass connectors. Therefore, if dielectrics are not viable or allowed, utilities conducting PLSLRs should (to the extent practically reasonable) consider using the connectors that released less lead.

ACKNOWLDGEMENTS

The authors acknowledge the financial support of the Robert Wood Johnson Foundation (RWJF) under the Public Health Law Research (PHLR) Program. Brandi Clark was supported by a National Science Foundation (NSF) Graduate Research Fellowship (GRF). Opinions and findings expressed herein are those of the authors and do not necessarily reflect the views of the RWJF or the NSF. The authors would also like to thank Casey Murray for her assistance with the experimental work for this study.

REFERENCES

American Water Works Association (AWWA), 2005. C800-05: AWWA Standard for Underground Service Line Valves and Fittings.

Arnold, R. B. and M. Edwards, 2012 Potential Reversal and the Effects of Flow Pattern on Galvanic Corrosion of Lead. *Environ. Sci. Technol.* 46:20:10941-10947.

Boyd, G. R., S. H. Reiber, M. S. McFadden and G. V. Korshin, 2012. Effect of Changing Water Quality on Galvanic Coupling. *Journal AWWA* 104:3:E136-E149.

Bradford, S. A., 2001. *Corrosion Control*. Edmonton, CASTI Pub.

Britton, A. and W. N. Richards, 1981. Factors Influencing Plumbosolvency in Scotland. *J. Inst. Water Eng. Scient.* 35:349-364.

Brown, M. J., J. Raymond, D. Homa, C. Kennedy and T. Sinks, 2011. Association between children's blood lead levels, lead service lines, and water disinfection, Washington, DC, 1998–2006. *Environmental Research* 111:1:67-74.

Cartier, C., R. B. Arnold Jr, S. Triantafyllidou, M. Prévost and M. Edwards, 2012. Effect of Flow Rate and Lead/Copper Pipe Sequence on Lead Release from Service Lines. *Water Research* 46:13:4142-4152.

Cartier, C., E. Dore, L. Laroche, S. Nour, M. Edwards and M. Prevost, 2013. Impact of Treatment on Pb Release from Full and Partially Replaced Harvested Lead Service Lines (LSLs). *Water Research* 47:2:661-671.

Davis, J. R., Ed. 2000. *Corrosion: Understanding the Basics*. Materials Park, OH, ASM International.

Dudi, A., 2004. Reconsidering Lead Corrosion in Drinking Water: Product Testing, Direct Chloramines Attack, and Galvanic Corrosion. Department of Civil and Environmental Engineering, Virginia Tech. M.S.

Edwards, M. A., 2012. Discussion: Effect of Changing Water Quality on Galvanic Coupling. *Journal AWWA* 104:12:65-82.

Frankel, G.S., 2012. Letters to the Editor, Galvanic Corrosion Article Draws Comment. *Journal AWWA* 104:12:8-11.

Frankel, G. S. and D. Landolt, 2007. Kinetics of Electolytic Corrosion Reactions. *Encyclopedia of Electochemistry*, Wiley-VCH Verlag GmbH & Co. KGaA.

Giammar, D. E., G. J. Welter and A. Cantor, 2012. Review of Previous Water Research Foundation Projects on Galvanic Corrosion. Accessed online July 2012 at http://www.waterrf.org/ProjectsReports/ProjectPapers/Lists/PublicProjectPapers/Attachments/3/4349_LiteratureReview.pdf.

Hack, H. P. and W. L. Wheatfall, 1995. Evaluation of Galvanic and Stray Curent Corrosion in 70/30 Copper-Nickel/Alloy 625 Piping Systems (CARDIVNSWC-TR-61-94/15).

Hu, J., F. Gan, S. Triantafyllidou, C. K. Nguyen and M. Edwards, 2012. Copper-Induced Metal Release from Lead Pipe into Drinking Water. *Corrosion* 68:11:1037-1048.

Jensen, J. A, 1918. Lead Pipe Couplings. *Journal AWWA* 5:4:407-411.

Lennox, T. J. and M. H. Peterson, 1971. Potential and pH Relationships in Cathodically Polarized Metal Crevices. Localized Corrosion, Williamsburg, VA.

Nguyen, C. K., K. R. Stone, A. Dudi and M. A. Edwards, 2010. Corrosive Microenvironments at Lead Solder Surfaces Arising from Galvanic Corrosion with Copper Pipe. *Environmental Science & Technology* 44:18:7076-7081.

Nguyen, C. K., B. N. Clark, K. R. Stone, and M. A. Edwards, 2011. Acceleration of Galvanic Lead Solder Corrosion Due to Phosphate. *Corrosion Science* 53:1515-1521.

Rosenfeld, I. L., 1971. Crevice Corrosion of Metals and Alloys. Localized Corrosion, Williamsburg, VA.

Salamat, G., G. A. Juhl and R. G. Kelly, 1995. Mechanism of Dissimilar Metal Crevice Corrosion of Superferritic Stainless Steels. *Corrosion* 51:11:826-836.

Sarver, E., M. Edwards and Y. Zhang, 2011. Revisiting Dezincification Performance Testing for Brass Plumbing Devices. *Materials Performance* 50:5:70-75.

St. Clair, J., C. Stamopoulos and M. Edwards, 2012. Increased Distance Between Galvanic Pb:Cu Pipe Connections Decreases Lead Release. *Corrosion* 68:9:779-783.

Standard Methods for the Examination of Water and Wastewater, 1998 (20th ed.) APHA, AWWA, WEF, Washington.

Triantafyllidou, S. and M. Edwards, 2011. Galvanic Corrosion After Simulated Small-Scale Partial Lead Service Line Replacements. *Journal AWWA* 103:9:85-99.

United States Environmental Protection Agency, 2011. SAB Evaluation of the Effectiveness of Partial Lead Service Line Replacements (EPA-SAB-11-015).

Wang, Y., J. He, V. Mehta, G. J. Welter and D.E. Giammar, 2012. Impact of galvanic corrosion on lead release from aged lead service lines, *Water Research* 46:5049-5060.

Zhang, Y. and M. Edwards, 2011. Brass Zn Content and its Influence on Lead Leaching. *Journal AWWA* 103:7.

CHAPTER 2. PROFILE SAMPLING TO CHARACTERIZE PARTICULATE LEAD RISKS IN POTABLE WATER

Brandi Clark[a], Sheldon Masters[a], and Marc Edwards[a]

[a]Virginia Polytechnic Institute and State University, Blacksburg, Va.

ABSTRACT

Traditional lead (Pb) profiling, or collecting sequential liters of water that flow from a consumer tap after a stagnation event, has recently received widespread use in understanding sources of Pb in drinking water and risks to consumer health, but has limitations in quantifying particulate Pb risks. A new profiling protocol was developed in which a series of traditional profiles are collected from the same tap at escalating flow rates. The results revealed marked differences in risks of Pb exposure from one consumer home to another as a function of flow rate, with homes grouped into four risk categories with differing flushing requirements and public education to protect consumers. On average, Pb concentrations detected in water at high flow without stagnation were at least three to four times higher than in first draw samples collected at low flow with stagnation, demonstrating a new "worst case" lead release scenario, contrary to the original regulatory assumption that stagnant, first draw samples contain the highest lead concentrations. Testing also revealed that in some cases water samples with visible particulates had much higher Pb than samples without visible particulates, and tests of different sample handling protocols confirmed that some EPA-allowed methods would not quantify as much as 99.9% of the Pb actually present (avg. 27% of Pb not quantified).

KEYWORDS: Drinking Water**,** Flow Rate**,** Corrosion Control**,** Sampling Protocol

INTRODUCTION

As the United States strives to reduce levels of elevated blood lead (Pb) in children,[1] accurate quantification of Pb risks from potable water taps in individual homes will become of greater concern.[2, 3] Recent studies have identified significant increases in blood Pb for children[4, 5] and young women[6] at water lead exposure levels that are common at many homes in older cities with Pb-bearing plumbing. Recent analyses of Pb exposure in U.S. schools,[7] Washington, DC,[8] and Germany[6] have confirmed expectations that public health interventions such as filters, flushing, and use of alternative water sources can markedly reduce blood Pb levels and even incidence of fetal death due to water Pb exposure.

Regulatory Limitations. Pb in drinking water is regulated by the U.S. Environmental Protection Agency (US EPA) under the Lead and Copper Rule (LCR). The LCR sets a Pb action level (AL) of 15 ppb in first draw samples collected from consumer taps after 6 hours of stagnation.[9] If the 90th percentile Pb concentration in these samples exceeds the 15 ppb AL, then the rule requires the utility to take measures that can include adding treatment to control plumbing corrosion, adding source water treatment, replacing lead service lines, and implementing consumer education on avoiding water lead risks.[9] Research by EPA scientists and others has confirmed that existing EPA sampling methods and analysis protocols can sometimes substantially underestimate Pb in drinking water, especially if Pb is present in particulate form or if Pb service lines are present.[2, 3, 10-12] The extent to which established EPA-approved analysis protocols can miss particulate Pb was recently verified,[10, 13] in that for some worst-case samples as much as 81% of the Pb was missed using the standard EPA sample handling methods, which involve acidification to pH 2 for 16 hours before removing an aliquot for analysis.[10] Furthermore, up to 98% of the Pb was missed if samples were not thoroughly mixed upon acidification, which is not explicitly required by some methods that are accepted by EPA for analysis.[10]

The LCR was also intended to provide a system-wide, community-based reduction in water Pb exposure, and it is acknowledged that it does not control or account for harmful exposures at individual taps.[14] Dependent on factors such as plumbing material, water use patterns, prior disturbances, and galvanic corrosion, Pb levels in individual homes can vary by two orders of magnitude or even more.[7, 8, 12, 15, 16] As public health programs begin to more carefully scrutinize individual cases of Pb poisoning and Pb exposure, it is important to identify and assess Pb in water risks at individual taps.[4, 7]

Traditional Pb Profiling. A tool that has recently been used to assess risks at individual taps is Pb profiling, or collecting a series of samples of Pb in water as it flows from the tap to ensure that water in contact with all types of Pb-bearing plumbing is sampled.[12, 15-19] Typical profiling produces graphs of Pb concentration versus either flushing time or flushing volume.[12, 16-20] Compared to collection of a standard EPA single "first-draw" sample, this method has the advantage of providing more detailed information about the sources of Pb present in the home's water supply and can often detect Pb hazards from the service line that first draw sampling can completely miss.[12, 15, 18, 19] Profiles have also been used to better estimate the required flushing time for consumers to protect public health[15, 17] and to identify homes with high risk lead service lines for additional scrutiny and public health protection.[21] However, many of these profiles

have been collected at a very low flow rate of less than 2 liters per minute,[2, 17, 18, 22] while other studies did not report the flow rate.[19]

Importance of Flow Rate to Pb-in-Water Risks. Several studies have investigated the link between higher flow rate and mobilization of Pb particulates to drinking water.[20, 22-25] If there is a reservoir of non-adherent particulate Pb on plumbing surfaces that is relatively easy to mobilize via hydraulic scour, much more Pb can be released at higher flow rate.[2, 22-24] However, if non-adherent particulate Pb reservoirs are absent within the pipe, higher flow rates during sampling will tend to have no effect or would even decrease soluble Pb concentrations due to dilution. This can explain why Britton reported that the concentration of Pb as a function of flow rate is minimized at intermediate flow rates in some systems.[20] Conceptually, using lower flow rates during sampling will either have no effect on or increase the concentration of soluble Pb dissolved from Pb-bearing plumbing into the water,[25] whereas lower flow rates minimize mobilization of particulate Pb.[20, 22-24] The release of total Pb (the sum of soluble Pb and particulate Pb) at various flow rates is highly dependent on the water chemistry, types and durability of Pb deposits, Pb solubility and dissolution rates, and specifics of the premise plumbing system, including pipe materials and pipe diameters.[23, 24] Flow rates at individual taps also vary according to design and consumer behaviors, which in turn can profoundly affect the concentration of Pb detected or the risk of consumer exposure.[2, 23] Thus, the tap flow rate during water sampling or consumer use represents an important dimension in assessing both the effectiveness of corrosion control programs across a system and public health risks in individual homes. After the link between flow rate and particulate lead release was discovered,[26] recent work adopted a high flow rate profiling approach, which was used to reveal significant problems with elevated lead in Chicago.[12]

An Updated Profiling Method. To quantify the release of Pb to drinking water as an explicit function of flow rate, a new Pb profiling method was conceptualized and tested. By collecting a conventional Pb profile at very low flow rate after a long stagnation event, and immediately thereafter collecting additional profiles at moderate and then high flow rates, risks from particulate Pb release can be explicitly quantified with appropriate analytical methods.[10, 11, 13] The importance of particulate release mechanisms has been highlighted in several recent studies, which linked spikes in particulate Pb release to water to physical pipe disturbances,[8, 12] galvanic corrosion,[27] and instances of childhood Pb poisoning from tap water.[11] Compared to traditional profiling conducted at low flow rates not representative of normal consumer use, this profiling approach can better quantify Pb exposures during a range of home water use scenarios, and results can be used to both provide improved public health advice to consumers and directly evaluate effectiveness of corrosion control for particulate Pb. The approach would also have potential to characterize health hazards from other inorganic contaminants in tap water such as arsenic[28, 29] and radionuclides,[30-32] which can be concentrated in pipe scale.

MATERIALS AND METHODS

Site Selection. Samples were collected in the summer of 2011 in two cities, Washington, DC and Providence, RI. These cities were selected due to a recent history of lead action level exceedence and partial lead service line replacement. Washington, DC exceeded the lead action

level after switching from chlorine to chloramine disinfectant in 2001[15] and now controls lead release by dosing an orthophosphate corrosion inhibitor.[27] Providence, RI exceeded the lead action level in 2006 after changing pH from 10.3 to 9.7, and has since reversed the pH change.[33] Detailed recent water quality information for both cities has been recently reported elsewhere.[27,34] At the time of sampling, Providence had not yet adjusted pH back to 10.3, and corrosion control was not optimized; in Washington, DC, traditional optimized corrosion control practices (orthophosphate) were already in place at the time of sampling. Individual homes were selected on a volunteer basis from a pool of homes with known or suspected lead service lines. Twelve sites were selected each city, and a breakdown of the sites into "full lead service line," "partial lead service line," or "unknown" is given in the Supporting Information (Table A-1). Due to inadequate representation of partial lead service lines in Washington, DC and full lead services lines in Providence, RI, a comparison of lead release from full versus partial lead service lines was not possible.

Flow Rate Selection. Flow rates were primarily selected to compare different consumer exposure scenarios. The low flow rate represents traditional profile sampling at 1 L/min, the medium flow rate represents the highest flow rate achieved during typical consumer use (kitchen tap fully open), and the high flow rate represents the worst-case scenario of the maximum achievable flow rate at the tap without an aerator. The latter flow rate is similar to that expected from some non-drinking-water taps such as Roman bath spouts and laundry room faucets. Differences in achievable flow rates at a given tap are responsible for the wide range of flow rates for the medium and high flow categories (Figure 2-1); flow rates used for sampling at each site are summarized in the Supporting Information (Table A-1). These different flow rates also have mechanistic significance in terms of a transition between laminar and turbulent flow. Although precise Reynolds numbers (Re) at each site cannot be calculated due to lack of pipe diameter information, the low flow sample is expected to be in the laminar region (Re = 994 for a ¾" service line).[35] On the other hand, flow in a ¾" service line can be expected to become turbulent (Re > 4000)[35] once the flow rate exceeds 4 L/min, which was exceeded at all sites for the high flow sample and at all but one site for the medium flow sample.

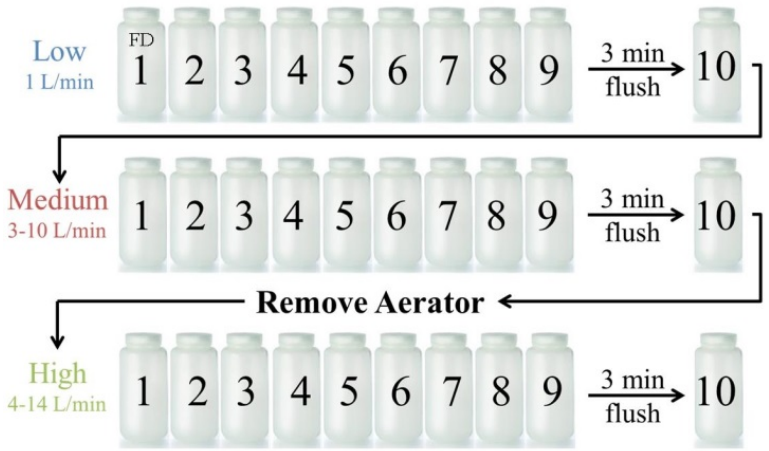

Figure 2-1. Illustration of the sequential sampling protocol used in each home. One-liter water samples are collected in the sequence shown at low, medium, and high flow rates after at least 6 hours of stagnation. The first liter of the low flow profile represents the first draw (FD) after stagnation.

Sample Collection. Profiles of Pb concentration in water were collected using new, wide-mouth, one-liter HDPE bottles (Fisher Scientific). Three sequential profiles were collected after a minimum of six hours stagnation in each home (Figure 2-1). For the first profile, nine sequential liters of water were collected at a low flow rate of approximately 1 L/min. The tap was then allowed to run at the same low flow rate for 3 minutes before collecting a tenth one-liter sample. Without allowing additional stagnation time, the tap was then fully opened (3-10 L/min) and the second profile, reported here as "medium flow," was collected in the same manner. The faucet aerator was then removed, and two one-liter samples were collected at a low (1 L/min) flow rate with 3 minutes of flushing between the first and second sample. These samples represent particles released due to aerator removal, and in some cases contain very high (more than 10 mg/L) lead levels as a result. The lead concentration in each of these samples is available in Table A-2 in the Supporting Information. These samples are not included in this analysis because they do not reflect lead levels resulting from normal water use patterns. For the final profile, reported here as "high flow," the tap was fully opened with the aerator off (4-14 L/min) and 10 liters were collected in the same way as for the first two profiles. An aliquot from liters 3 and 5 from each of the three profiles (Figure 2-1) was filtered in the field through a 0.45 μm nylon syringe filter (Whatman). These samples were selected for filtering because the 3rd to 5th liters of a profile often contain the water (and soluble or particulate Pb) derived from service lines,[21] either by dissolution during stagnation or via particulate detachment caused by abrupt changes in flow.

Sample Analysis. This part of the study explored whether observations from previous work regarding the limitations of EPA-approved methods[10] hold true for field samples designed to capture particulate Pb risks.

General Sample Analysis. Before analysis, samples were screened by eye for visible particles (Figure A-1). Samples without visible particles, including all field-filtered aliquots, were acidified in the sampling container to 1% nitric acid (trace metal grade, Fisher Scientific) by volume. An aliquot was removed from each sample and adjusted to 2% nitric acid by volume for analysis a minimum of 30 hours after acidification. For samples containing visible particles, most samples were acidified in the sampling container to 2% nitric acid by volume immediately after particulate screening. An aliquot was removed from each sample for analysis a minimum of 48 hours after acidification.

Detailed Sample Analysis. A subset of the samples with visible particulates was subjected to a more detailed sequential sample preparation procedure (Figure A-2). Only samples with accompanying field-filtered aliquots were chosen for this detailed analysis. Five samples were collected with increasingly rigorous sample handling methods to detect particulate Pb. The first and second samples were taken directly from the un-acidified bottle without and with shaking, respectively, as 20 mL aliquots. These aliquots were then acidified with 2% nitric acid by volume for 48 hours before analysis. After taking Samples 1 and 2, the original sampling container was acidified to pH <2 with nitric acid. After 16 hours, Samples 3 and 4 were taken without and with shaking, respectively. These aliquots were also adjusted to 2% nitric acid by volume for analysis. After taking the third and fourth sample, the original sampling container was adjusted to 2% nitric acid by volume. The fifth and final sample was taken 48 hours after acidification with shaking and is deemed representative of "total Pb" herein, even though other

research has indicated that, in rare instances, hydrochloric acid, heat, and/or days of digestion can be required to dissolve all Pb present in drinking water.[11, 13] All samples were analyzed for total metals by inductively coupled plasma – mass spectrometry (ICP-MS; Thermo Scientific Thermo Electric X Series) using Standard Method 3125B.[36]

RESULTS AND DISCUSSION

Pb Profiling and Consumer Risk. The concentration of Pb in water from a consumer tap as a function of time and flow rate as measured using the new profiling method (Figure 2-1) was variable and site-specific. However, homes could be grouped into four general categories of behavior, which also fit into current conceptualizations of behavior based on effectiveness of corrosion control as measured by levels of soluble lead in each system (Figure 2-2). Traditional corrosion control is based on lead solubility, and can include changes in alkalinity or pH or the addition of orthophosphate to form insoluble lead phosphate scales.[37] As we gain appreciation for the important role of particulate lead as a key route of exposure in modern premise plumbing systems, the concept of "corrosion control" must be expanded to explicitly consider aspects of scale durability and adherence as well as lead solubility. Ultimately, it is likely that particular mineralogies and co-factors such as iron and manganese will play critical roles in creating reservoirs of non-adherent lead as has been suggested in prior research.[11,27,33,37-40]

In the first group of homes (Case A), the Pb concentration remained low in all samples at all flow rates (Figure 2-2, part A). For the example profile shown, Pb was less than 2 ppb in all samples. This type of Pb profile is expected in homes in which traditional corrosion control is optimized, leading to low soluble Pb, and also for which pipe scales are durable and adherent, leading to a low incidence of particulate Pb release. At these taps, the risk of Pb exposure was low regardless of flow rate.

In a second group of homes (Case B), the Pb concentration at low flow rate increased over the first few liters, reached a maximum value when collecting water that had been sitting in the Pb service line, and then decreased (Figure 2-2, part B). For these homes, the resulting profile was consistent with conventional wisdom that the highest risk from soluble lead derives from the water sitting in the lead service line.[12, 17, 18] In the example shown, the Pb concentration reaches a maximum value of nearly 100 ppb in the fourth liter, which is the water contacting the lead service line, but is reduced to 15 ppb by the sixth liter as the water in the service line mixes with water from the main. At taps with a Pb release pattern dominated by soluble lead, very little additional Pb was released when the flow rate was increased to moderate and high flow rates without additional stagnation. This type of release is expected to occur when soluble Pb dominates (non-optimized traditional corrosion control) and there are few reservoirs of detachable particulate Pb on plumbing surfaces (durable scale).[25]

In the third group of homes (Case C), profiles collected at low flow showed very little Pb release, as in Case A; however, increases in flow rate caused spikes in Pb concentration due to particulate Pb detachment. In an exemplary profile (Figure 2-2, part C), the Pb concentration is less than 3 ppb for all samples collected at both low and medium flow rates, but spikes as high as 35 ppb were present at the highest flow rate. This release pattern is representative of a case in which

traditional corrosion control is optimized, resulting in low soluble Pb concentrations, but the scales present on the lead-bearing plumbing are not durable, resulting in erratic release of particulate Pb. If this home had been sampled using LCR methods or even a traditional lead profile, consumption of water in this home would have been erroneously classified as presenting little or no risk to consumers, when, in fact, a relatively high risk of particulate Pb exposure risk exists.

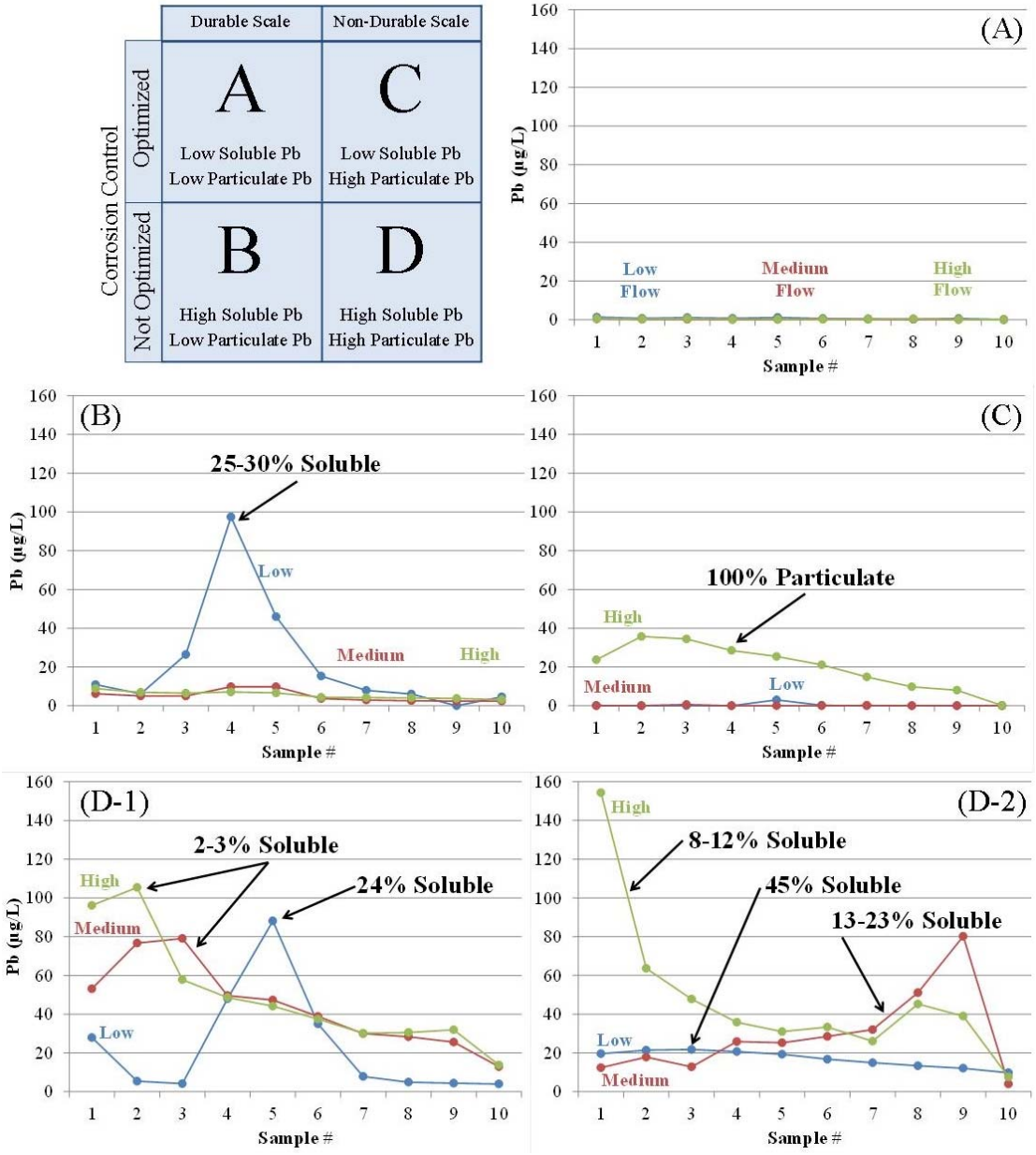

Figure 2-2. Upper left indicates four theoretical lead (Pb) release patterns and representative lead profiles based on patterns of release for (A) Washington, D.C. (Site 24); (B) Providence (Site 9); (C) Washington, D.C. (Site 4); (D-1) Providence (Site 16); (D-2) Providence (Site 12). "Soluble Pb" is defined as the Pb measured in the field-filtered aliquot taken from the 3rd and 5th liter in each profile, and is given as a percentage of the total lead measured in the sample.

In the fourth and final group of homes (Case D), high soluble Pb concentrations were observed as in Case B; however, particulate Pb spikes at higher flow rates also occurred that were equal to or worse than the peak Pb concentration from the service line after long stagnation (Figure 2-2, parts D-1 & D-2). These homes represent the worst case for exposure, since traditional corrosion control for soluble lead is not optimized and non-durable scales are present, resulting in release of high levels of both soluble and particulate Pb. In one of these homes (Case D-1; Figure 2-2, part D-1), the Pb profile at low flow was similar to the Case B profile (Figure 2-2, part B), but when flow was increased, particulate Pb was released at high levels: up to 79 ppb at moderate flow and up to 105 ppb at high flow. In total, 17 minutes of cumulative flushing (12.5 min low flow; 4.6 min high flow) were required before Pb dropped below 15 ppb at a moderate flow rate. When the flow rate was increased, an additional 11 minutes of flushing were required to reach 15 ppb again. This demonstrates that in homes of this type, routine advice to flush lines for 30 seconds to 2 minutes is not adequately protective of public health. As with Case C, if this home had been sampled using typical Pb profiling, the markedly different health risk to consumers in homes corresponding to Case B and Case D-1 would not be distinguishable. In some Case D homes, particulate Pb release was less predictable. For one home (Case D-2; Figure 2-2, part D-2), the Pb concentration was only slightly elevated at low flow, but higher flows were typified with two relatively large spikes of 80 ppb and 154 ppb. It is believed that this type of behavior is caused by sporadic release of larger Pb particulates. As a rule the Pb levels did not systematically decrease with increased flushing time in Case D-2 situations.

Public health advice for consumers could be tailored dependent on which of these four categories a given home falls into (Table 2-1). This case-specific advice may be especially important in homes with particulate Pb contamination, which in some cases can increase with flushing and is relatively unaffected by stagnation time,[41] contrary to conventional wisdom and current consumer guidance based on soluble Pb release. Case A has low Pb regardless of flow rate or flushing time, while Case B can be considered dominated by soluble Pb and risks are expected to be mitigated after standard EPA advice to flush Pb service lines for 30 seconds to 2 minutes. However, problems associated with Cases C and D are dominated by particulate Pb, and in such situations consumers should probably use filters certified to remove Pb because risks cannot be adequately mitigated by realistic flushing times.

Table 2-1. Potential public health advice for individual homes in each category represented in Figure 2-2, part A.

Case	Potential Flushing Advice
A	No special precautions needed.
B	Flush tap at high flow rate for 30 sec – 2 min before using water for cooking or drinking.
C, D	Flush tap at high flow rate for AT LEAST 10 min before using water for cooking or drinking*

*Flushing time is likely unrealistic, and use of filters certified to remove Pb particles is recommended as an alternative.

Sampling the Worst Case. Another goal of this work was to illustrate the extent to which sampling conditions could detect worst-case exposure. To do this, samples were separated into

categories as follows: Case A = no samples above 15 ppb; Case B = at least one sample above 15 ppb at low flow, but no samples above 15 ppb at high flow; Case C = no samples above 15 ppb at low flow, but at least one sample above 15 ppb at medium or high flow; Case D = at least one sample at low flow and one sample at medium or high flow is above 15 ppb. Using these criteria produced a fairly even split, assigning 8 homes to Case A, 5 homes to Case B, 6 homes to Case C, and 5 homes to Case D. Boxplots for each category at each flow rate (Figure 2-3) demonstrate that C and D homes have greater variability in lead release, especially at high flow rates, which is expected based on the sporadic nature of particulate lead release. To determine the worst case, 90th percentile values for each category and flow rate were compared (Figure 2-3; Table A-3). As might be expected, the flow rate required to sample the "worst case" Pb concentration was dependent on the Pb release category. For the best and worst homes (Cases A and D), the first draw sample contained the highest 90th percentile Pb concentration, and the EPA LCR sampling protocol generally detected the risks to public health. For Case B, the highest Pb concentrations were observed at low flow, but not in the first draw sample, consistent with expectations based on a traditional profiling approach.[12] For Case C, the highest Pb concentration was observed at the highest flow rate, reflecting a particulate Pb hazard.

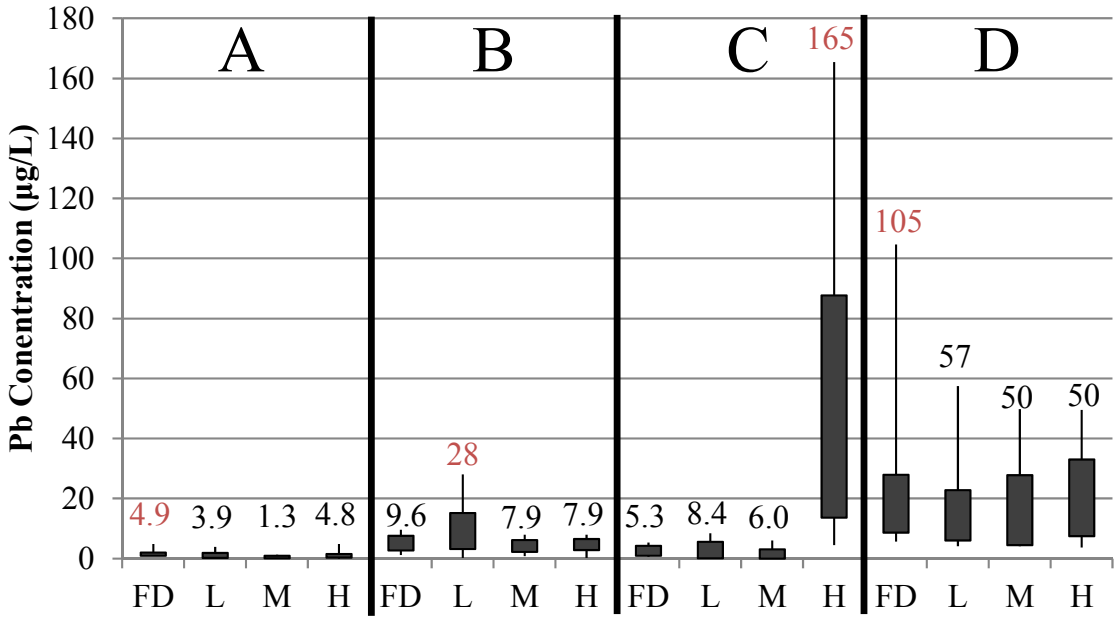

Figure 2-3. Box plot showing the lead concentrations for first draw (FD), low flow (L), medium flow (M), and high flow (H) samples for lead release categories A-D. The top and bottom of the box represent the 75th and 25th percentiles, respectively. The top and bottom whiskers represent the 90th and 10th percentiles, respectively. 90th percentile values are shown on the chart, with the highest value for each lead release category shown in red.

When all sites are considered together, samples collected at the highest flow rate had a 90th percentile value more than 4X higher than the first draw and 3.5X higher than samples collected by typical profiling at low flow rate (Table A-3). Since the samples collected at the highest flow rate had been previously flushed for a cumulative 20 minutes at low and moderate flow rates and had no stagnation time, whereas samples collected at low flow rates had a minimum of 6 hours stagnation, it is clear that flow rate can have a much greater impact on compliance with the EPA

90th percentile action level of 15 ppb than stagnation time in the systems studied herein. This confirms a previous research report that noted compliance with EPA standards can be "all in the wrist," and recommended LCR sampling rates of less than 1 L/min in order to meet EPA standards.42 The obvious downside of this approach is that the actual lead in water when it is consumed can be much higher than when it is sampled, and the public would not be alerted to the true health risk that is present or instructed as to how to avoid it. Worst case sampling protocols designed to detect the health risk would require sampling of first draw after stagnation at a realistic (moderate to high) flow rate and also collection of a second draw sample that is representative of soluble and particulate lead from the service line. If a single profile is used to determine health risks and/or provide flushing advice, samples should be collected at flow rates consistent with the highest flow rate realistically expected to be used by consumers.

Analytical Method and Pb Recovery. Field samples from this profiling study were also used to determine the extent to which Pb concentrations may be underestimated by some accepted sample handling methods and acidification procedures.[10, 13]

Trends in Visible Particle Release. In the first part of this analysis, the idea that samples with high Pb could be identified visually, contrary to conventional wisdom and regulatory assumptions[43] derived from experiences with dissolved lead, was investigated. Samples with visible particles identified before sample preparation and analysis had higher Pb concentrations, on average, than those without visible particles (Table 2-2). In Washington, D.C., this difference was large and statistically significant (two-sided t-test, $p = 0.0045$), with samples containing visible particulates having nearly 15X higher Pb on average when compared to samples without visible particles. However, both in Providence samples and another recent study in Chicago,[12] there were no significant differences in Pb concentration for samples with and without visible particles. One possible reason for this finding in Providence is a large number of non-lead particles due to a substantial iron corrosion problem at the time of sampling.[33] Similarly, in Chicago, some sampling took place during the fire department's annual valve exercising activity, resulting in high levels of non-lead particulates.[12]

Table 2-2. Summary of the lead concentration and number of samples (N) with and without visible particles. Concentrations are reported for the most rigorous digestion method used in each case (1% nitric acid without visible particles, 2% nitric acid with visible particles). On average, the lead concentration is nearly 4X higher when particles are visible.

		N	Average (ppb)	Median (ppb)	Range (ppb)
Washington, DC	WITH Visible Particles	182	32.3	3.2	ND – 1801
	NO Visible Particles	158	2.2	1.2	ND – 12.7
Providence, RI	WITH Visible Particles	255	13.5	5.0	ND – 155.8
	NO Visible Particles	105	10.9	4.3	ND – 110.1

The number of samples collected in this study with visible particles was large, with over two-thirds of all samples collected containing visible particles. Of these samples, approximately 40% were collected at high flow, 35% at medium flow, and 25% at low flow. Although no direct isolation and characterization of particles was undertaken during this study, some further information about the type of particles released can be gained by examining the concentrations of non-lead elements in each sample (Tables A-4, A-5). For example, in Providence, lead was often found to be correlated with iron, a trend which was further explored with follow-up sampling and reported elsewhere.[33] In Washington, DC, lead particles were sometimes associated with phosphate, implying that lead phosphate solids were released, but at other times associated with tin or zinc, implying that brass or solder sources existed within the home.

Effect of Digestion Procedure. When samples were subjected to the more detailed sequential analysis, the standard EPA method gave similar results, on average, to the 2% acid digestion (Figure 2-4). However, if these samples were not shaken, 0-99.9% (27% average) of the Pb was missed. If samples are not digested in the original bottle, as occurs in some customer service sampling by utilities,[10] very large errors in quantification can occur. In this study, digesting samples outside of the original bottle missed 0-100% (88% average) and 0-100% (32% average) of the Pb without and with shaking before aliquot removal, respectively.

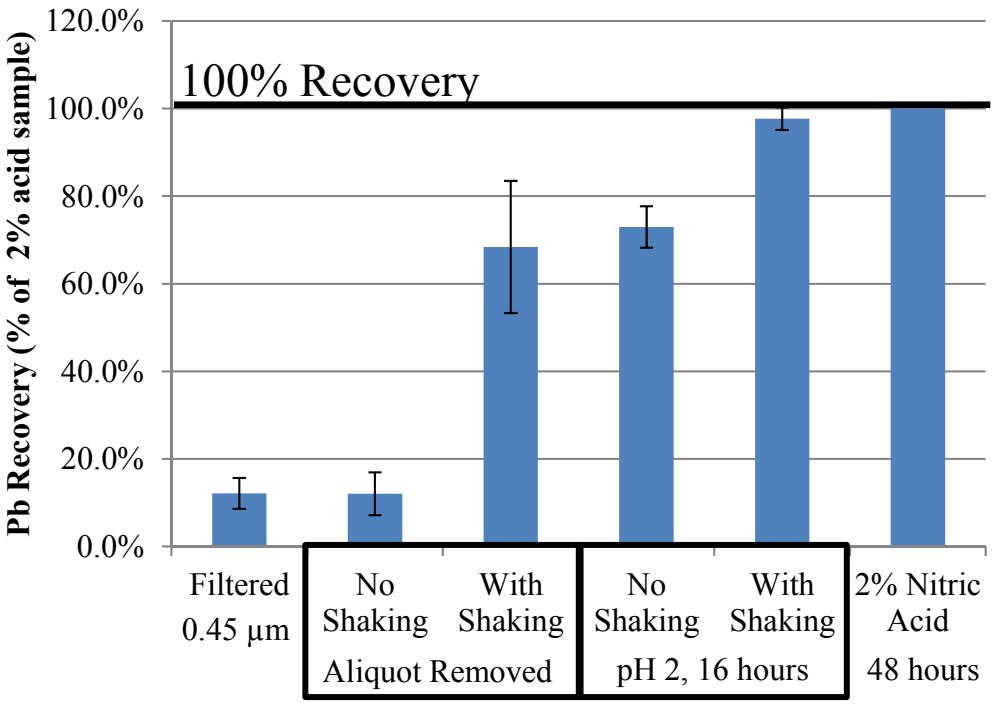

Figure 2-4. Plot of average lead recovery for each analytical procedure, calculated by dividing the concentration in the aliquots for each digestion procedure by the concentration of the most rigorously digested sample (2% nitric acid for 48 hours). Error bars represent 95% confidence. Moving from left to right on the chart, the digestion procedure becomes more rigorous and the average lead recovery increases. A total of N=88 particulate-containing samples were used for this analysis; at least one sample from each of the 24 sites was used.

Regulatory Implications. As the EPA continues to consider changes to be made in the Long-Term Revisions to the LCR, revising site selection and sampling protocols will be a key consideration.[44] This work demonstrates that Pb release/exposure can be a strong function of sample flow rate and site selection. In some cases, sampling at flow rates typical during normal use ("medium" flow) detected lead levels 4X higher than in a low flow first draw sample, even without any stagnation time. In general, medium flow samples gave 60% of the average and 40% of the peak lead concentrations determined at low flow, demonstrating that flow rate is almost as important as stagnation in detecting worst-case consumer exposures. Furthermore, samples collected at realistic flow rates in homes believed to have lead service lines, which would be considered "worst case" sites under the current site selection criteria, ranged from non-detect to 180 ppb, demonstrating that the true "worst case" is not simply a function of service line material and is probably related to total water use, presence of disturbed service lines, longer service lines, particulate iron, and other factors.[12,21-22,33,40,45]

ACKNOWLEDGEMENTS

The authors acknowledge the financial support of the National Science Foundation under NSF CBET-0933246 and the Graduate Research Fellowship Program (GRFP). The authors would also like to acknowledge the financial support of the Sussman Foundation and the Robert Wood Johnson Foundation (RWJF) under the Public Health Law Research program. Opinions and findings expressed herein are those of the authors and do not necessarily reflect the views of the NSF, RWJF, or Sussman Foundation. The authors would further like to thank Amanda Martin and Navarre Bartz for their assistance with in-home sampling, the homeowners who volunteered to participate in this study, and DC Water for assistance with site selection.

SUPPORTING INFORMATION AVAILABLE

Supporting information for this study is available in Appendix A, including site-specific information, concentrations of non-lead elements, and illustrations for sampling protocols.

REFERENCES

1. U.S. Department of Health and Human Services. *Healthy People 2020 Summary of Objectives*. [cited Sept 3, 2012; Available from: http://healthypeople.gov/2020/topicsobjectives2020/pdfs/EnvironmentalHealth.pdf.
2. Triantafyllidou, S. and Edwards, M. Lead (Pb) in Tap Water and in Blood: Implications for Lead Exposure in the United States. *Critical Reviews in Environmental Science and Technology*. **2011**, *42* (13), p. 1297-1352.
3. Brown, M.J. and Margolis, S. Lead in Drinking Water and Human Blood Lead Levels in the United States. *Morbidity and Mortality Weekly Report (MMWR) Supplements*. **2012**, *61* (4).

4. Triantafyllidou, S.; Gallagher, D.; Edwards, M. Assessing risk with increasingly stringent public health goals: the case of water lead and blood lead in children. *Journal of Water and Health*. **2013**, *In Press*.
5. Deshommes, E.; Prévost, M.; Levallois, P.; Lemieux, F.; Nour, S. Application of lead monitoring results to predict 0–7 year old children's exposure at the tap. *Water Research*. **2013**, *47* (7), p. 2409-2420.
6. Fertmann, R.; Hentschel, S.; Dengler, D.; Janßen, U.; Lommel, A. Lead exposure by drinking water: an epidemiologial study in Hamburg, Germany. *International Journal of Hygiene and Environmental Health*. **2004**, *207* (3), p. 235-244.
7. Triantafyllidou, S.; Le, T.; Gallagher, D.; Edwards, M. Reduced risk estimations after remediation of lead (Pb) in drinking water at two US school districts. *Science of The Total Environment*. **2014**, *466–467* (0), p. 1011-1021.
8. Edwards, M. Fetal Death and Reduced Birth Rates Associated with Exposure to Lead-Contaminated Drinking Water. *Environmental Science & Technology*. **2013**, *48* (1), p. 739-746.
9. United States Environmental Protection Agency. Maximum Contaminant Level Goals and National Primary Drinking Water Regulations for Lead and Copper. *Federal Register*. **1991**, *56* (110), p. 26460-26564.
10. Triantafyllidou, S.; Nguyen, C.; Zhang, Y.; Edwards, M. Lead (Pb) quantification in potable water samples: implications for regulatory compliance and assessment of human exposure. *Environmental Monitoring and Assessment*. **2012**, p. 1-11.
11. Triantafyllidou, S.; Parks, J.; Edwards, M. Lead Particles in Potable Water. *Journal AWWA*. **2007**, *99* (6), p. 107-117.
12. Del Toral, M.A.; Porter, A.; Schock, M.R. Detection and Evaluation of Elevated Lead Release from Service Lines: A Field Study. *Environmental Science & Technology*. **2013**, *47* (16), p. 9300-9307.
13. Haas, C.; Koch, L.; Kelty, K.; Triantafyllidou, S.; Lytle, D., *Effectiveness of the Preservation Protocol within EPA Method 200.8 for Soluble and Particulate Lead Recovery in Drinking Water (EPA/600/R-13/222)*, U.S. Environmental Protection Agency, Editor, 2013
14. United States Environmental Protection Agency. *Is There Lead in my Drinking Water? (EPA 816-F-05-001)*. 2005 [cited 2014 Feb 28]; Available from: http://water.epa.gov/drink/info/lead/leadfactsheet.cfm.
15. Edwards, M. and Dudi, A. Role of Chlorine and Chloramine in Corrosion of Lead-Bearing Plumbing Materials. *Journal AWWA*. **2004**, *96* (10), p. 69-81.
16. Cartier, C.; Nour, S.; Richer, B.; Deshommes, E.; Prévost, M. Impact of water treatment on the contribution of faucets to dissolved and particulate lead release at the tap. *Water Research*. **2012**, *46* (16), p. 5205-5216.
17. Giani, R.; Edwards, M.; Chung, C.; Wujek, J., *Use of Lead Profiles to Determine Source of Action Level Exceedences from Residential Homes in Washington, D.C.*, presented at *Water Quality Technology Conference*: San Antonio, TX, 2004
18. HDR Engineering Inc., *An Analysis of the Correlation Between Lead Released from Galvanized Iron Piping and the Contents of Lead in Drinking Water*. HDR Engineering Inc.: Bellevue, WA, 2009

19. Sandvig, A.; Maynard, B.; Mast, D.; Trussel, R.R.; Trussel, S.; Cantor, A.; Prescott, A., *Contribution of Service Line and Plumbing Fixtures to Lead and Copper Rule Compliance Issues*. American Water Works Association Research Foundation: Denver, CO, 2008
20. Britton, A. and Richards, W.N. Factors Influencing Plumbosolvency in Scotland. *J. Inst. Water Eng. Scient.* **1981**, *35*, p. 349-364.
21. Cartier, C.; Bannier, A.; Pirog, M.; Nour, S.; Prévost, M. A rapid method for lead service line detection. *Journal: American Water Works Association*. **2012**, *104* (11), p. E596-E607.
22. Cartier, C.; Arnold Jr, R.B.; Triantafyllidou, S.; Prévost, M.; Edwards, M. Effect of Flow Rate and Lead/Copper Pipe Sequence on Lead Release from Service Lines. *Water Research*. **2012**, *46* (13), p. 4142-4152.
23. Schock, M.R. Causes of temporal variability of lead in domestic plumbing systems. *Environmental Monitoring and Assessment*. **1990**, *15* (1), p. 59-82.
24. Deshommes, E.; Laroche, L.; Nour, S.; Cartier, C.; Prévost, M. Source and occurrence of particulate lead in tap water. *Water Research*. **2010**, *44* (12), p. 3734-3744.
25. Cardew, P.T. Development of a convective diffusion model for lead pipe rigs operating in laminar flow. *Water Research*. **2006**, *40* (11), p. 2190-2200.
26. Clark, B.; Masters, S.; Edwards M. *3-D Lead Profiling Detects Particulate Lead-in-Water Risks as a Function of Flow Rate,* presented at Water Quality Technology Conference: Toronto, ON, 2012.
27. Wang, Y.; Mehta, V.; Welter, G.J.; Giammar, D.E. Effect of connection methods on lead release from galvanic corrosion (PDF). *Journal-American Water Works Association*. **2013**, *105* (7), p. E337-E351.
28. Lytle, D.A.; Sorg, T.J.; Frietch, C. Accumulation of Arsenic in Drinking Water Distribution Systems. *Environmental Science & Technology*. **2004**, *38* (20), p. 5365-5372.
29. Lytle, D.A.; Sorg, T.J.; Muhlen, C.; Lili, W. Particulate arsenic release in a drinking water distribution system. *Journal: American Water Works Association*. **2010**, *102* (3), p. 87-98.
30. Schock, M.R.; Hyland, R.N.; Welch, M.M. Occurrence of Contaminant Accumulation in Lead Pipe Scales from Domestic Drinking-Water Distribution Systems. *Environmental Science & Technology*. **2008**, *42* (12), p. 4285-4291.
31. Valentine, R.L. and Stearns, S.W. Radon release from water distribution system deposits. *Environmental Science & Technology*. **1994**, *28* (3), p. 534-537.
32. Lytle, D.A.; Sorg, T.; Wang, L.; Chen, A. The accumulation of radioactive contaminants in drinking water distribution systems. *Water Research*. **2014**, *50* (0), p. 396-407.
33. Masters, S. and Edwards, M. *Holistic Examination of Lead Corrosion Control in Low Alkalinity High pH Water Distributed Though Unlined Iron Mains*, presented at Water Quality Technology Conference: Long Beach, CA, 2013.
34. Wang, Y.; Jing, H.; Mehta, V.; Welter, G.J.; Giammar, D.E. Impact of galvanic corrosion on lead release from aged lead service lines. *Water Research*. **2012**, *46*, p. 5049-5060.
35. Young, D.; Munson, B.; Okiishi, T.; Huebsch, W. *A Brief Introduction to Fluid Mechanics*. 4th ed; John Wiley & Sons: Hoboken, NJ, 2007.
36. APHA. *Standard Methods for the Examination of Water and Wastewater*. 20th ed; APHA, AWWA, WEF, 1998
37. Brown, R.; McTigue, N.; Cornwell, D. Strategies for assessing optimized corrosion control treatment of lead and copper. *Journal AWWA*. **2013**, *105* (5), p. 62-75.
38. Cantor, A.; Denig-Chakroff, D.; Vela, R.; Oleinik, M.; Lynch, D. Use of polyphosphate in corrosion control. *Journal AWWA*. **2000**, *92* (2), p. 95-102.

39. Camara, E., & Gagnon, G. A. *The Relationship between Iron Particles from Water Mains and Lead Release*, presented at AWWA Annual Conference & Exposition, Dallas, TX, 2012.
40. Camara, E.; Montreuil, K.; Knowles, A.; Gagnon, G. Role of the water main in lead service line replacement: A utility case study. *Journal AWWA*. **2013**, *105* (8), p. E423-E431.
41. De Rosa, S. and Williams, S.M., *Particulate Lead in Water Supplies (TMU 9024). Final Report to the Department of the Environment.* Water Research Center: Swindon, England, 1992
42. Reiber, S.; Poulsom, S.; Perry, S.A.L.; Edwards, M.; Patel, S.; Dodrill, D.M. *A General Framework for Corrosion Control Based on Utility Experience*; AWWA Research Foundation and American Water Works Association: Denver, CO, 1997
43. U.S. Environmental Protection Agency, *Long-Term Lead and Copper Rule Revision Public Meeting, October 14-15*, 2008
44. U.S. Environmental Protection Agency, *Lead and Copper Rule.* [cited 2014 May 23]; Available from: http://water.epa.gov/lawsregs/rulesregs/sdwa/lcr.
45. Arnold, R. and Edwards, M. Potential reversal and the effects of flow pattern on galvanic corrosion of lead. *Environmental Science & Technology*, **2012**, *46* (20) p. 10941-10947.

CHAPTER 3. LEAD RELEASE TO DRINKING WATER FROM GALVANIZED STEEL PIPE COATINGS

Brandi Clark[a], Sheldon Masters[a], and Marc Edwards[a]

[a]Virginia Polytechnic Institute and State University, Blacksburg, Va.

ABSTRACT

Problems identified with elevated lead in drinking water associated with galvanized steel pipe were recently hypothesized to result from lead accumulation on galvanized steel pipe surfaces from upstream lead service pipes. However, historical research documents that the grade of zinc typically used for galvanizing contains a minimum of 0.5% lead and can itself be a significant long-term source of lead, which may explain some recent lead contamination problems associated with galvanized steel. Surface analysis of various galvanized steel pipes and fittings installed from 1950-2008 demonstrated that the concentration of lead in the original zinc coating can range from non-detect to nearly 2%, dependent on manufacturer and fitting type. Since cadmium is also present in many zinc coatings, but not in lead pipe, leaded solder, or brass, correlation of zinc concentration to both lead and cadmium concentrations in water was considered as a possible "fingerprint" implicating the coating on galvanized steel as a lead source; bench scale tests of metal leaching from harvested galvanized steel pipes were used to validate this approach. Using profile sampling, individual homes with galvanized steel pipe as a primary lead source were identified in Washington, D.C., Providence, RI, Chicago, IL, and a city in Florida. In some cases the levels of lead from this source were very significant (> 100 μg/L) and can be exacerbated by installation of copper pipe upstream during partial service line replacements.

This chapter is currently under review for publication in *Environmental Engineering Science*.

INTRODUCTION

Exposure to lead in water remains a significant public health concern and is receiving increased attention as other sources are addressed and public health goals become more stringent (Shannon and Graef 1989; Triantafyllidou and Edwards 2011; Deshommes et al. 2013; Etchevers et al. 2014; Triantafyllidou et al. 2014). Historically, lead pipes, leaded solders, and lead-containing brass and bronze have been considered the dominant sources of water lead, and continue to dominate lead release in many homes, although galvanized steel pipes have been acknowledged to be significant in some cases (Korshin 1999; Triantafyllidou and Edwards 2011). In this work, the term "galvanized steel pipe" refers to a steel pipe coated with sacrificial zinc coating, which may contain lead, and the term "zinc coating" refers to the zinc layer only.

Zinc Coating as a Source of Lead. Although galvanized steel pipes have fallen out of favor in the U.S., they were the most commonly installed pipe material for most of the 20th century (AWWA 1996) and are still installed in some present-day buildings. In a large national water utility survey, 52% of utilities (N = 898) reported the presence of steel or galvanized steel service lines within their distribution system, and an estimated 7.5% of households overall had steel or galvanized steel services (American Water Works Association 1996). The source of lead in galvanized steel pipes is the zinc coating. It is common practice to use Prime Western Grade zinc in galvanizing baths (AWWA 1996), which contains a *minimum* of 0.5% lead by weight and a maximum of 1.4% lead by weight (AWWA 1996; ASTM 2013; ASTM 2013). While galvanizing can be accomplished with zinc containing lower levels of lead, the presence of lead in the galvanizing kettle has processing advantages, including increased fluidity (American Galvanizers Association 2006). In comparison, the level of lead in "lead free" components for potable water use was recently reduced to a maximum of 0.25% in the wetted surface material (United States Environmental Protection Agency 2012), making the level of lead found in many zinc coatings unacceptable for potable use if judged by the new standard. When lead is present in the zinc coating, it can be released to water either in soluble form through dissolution of the zinc coating or in particulate form through the scouring of zinc corrosion products at high flow rates (Figure 3-1a). In this work, this is referred to as *direct* lead release.

Cadmium as a Fingerprint for Galvanized Steel Pipe. In situations where lead release is dominated by dissolution of zinc coatings, it is expected that lead and zinc concentrations will tend to be correlated. However, several attempts to study lead release from galvanized steel pipe have been confounded by the presence of brass fittings (Neff et al. 1987; Lee et al. 1989), which also contain both lead and zinc. One possible way to distinguish lead from galvanized steel and lead from brass in the field is by using the cadmium concentration as a "fingerprint." Prime Western Grade zinc can contain up to 0.2% cadmium (AWWA 1996; ASTM 2013), and bench scale experiments under intermittent flow conditions have demonstrated that the concentrations of zinc, cadmium, and lead released from galvanized steel pipes can correlate with each other (Meyer 1980). Such correlations between lead and cadmium release were successfully used in Poland to identify galvanized steel as a water lead source (Barton et al. 2002; Barton 2005).

Other Sources of Cadmium in Drinking Water. According to EPA, the primary sources of cadmium in drinking water are the corrosion of galvanized pipes, erosion of natural deposits, discharge from metal refineries, and runoff from waste batteries and paints (United States

Environmental Protection Agency 2013). Other than galvanized steel pipe corrosion, these major sources of cadmium are expected to affect the cadmium concentration in the source water, which can be identified by taking samples for cadmium at the treatment plant or checking the cadmium concentration of well-flushed field samples. Brass tends to have only traces of cadmium releative to lead (e.g., Schock and Neff 1988). In the field, the amount of cadmium released from galvanized steel pipe has been sufficient to distinguish it from other materials despite possible confounding factors; in Seattle, homes with galvanized steel pipe had cadmium concentrations at least ten times higher than homes with copper pipe (Sharrett et al. 1982).

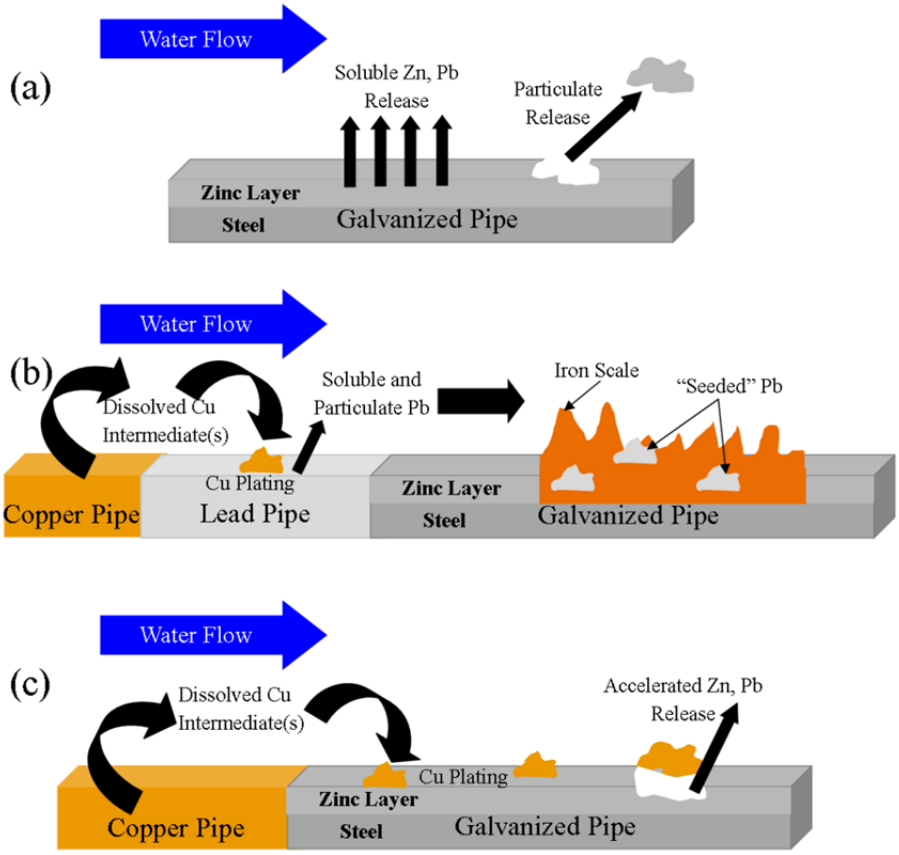

Figure 3-1. Schematic showing three different possible lead release scenarios for galvanized pipe. (a) Galvanized pipe with no other plumbing materials is expected to release zinc (Zn) and lead (Pb) in both soluble and particulate forms. (b) In the "lead seeding" hypothesis, upstream Pb release causes Pb adsorption/deposition on downstream iron scales, which can act as a reservoir of Pb. If copper (Cu) pipe is also present upstream, galvanic and deposition corrosion can increase the corrosion rate of the Pb pipe. (c) In the presence of Cu, galvanized pipe is also expected to undergo deposition corrosion, leading to accelerated release of Zn and Pb.

Galvanized Steel Pipe as a Direct Lead Source. A literature review identified numerous laboratory and field studies (Table 3-1) demonstrating that galvanized steel pipe can be a significant source of lead in drinking water (McFarren et al. 1977; Center for Disease Control 1978; Meyer 1980; Lee et al. 1989; AWWA 1996; Quevauviller and Thompson 2005; Lasheen et al. 2008). Experiences with samples in France found that lead concentrations from galvanized steel are typically below 10 µg/L, but can frequently reach 25 µg/L and are sometimes as high as

100 µg/L (Quevauviller and Thompson 2005). Similarly, data taken from homes with galvanized steel pipe in Portland, OR showed a median lead level of 10 µg/L and a 90th percentile value of 20 µg/L (AWWA 1996). These data imply that pre-2014 galvanized steel could contribute enough lead to create problems with action level compliance and human health (Triantafyllidou et al. 2014). It is expected that the levels of lead released from galvanized steel pipe will tend to decrease as the zinc coating is depleted; however, one three-year intermittent-flow study demonstrated that lead can be released above the action level for at least several years after installation (Meyer 1980).

Table 3-1. Literature Review of Galvanized Pipe as a Source of Lead

Reference	Study Type	pH	Lead Levels	Sampling Details
(AWWA 1996)	Field	7	Median: 10 µg/L 90th %tile: 20 µg/L	Samples from homes in Portland, OR with galvanized pipe
(CDC 1978)	Field	5.5 – 6.5	1st Draw Mean: 59 µg/L Grab Mean: 63 µg/L Flushed Mean: 30 µg/L	Samples from 8 homes with galvanized service lines.
(Lasheen et al. 2008)	Lab	6-8	Mean: 50 – 70 µg/L	Dump and fill tests at multiple pH and alkalinity levels
(Lee et al. 1989)	Field	Various[a]	Mean: 4.2 µg/L	Survey of 94 utilities including 193 homes with galvanized pipe
(McFaren et al. 1977)	Lab	NR[b]	Ranged from 3.2 – 24.1 µg/L; cadmium < 0.2 µg/L	Intermittent flow pattern (200 gal/day), corrosive water through 160 ft of pipe; only overnight standing samples analyzed
(Meyer 1980)	Lab	7	60 µg/L at beginning 20 µg/L after 30 months	Three year study with intermittent flow
(Sharrett et al. 1982)	Field	6-7	Standing Median: 3.7 µg/L Running Median: 1.9 µg/L Median Cadmium: 0.25-0.63 µg/L	Samples from homes in Seattle, WA with galvanized pipe
(Quevauviller and Thompson 2005)	Field	NR[b]	"Normally": 1-10 µg/L "Frequently": 10-25 µg/L As high as 100 µg/L	General comments based on "experience in France"

[a]Majority of sites (68%) were between pH 7-8; detailed pH distribution available in (Lee et al. 1989)
[b]NR = not reported

Galvanized Steel Pipe as an Indirect Lead Source. Recent work identified problems with elevated lead in homes with galvanized steel in Washington D.C. and concluded that the lead present on the old galvanized steel pipe surfaces originated from upstream lead pipes (Sandvig et

al. 2008; HDR Engineering Inc. 2009; McFadden et al. 2011), causing other researchers to draw similar conclusions when galvanized steel is serving as a source of lead in water (Deshommes et al. 2010). Conceptually, this mechanism is the result of the strong tendency for iron to adsorb lead; these iron scales can form on the galvanized steel pipe surface once the zinc coating has been lost (Figure 3-1b). If lead-rich iron scales form, they can serve as a reservoir for *indirect* release of lead from galvanized steel pipe, even once the original lead source has been removed. The mechanism was supported by surface analysis of iron scale scrapings from harvested galvanized steel pipes, which identified lead-rich regions within the iron scale; the authors stated that the zinc layer was no longer present in these pipes and did not consider its possible contribution to lead release (HDR Engineering Inc. 2009; McFadden et al. 2011). It was further acknowledged that the "seeding" of lead from services on downstream galvanized steel is a complex process dependent on pipe age, mineralogy, and water chemistry, particularly the presence of phosphate corrosion inhibitors (HDR Engineering Inc. 2009; Wasserstrom 2014), which implies that it may not occur universally to a significant extent when lead is present upstream of galvanized steel pipe. For example, HDR's attempt to deposit lead on unlined iron tubing in a pipe loop setup led to weak adherence of lead to iron, with only 25% adhering to the surface, and half of this desorbing in the first week without lead dosing (2009).

Role of Deposition Corrosion. Deposition corrosion can occur whenever ions from a more noble metal (e.g., copper(I) and copper(II) ions) are present in water that contacts a less noble pipe material (e.g. lead or galvanized steel), form micro galvanic cells on the pipe surface, and dramatically accelerate corrosive attack, failure rates, and metal release (Kenworthy 1943). Most study of deposition corrosion has focused on the galvanized steel / copper system, and practical experiences with devastating consequences have led to recommendations against the installation of copper before galvanized steel in the flow sequence and general guidance to avoid installation of more noble metals before less noble metals in the pipe flow sequence (Cruse 1971; AWWA 1986; NACE 1995). Nevertheless, the practice continues, particularly in large buildings and when lead service lines are partially replaced with copper in homes with galvanized steel premise plumbing (HDR Engineering Inc. 2009; Noble 2013). In the case of lead release from galvanized steel pipe, the presence of upstream copper is expected to accelerate lead release in both the direct and indirect cases of lead release from galvanized steel pipe (Figure 3-1c).

Objectives. The overall goal of this work is to re-examine the role of galvanized steel as a lead source in modern homes, schools, and large buildings. Specifically, this work examined (1) the concentration of lead on the surface of galvanized steel pipes of various ages and types, (2) the level of lead released to water from galvanized steel pipe in well-controlled bench-scale studies, and (3) the use of cadmium as a "fingerprint" to detect galvanized steel pipe a source of lead in both homes and schools.

MATERIALS AND METHODS

Pipe Coating Analysis. The concentration of lead on the surface of the galvanized steel pipes was measured using a handheld x-ray fluorescence (XRF) analyzer (Innov-X Alpha 800 LZX). The measurement time for each XRF reading was 45 seconds. Unless noted otherwise, readings were taken on the clean outside surface of the pipe and represent the concentrations in the zinc

coating before exposure to water. To confirm XRF results, sections of scale were removed from one set of pipes and digested using a mixture of nitric acid and hydroxylamine hydrochloride and analyzed for total metals by inductively coupled plasma – mass spectrometry (ICP-MS; Thermo Scientific Thermo Electron X Series) using Standard Method 3125B (APHA 1998).

Bench Scale Study. Galvanized steel pipes (3/4" diameter) were harvested from a distribution system in Florida and cut into 6" sections. Twenty pipes were exposed to finished water from the city's treatment plant using a dump-and-fill protocol with water changes three times per week (MWF). During week one, no disinfectant residual was present; for the remaining weeks, free chlorine was added to a concentration of 2.1 mg/L to match the disinfectant residual measured leaving the treatment plant at the Florida utility. Water changes continued for three weeks, and samples were collected as weekly composites for each pipe. All samples were digested in the bottle by adding 2% trace metal grade nitric acid and 0.1% hydroxylamine hydrochloride, with a minimum of 24 hours of digestion at room temperature and 24 hours of digestion at 50 °C before analysis. Samples were analyzed for total metals by ICP-MS as above.

Household Sampling. Except for the data collected in the case of a child's elevated blood lead (EBL), all household samples were collected as part of sequential (profile) sampling using the protocol outlined in (Clark et al. 2014). At the sites in Washington D.C. and Chicago, IL, sequential profiles were collected at a low flow rate of 1 L/min with the aerator on, the highest possible flow rate with the aerator on, and the highest possible flow rate with the aerator off. Samples collected in Florida included only the two profiles with the aerator on. For the EBL case study, both first draw and 45 second flush samples were taken according to the standard EPA protocol (United States Environmental Protection Agency 1991; Triantafyllidou et al. 2012) at normal household flow rates with the aerator on at all taps in the home. All samples were acidified with 2% trace metal grade nitric acid and analyzed for total metals using the same ICP-MS method outlined above.

School Sampling. Samples in schools were collected according to the protocol outlined by EPA for voluntary monitoring in schools (United States Environmental Protection Agency 2006), which involves collecting a 250 mL sample rather than the 1 L sample typical in residential sampling. After overnight stagnation, both first draw and 45 second flushed samples were collected at all taps in the school used for drinking.

RESULTS AND DISCUSSION

After assessing the extent to which modern (pre-2014) galvanized steel pipes used in potable water systems contain lead, bench and field studies from a case study of a Florida utility with instances of elevated lead from galvanized steel service lines are reviewed. Results from a home in Chicago explored the effect of flow rate on lead release from galvanized steel pipe and confirmed the presence of cadmium as a "fingerprint" for lead derived from galvanized steel pipe coatings. This is followed by field results from home profile sampling, school sampling, and sampling in the EBL case study, demonstrating widespread significance of galvanized steel pipe as a lead source when it is present.

Concentration of Lead in Galvanized Steel Pipe Coatings. Significant concentrations of lead up to 1.8% were measured in the zinc coating of galvanized steel pipes and fittings (Figures 3-2,3-3). In 60-year-old galvanized steel service lines harvested from a distribution system in Florida, the coating on the outside of the pipe after surface cleaning contained 0.8 – 1.7% lead by weight (Figure 3-2). To put the amount of lead available for release from galvanized steel service lines in context, a calculation of "effective lead surface area" was performed for a representative household plumbing system with a galvanized steel service line and compared to a representative mix of 6 brass utility service parts commonly found in home plumbing (as described in Maas et al. 2002).

For galvanized schedule 80 steel pipe, the surface area was calculated for a 25 ft, ¾" service line and multiplied by 1.4%. For brass, the total surface area was estimated using volumes from the literature (Maas et al. 2002) and a surface area to volume ratio of 0.008 in^2/mL (Triantafyllidou and Edwards 2007), which was then multiplied by the percentage of lead to give the effective lead area. The effective lead area was 63 cm^2 for the galvanized steel service line, whereas the range of effective lead areas was only 0.03-1.1 cm^2 for brass with lead levels from 0.25%- 8% lead.

From a different perspective, the total mass of lead in the galvanized steel service line would be 3.4 – 11.2 g over the range of coating thicknesses documented in the literature (Fox et al. 1983), compared to 100 – 300 g estimated to be available in pre-2014 lead-free brass (Triantafyllidou and Edwards 2011). A key implication of these calculations is that for galvanized steel pipe, a relatively small mass of lead is concentrated in the area contacting the water via the thin zinc coating, causing a disproportionate impact. For example, 11.2 g of lead is sufficient to contaminate an entire four-person household's daily water use (100 gal/day) to the 15 µg/L action level for more than five years, if it was all released uniformly over that period.

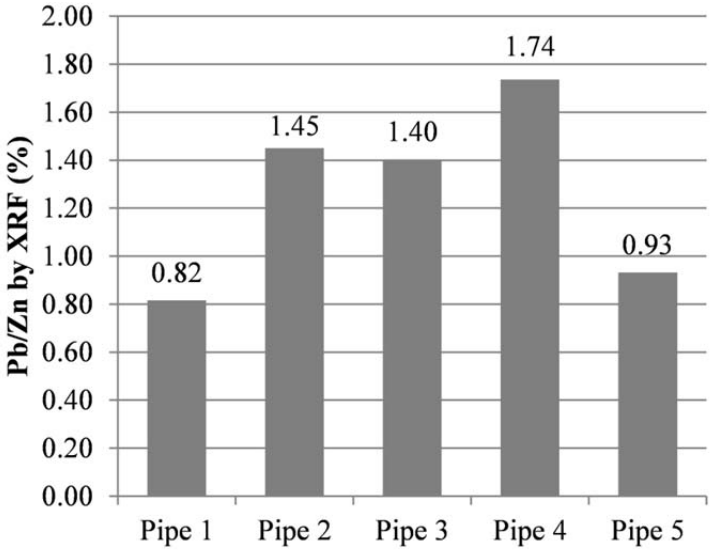

Figure 3-2. The ratio of lead (Pb) to zinc (Zn) detected on the *outside* of 60-year-old galvanized service lines harvested from a distribution system in Florida by XRF.

For galvanized steel premise plumbing installed from 1990-2008, lead concentration varied significantly by manufacturer and fitting type (Figure 3-3). In large (10-12") diameter galvanized steel pipes installed between 2005 and 2008 in a large public building in Indiana, lead concentrations on the outside of the pipe measured by XRF ranged from non-detect to 1.8% (Figure 3-3a). Dissolution and ICP-MS analysis of scale harvested from the inside of the same pipes was consistent with XRF results, with lead/zinc ratios ranging from ND – 2.2%. Using this more sensitive technique, for which the method detection limit (MDL) in the dissolved sample was 0.1 μg/L, cadmium was detectable in 5 / 18 samples, and was highest when lead was highest, implying that cadmium can serve as a positive indicator of galvanized steel pipe as a lead source, but that lead contributions from galvanized steel cannot be ruled out in the absence of cadmium. Similarly, in 1990s household plumbing harvested from a home in Chicago, lead concentrations on the outside of the pipe ranged from non-detect to 1.4% (Figure 3-3b). These results are consistent with expectations based on the use of Prime Western Grade zinc, which contains up to 1.4% lead, in the galvanizing process (AWWA 1996; ASTM 2013). The measurement of concentrations higher than 1.4% is consistent with the fact that XRF is a surface-sensitive measurement technique, and impurities, such as lead, are known to concentrate in the (eta) layer of zinc, furthest from the underlying steel (AWWA 1996).

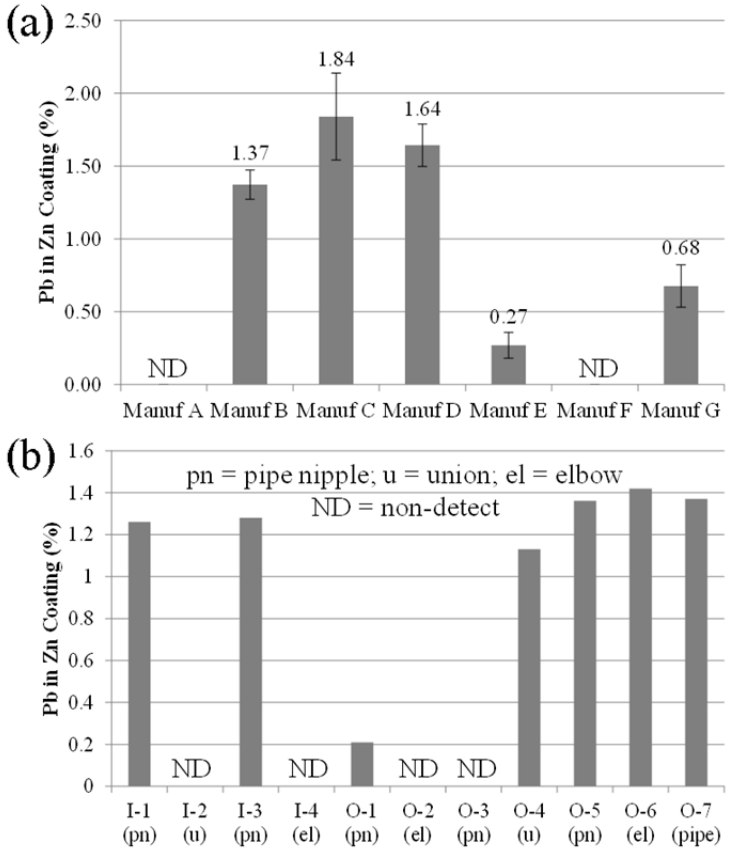

Figure 3-3. XRF results for the lead (Pb) concentration in the zinc (Zn) coating on galvanized pipes from several manufacturers in (a) large (10-12" diameter) galvanized pipes harvested from a building in Indianapolis (installed 2005-2008) and (b) premise potable water pipes from different manufacturers harvested from a home in Chicago (installed 1990). For (b), Pipe sections are numbered in flow sequence, with "1" representing the furthest pipe upstream. "I" pipes were located on the inlet to a water heater, and "O" pipes were located on the outlet.

Lead Release from Galvanized Steel in Florida. Exposure of sections of the harvested 60-year-old Florida service lines described above to finished water during bench-scale tests demonstrated that the zinc coating can contribute significant lead levels to water. During a three-week dump-and-fill study, the concentration of lead in water reached a maximum concentration of 172 µg/L, more than ten times the EPA action level. Throughout the test, the ratio of lead/zinc in water was similar to the ratio of lead/zinc expected in the zinc coating, ranging from 0.2 – 1.5% with an average of 0.5%. When lead concentration is plotted as a function of zinc concentration, the two metals are correlated with $R^2 = 0.46$ (Figure 3-4a). A relatively strong correlation is also present between zinc and cadmium with $R^2 = 0.69$ (Figure 3-4a). For both lead and cadmium, the sample with the highest zinc concentration has a large effect on the linear fit; if this point is excluded, the R^2 values change to 0.34 for lead and 0.77 for cadmium. If lead and cadmium are plotted against one another (Figure 3-4b), a moderate correlation with $R^2 = 0.44$ is observed. As expected based on the composition of Prime Western Grade zinc, the concentrations of cadmium are lower than lead (maximum cadmium = 13 µg/L; average cadmium/zinc = 0.05%). Despite the low concentrations, the relationship between the concentrations of zinc, lead, and cadmium provided further support for the use of cadmium as a "fingerprint" element for the presence of galvanized steel pipe.

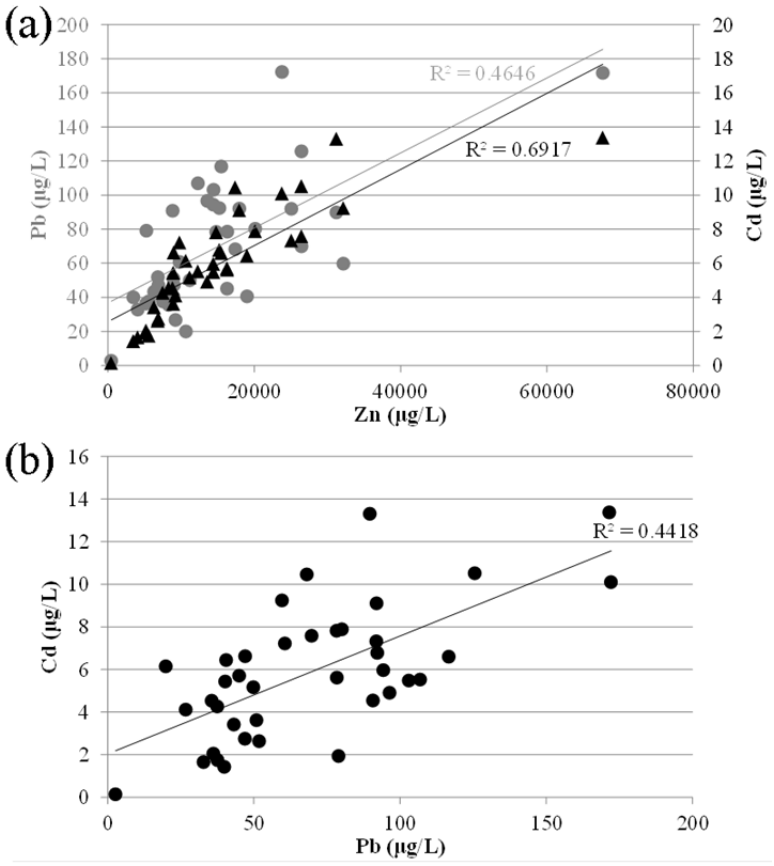

Figure 3-4. Correlations observed between (a) zinc (Zn) and lead (Pb; gray circles) and Zn and cadmium (Cd; black triangles) as well as (b) Cd and Pb during a three-week *bench scale study* conducted with galvanized pipes harvested from a distribution system in Florida. The average Pb/Zn ratio was 0.53%, and the average Cd/Zn ratio was 0.05%. This also illustrates the possible use of the presence of Cd as a "fingerprint" for Pb resulting from a galvanized pipe.

Field sampling in the same city in Florida, which is believed to have no lead service pipes, revealed lead concentrations as high as 67 μg/L in samples collected at high flow rate, even after several minutes of flushing. The highest lead sample had more than 3000 μg/L zinc, giving a lead/zinc ratio of 2%, similar to that detected in the galvanized steel pipe removed from the system. The sample also contained high levels of iron (22,000 μg/L) and detectable cadmium (> 0.1 μg/L). Interestingly, the sample also contained 1000 μg/L copper, implying either the presence of brass or that deposition corrosion is occurring. In some cases, lead and zinc concentrations were correlated; in one particular home, samples collected at high flow rate demonstrated a very strong correlation with $R^2 = 0.976$, and the presence of detectable cadmium (> 0.1 μg/L) indicated galvanized steel pipe as a lead source.

Role of Flow Rate in Lead Release from Galvanized Steel Pipe. Sequential (profile) sampling at a home in Chicago, IL revealed that lead release from galvanized steel pipe is sensitive to changes in flow rate and removal of the aerator (Figure 3-5). This home contained multiple lead sources, including both a lead service line and galvanized steel premise plumbing. Despite this, both lead and cadmium concentrations in water were correlated to the zinc concentration in water for all samples collected (Figure 3-5a), implying that the zinc coating on the premise pipes is a dominant source. Furthermore, when only samples taken at the highest flow rate with the aerator removed are included, the correlation becomes even stronger ($R^2 > 0.90$; Figure 3-5b). One possible reason for this is the dominance of particulate metal release in these samples (Clark et al. 2014), and it is expected that elevated lead levels in this home are the result of scale being scoured from galvanized steel pipe walls at high flow. For example, the sample with the highest lead concentration (63 μg/L, 0% soluble) also contained high levels of particulate zinc (600 μg/L, 10% soluble) and iron (1160 μg/L, 0% soluble). The particulate copper concentration in this sample was also elevated (44 μg/L, 2% soluble), an observation consistent with the scouring of copper-containing deposits from the galvanized pipe wall. This result implies that deposition corrosion could play a role in metal release to water for this home, which was known to have experienced a recent partial lead service pipe replacement with copper.

Household Correlations of Lead, Cadmium, and Zinc at High Flow Rate. Strong correlations between lead, cadmium, and zinc found in Chicago were also present in field samples from Washington, D.C. and Providence, RI (Clark et al. 2014). Of 12 homes with lead service lines sampled in Washington, D.C., five demonstrated a correlation between lead and zinc (> 0.8) at high flow with no aerator (Figure 3-6). Similarly, 4 out of 12 homes with lead service lines sampled in Providence showed the same correlation ($R^2 > 0.7$; Figure 3-6a). Correlations were also found between zinc and cadmium, iron, and copper in some homes (Figure 3-6a). Both cadmium and iron could be expected if release is due to galvanized steel pipe, and the correlation to copper could be a result of deposition corrosion effects. It is important to note that for many of these homes, galvanized steel was not indicated as a lead source by co-occurrence of cadmium. Only 8% of samples in both Washington, D.C. and Providence contained detectable (> 0.1 μg/L) cadmium. Among the samples with non-detect cadmium were several extremely high lead samples (1800 μg/L in Washington, D.C. and 7700 μg/L in Providence), which are believed to result from scouring of particles from the lead service line, as well as samples containing high levels of both lead and tin believed to result from dislodged solder particles (Clark et al. 2014).

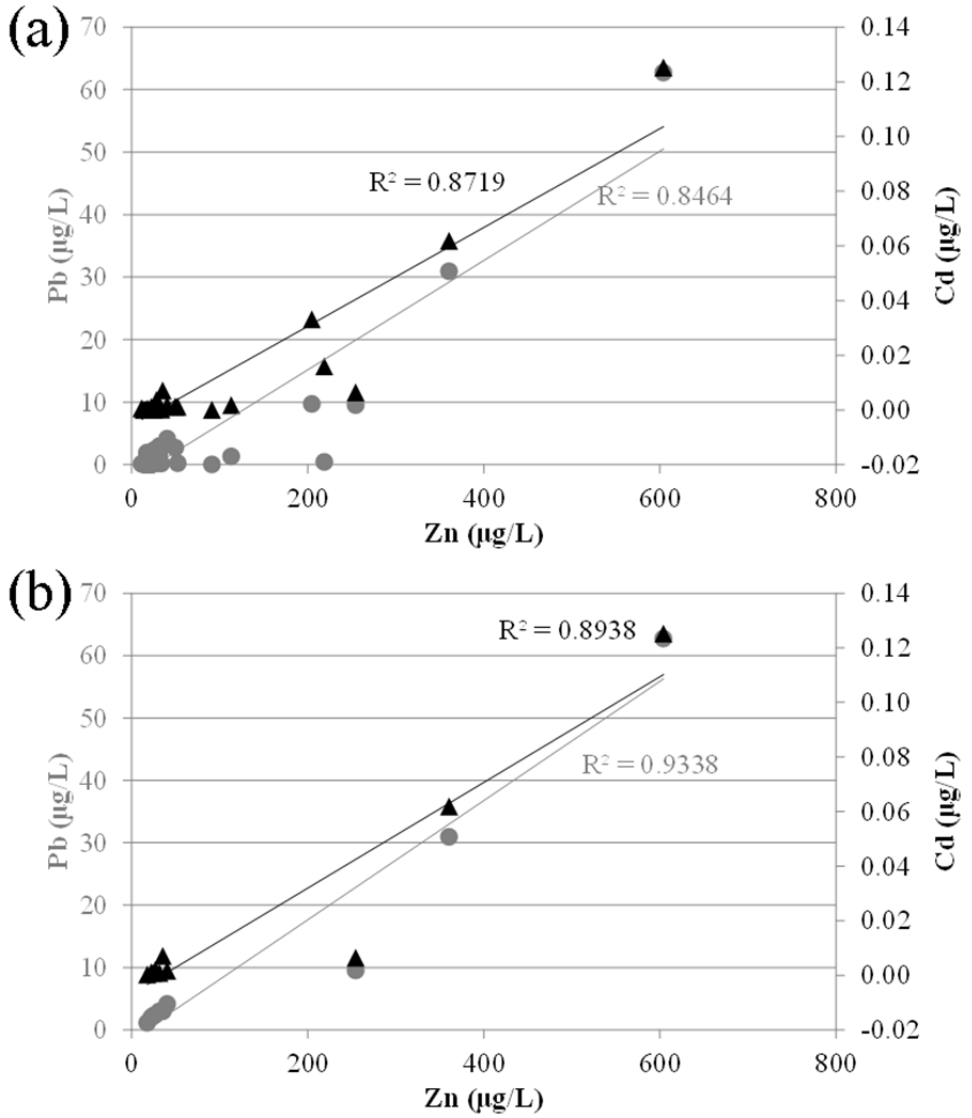

Figure 3-5. Plots of the lead (Pb; gray circles) and cadmium (Cd; black triangles) concentrations as a function of the zinc (Zn) concentration in water for a home in Chicago using (a) all samples collected (low flow, high flow with aerator, and high flow, no aerator) and (b) high flow, no aerator samples only. Pb and Cd are most correlated to Zn in the highest flow samples, in which metals are in primarily particulate form and at their highest concentrations.

Lead Release from Galvanized Steel Pipe in Schools. Analysis of results from 92 samples collected from different taps in a Washington, D.C. school did not demonstrate a consistent correlation between zinc and lead or cadmium, as expected given variability in coatings. However, when samples are separated into two groups based on the detection limit for cadmium of 0.1 µg/L, cadmium > MDL (N = 44) and cadmium < MDL (N = 48), the detectable cadmium group had an average lead concentration of 194 µg/L, more than ten times higher than the average lead concentration of the non-detect cadmium group (18 µg/L). This result implies that the presence of a galvanized steel pipe, as flagged by the presence of cadmium as a "fingerprint," is associated with elevated lead in water.

(a)

	Zn-Pb R^2	Zn-Cd R^2	Zn-Cu R^2	Zn-Fe R^2
Site 3	0.805	ND*	0.164	0.652
Site 18	0.894	0.617	0.835	0.946
Site 19	0.973	0.965	0.846	0.991
Site 21	0.989	0.971	0.956	0.978
Site 22	0.868	ND*	0.622	0.838
Site 6	0.946	ND*	0.887	0.614
Site 12	0.856	ND*	0.342	0.130
Site 14	0.998	ND*	0.888	0.803
Site 16	0.720	0.764	0.850	0.786

*ND = all Cd samples non-detect

(b)

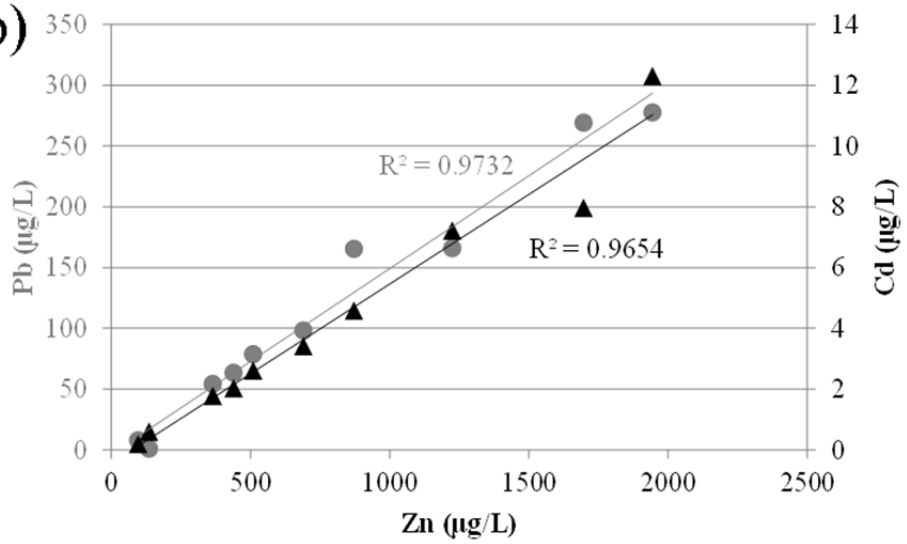

Figure 3-6. (a) For 5 / 12 sampling sites in Washington, D.C. (top half of table) and 4 / 12 sampling sites in Providence, RI (bottom half of table), zinc (Zn) was found to be correlated ($R^2 > 0.700$) to lead (Pb) in high flow (no aerator) samples. R^2 values are shown for these sites for Zn with Pb, cadmium (Cd), copper (Cu), and iron (Fe). (b) Plot of the Pb (gray circles) and Cd (black triangles) concentrations as a function of the Zn concentration in water samples collected at high flow (no aerator) at Site 19 (Washington, D.C.).

Galvanized Steel Pipe and EBL. In 2008, a case of childhood elevated blood lead (EBL) in Washington D.C. led to water sampling, which revealed extremely high lead levels (nearly 1,000 µg/L). Further analysis revealed that the concentration of lead in this home, which was known to contain galvanized steel pipe, was highly correlated to the zinc concentration (Figure 3-7). Furthermore, zinc and cadmium were correlated, the "fingerprint" for lead release from galvanized steel, implying that galvanized steel pipe contributed a significant fraction of the lead in water in this case.

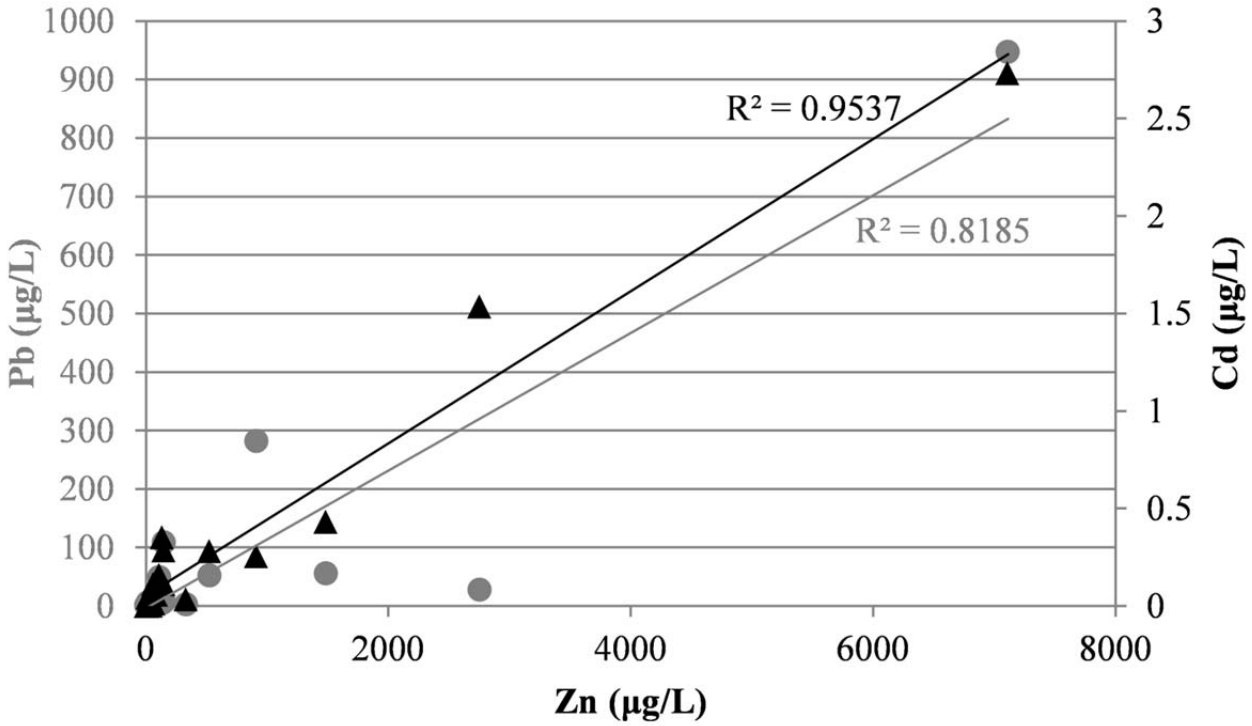

Figure 3-7. Water samples taken from a home in Washington, D.C. where a child was found to have elevated blood lead demonstrate a strong correlation between both lead (Pb) and zinc (Zn) (gray circles) and cadmium (Cd) and Zn (black triangles), implicating galvanized iron as a possible source of lead in water.

Relative Importance of Direct and Indirect Lead Release. Although recent work has appropriately drawn attention to galvanized steel pipe as an important source of lead in drinking water (HDR Engineering Inc. 2009; Wasserstrom 2014), the HDR work has focused exclusively on *indirect* release of lead via seeding. While lead "seeding" can and does occur in some cases, it is important to not overlook *direct* release of lead from the zinc coating itself. For galvanized steel pipes harvested from a home in Chicago, IL with a lead service line, which serves as an upstream lead source, a comparison of the concentration of lead on the inside of the pipe compared to the outside can provide insight into the relative contribution of direct and indirect sources of lead release (Figure 3-8).

The concentration on the outside of the pipe represents the concentration of lead in a new pipe coating available for direct release, while the concentration on the inside reflects residual direct release lead and any seeded lead available for indirect release. In this home, the concentration of lead by weight detected by XRF on the inside of the pipe was never more than 2%, and was on average less than 1%, which is similar to the concentration found on the outside of the pipe (Figure 3-8). This provides an example of a case where direct release of lead dominates relative to indirect release, and highlights the need to consider both mechanisms when evaluating lead-in-water contributions from galvanized steel pipe.

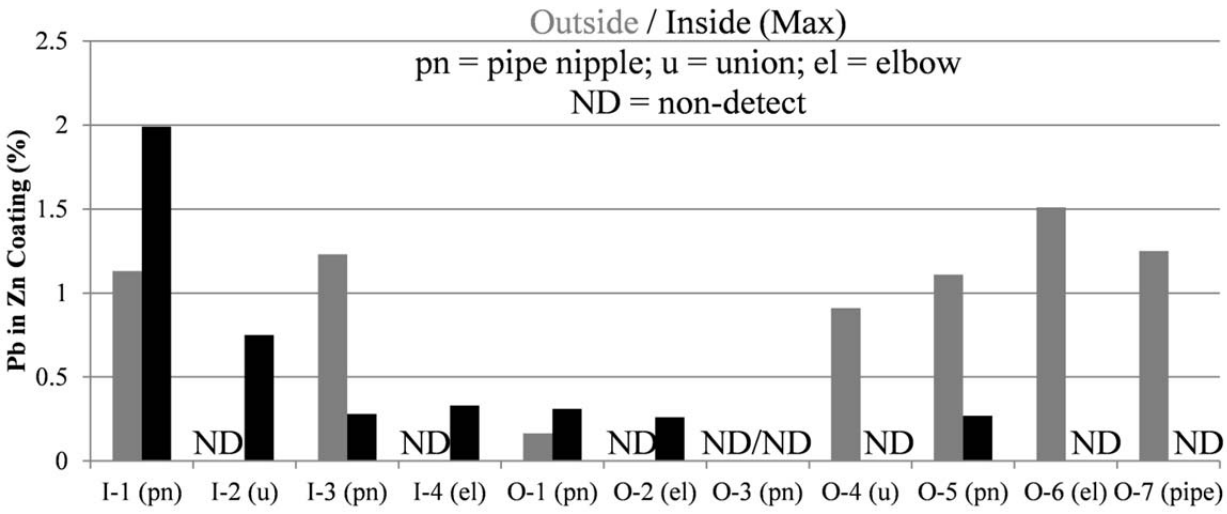

Figure 3-8. For pipes harvested from a home in Chicago (see Figure 3-3b), the concentration of lead (Pb) by XRF in the zinc (Zn) coating (gray) is compared to the maximum concentration of Pb measured on the inside by XRF (black), which represents a mix of the remaining Pb from the coating and any "seeded" lead.

CONCLUSIONS

Analysis of pipe surfaces, bench scale studies, and field samples for lead leaching from galvanized steel pipe yielded the following conclusions:

- Surface analysis of galvanized steel pipe coatings removed from modern buildings, revealed surface concentrations up to 1.8% lead, which is roughly consistent with the composition of Prime Western Grade zinc.
- Bench-scale tests with harvested galvanized steel pipe revealed concentrations as high as 172 μg/L lead could be released from galvanized steel pipe under dump-and-fill conditions, and that lead and cadmium are correlated to zinc when galvanized steel pipes are the source of lead release to water.
- Samples collected from homes in Washington D.C., Providence, RI, and Chicago, IL, and a city in Florida revealed strong correlations between cadmium, lead, and zinc indicative of galvanized steel as a significant source of lead in these homes.
- The above correlations were strongest at high flow rates, especially without aerators, implying that particulate release from zinc coatings can be the dominant source of lead at these flow rates
- When samples collected at a school in Washington, D.C. were divided into two groups based on a cadmium threshold of 0.1 μg/L (the MDL for cadmium by ICP-MS), the samples with detectable cadmium had an average lead concentration 10X higher than the samples without cadmium, implicating galvanized steel pipe as a significant source of lead in this school.
- Although indirect lead release via lead "seeding" onto galvanized steel pipes can occur under some conditions, considering only this mechanism gives an incomplete picture of lead release from galvanized steel pipe, and the contribution of direct release from the

zinc coating to lead in water should be considered when the overall risk of lead exposure from galvanized steel pipes is estimated.

ACKNOWLEDGEMENTS

The authors acknowledge the financial support of the National Science Foundation under NSF CBET-0933246 and the Graduate Research Fellowship Program (GRFP). The authors would also like to acknowledge the financial support of the Robert Wood Johnson Foundation (RWJF) under the Public Health Law Research program and the Abel Wolman Fellowship (American Water Works Association). Opinions and findings expressed herein are those of the authors and do not necessarily reflect the views of the NSF, RWJF, or AWWA. The authors would further like to thank Yanna Lambrinidou at Parents for Nontoxic Alternatives (PNA), the DC Department of the Environment (DDOE), and the homeowners who participated in the field sampling studies in Washington D.C., as well as the DC Public Schools (DCPS), Eastern High School, and the student sampling volunteers at Washington International School (WIS).

AUTHOR DISCLOSURE STATEMENT

No competing financial interests exist.

REFERENCES

American Galvanizers Association (2006). *Alloy Additions to the Kettle and Their Purposes*. Available at: http://www.galvanizeit.org/education-and-resources/resources/technical-faq-dr-galv/alloy-additions-to-the-kettle-and-their-purposes.

American Water Works Association (1996). WATER:\STATS 1996 Survey.

APHA (1998). *Standard Methods for the Examination of Water and Wastewater*: APHA, AWWA, WEF.

ASTM (2013). ASTM Standard A123M - 13, "Standard Specification for Zinc (Hot-Dip Galvanized) Coatings on Iron and Steel Products". West Conshohocken, PA, ASTM International.

ASTM (2013). ASTM Standard B6-13, "Standard Specification for Zinc". West Conshohocken, PA, ASTM International.

AWWA (1986). *Corrosion Control for Operators*. Denver, CO: American Water Works Association.

AWWA (1996). *Internal corrosion of water distribution systems*: American Water Works Association.

Barton, H. (2005). Predicted intake of trace elements and minerals via household drinking water by 6-year-old children from Krakow, Poland. Part 2: Cadmium, 1997-2001. *Food Additives & Contaminants* 22(9), 816-828.

Barton, H., Z. Zachwieja and M. Folta (2002). Predicted intake of trace elements and minerals via household drinking water by 6-year-old children from Krako'w (Poland). Part 1: Lead (year 2000). *Food Additives and Contaminants* 19(10), 906-915.

Center for Disease Control (1978). Internal Memo: Childhood Health Effects of Lead in Drinking Water, Bennington, Vermont.

Clark, B., S. Masters and M. Edwards (2014). Profile Sampling to Characterize Particulate Lead Risks in Potable Water. *Environmental Science & Technology*.

Cruse, H. (1971). Dissolved-Copper Effect on Iron Pipe. *Journal AWWA* 63(2), 79-81.

Deshommes, E., L. Laroche, S. Nour, C. Cartier and M. Prévost (2010). Source and occurrence of particulate lead in tap water. *Water Research* 44(12), 3734-3744.

Deshommes, E., M. Prévost, P. Levallois, F. Lemieux and S. Nour (2013). Application of lead monitoring results to predict 0–7 year old children's exposure at the tap. *Water Research* 47(7), 2409-2420.

Etchevers, A., P. Bretin, C. Lecoffre, M.-L. Bidondo, Y. Le Strat, P. Glorennec and A. Le Tertre (2014). Blood lead levels and risk factors in young children in France, 2008–2009. *International Journal of Hygiene and Environmental Health* 217(4–5), 528-537.

Fox, K. P., C. H. Tate and E. Bowers (1983). The interior surface of galvanized steel pipe: a potential factor in corrosion resistance. *Journal (American Water Works Association)*, 84-86.

HDR Engineering Inc. (2009). An Analysis of the Correlation Between Lead Released from Galvanized Iron Piping and the Contents of Lead in Drinking Water. Bellevue, WA, HDR Engineering Inc.

Kenworthy, L. (1943). The Problem of Copper and Galvanized Iron in the Same Water System. *The Journal of the Institute of Metals* 69.

Korshin, G. V. (1999). *Corrosion and Metal Release for Lead-Containing Materials: Influence of NOM*: American Water Works Association.

Lasheen, M. R., C. M. Sharaby, N. G. El-Kholy, I. Y. Elsherif and S. T. El-Wakeel (2008). Factors influencing lead and iron release from some Egyptian drinking water pipes. *Journal of Hazardous Materials* 160(2–3), 675-680.

Lee, R. G., W. C. Becker and D. W. Collins (1989). Lead at the Tap: Sources and Control. *Journal (American Water Works Association)* 81(7), 52-62.

Maas, R. P., S. C. Patch, J. Berkowitz and M. LaGasse. (2002). *Comparison of Lead Discharge from Conventional Leaded Brass Versus "No-Lead" Type Water Service Valves and Fittings*. Available at: http://www.environmentalqualityinstitute.org/lead/pdf/Lead-02-097-EQI.pdf.

McFadden, M., R. Giani, P. Kwan and S. H. Reiber (2011). Contributions to Drinking Water Lead from Galvanized Iron Corrosion Scales (PDF). *Journal-American Water Works Association* 103(4), 76-89.

McFarren, E. F., R. W. Buelow, R. C. Thurnau, M. Gardels, R. K. Sorrell, P. Snyder and R. C. Dressman (1977). Water Quality Deterioration in the Distribution System. Presented at *Water Quality Technology Conference*, Kansas City, MO.

Meyer, E. (1980). Beeinträchtigung der Trinkwassergüte durch Anlagenteile der Hausinstallation–Bestimmung des Schwermetalleintrags in das Trinkwasser durch Korrosionsvorgänge in metallischen Rohren. *DVGW-Schriftenreihe Wasser*(23), 113-131.

NACE (1995). *Prevention & Control of Water-Caused Problems in Building Potable Water Systems*. Houston: NACE International.

Neff, C. H., M. R. Schock and J. I. Marden (1987). Relationships between water quality and corrosion of plumbing materials in buildings. *Project Report for Grant No. CR80856010*(EPA/600/S2-87/036).
Noble, C. (2013). Corrosion of Galvanized Piping in Domestic Water Systems. *The Conduit (M&M Engineering Associates, Inc.)* 13(1), 1-3.
Quevauviller, P. P. and C. Thompson (2005). *Analytical methods for drinking water: advances in sampling and analysis*: John Wiley & Sons.
Sandvig, A., B. Maynard, D. Mast, R. R. Trussel, S. Trussel, A. Cantor and A. Prescott (2008). Contribution of Service Line and Plumbing Fixtures to Lead and Copper Rule Compliance Issues. Denver, CO, American Water Works Association Research Foundation.
Schock, M. R. and C. H. Neff (1988). Trace metal contamination from brass fittings. *Journal AWWA* 80(11), 47-56.
Shannon, M. and J. W. Graef (1989). Lead Intoxication: From Lead-contaminated Water Used to Reconstitute Infant Formula. *Clinical Pediatrics* 28(8), 380-382.
Sharrett, A. R., A. P. Carter, R. M. Orheim, and M Feinleib (1982). Daily intake of lead, cadmium, copper, and zinc from drinking water: the Seattle stud of trace metal exposure. *Environmental Research* 28(2), 456-475.
Triantafyllidou, S. and M. Edwards (2007). Critical evaluation of the NSF 61 Section 9 test water for lead. *Journal AWWA* 99(9), 133-143.
Triantafyllidou, S. and M. Edwards (2011). Lead (Pb) in Tap Water and in Blood: Implications for Lead Exposure in the United States. *Critical Reviews in Environmental Science and Technology* 42(13), 1297-1352.
Triantafyllidou, S., D. Gallagher and M. Edwards (2014). Assessing risk with increasingly stringent public health goals: The case of water lead and blood lead in children. *Journal of water and health* 12(1), 57-68.
Triantafyllidou, S., C. Nguyen, Y. Zhang and M. Edwards (2012). Lead (Pb) quantification in potable water samples: implications for regulatory compliance and assessment of human exposure. *Environmental Monitoring and Assessment*, 1-11.
United States Environmental Protection Agency (1991). Maximum Contaminant Level Goals and National Primary Drinking Water Regulations for Lead and Copper. *Federal Register* 56(110), 26460-26564.
United States Environmental Protection Agency (2006). *3Ts for Reducing Lead in Drinking Water in Schools*. Available at: http://water.epa.gov/drink/info/lead/index.cfm.
United States Environmental Protection Agency (2012). Public Meeting: Potential Regulatory Implications of the Reduction of Lead in Drinking Water Act of 2011. *Federal Register* 77(146), 44562.
United States Environmental Protection Agency (2013). *Basic Information about Cadmium in Drinking Water*. Available at: http://water.epa.gov/drink/contaminants/basicinformation/cadmium.cfm.
Wasserstrom, L. W. (2014). Uptake of Lead by Iron Corrosion Scales: Effects of Iron Mineralogy and Orthophosphate. Department of Geology. Cincinati, OH, University of Cincinnati. **M.S.**

CHAPTER 4. DEPOSITION CORROSION OF GALVANIZED IRON IN THE PRESENCE OF COPPER

Brandi Clark[a], Marc Edwards[a]

[a]Virginia Polytechnic Institute and State University, Blacksburg, Va.

ABSTRACT

Deposition corrosion, via formation of microgalvanic cells from copper ions (e.g., Cu^{+}, Cu^{2+}) on iron or galvanized (zinc coated) steel pipes, has been linked to disastrous field corrosion failures. Key factors expected to control deposition corrosion, including soluble copper concentration, copper ion speciation, and flow pattern (stagnant versus recirculating), were examined. The mass of copper plated was directly proportional to the soluble copper concentration in solution. The presence of flow, which allowed greater mass transport of reactants to the pipe surface, proved to be crucial to replicating deposition corrosion in the laboratory: tests with flow demonstrated up to 7X more zinc release and 55X more iron release when copper was present than when it was absent, compared to increases of only ≈2X in the same water under stagnant conditions. Scale dissolution, x-ray fluorescence (XRF), and scanning electron microscopy (SEM) were used to characterize copper-rich deposits on the surface of both field and laboratory samples that were consistent with metallic copper, supporting a deposition corrosion mechanism.

This chapter is currently under review for publication in *CORROSION*

INTRODUCTION

Corrosion of drinking water distribution systems can cost water utilities and homeowners tens of billions of dollars each year in infrastructure damage, adversely impact public health, and cause water loss through leaks.[1] The corrosion of iron is particularly costly, because the majority of water mains currently in service are composed of iron and its alloys.[2, 3] Despite early reports that the presence of dissolved copper could dramatically increase the rate of failure for iron and galvanized steel, this "dissolved copper effect," or deposition corrosion, has received little recent attention.[4-7] Mechanistically, plating of copper ions (e.g., Cu^{+}, Cu^{2+}) onto an iron pipe surface forms micro-galvanic cells, dramatically accelerating corrosive attack and causing rapid pipe failures.[4, 5] If enough copper "islands" are present, an overall acceleration of the corrosion rate may be observed electrochemically or by depletion of chlorine/oxygen in water due to cathodic reactions. Acknowledged as "disastrous" in the field,[4] laboratory work has not always been successful in reproducing the phenomenon, limiting the development of remedial measures.

Sources of Upstream Copper. In spite of predicted damage to iron infrastructure from dissolved copper in water, a range of copper sources upstream of steel water pipes persists, and new sources are being considered. For instance, trace levels of copper sulfate have been used to control algal blooms in reservoirs for more than a century, and although this practice has become restricted in some locations due to detrimental effects on aquatic ecosystems,[8, 9] many alternative algaecides are also copper-based.[10, 11] More recently, copper dosing at the treatment plant has been identified as a possible remedy for distribution system nitrification,[12] and copper-silver ionization systems are being used in hospital plumbing systems for *Legionella* control.[13] For premise plumbing, the installation of galvanized steel and copper pipes within the same building, particularly in the hot water recirculating system, is known to lead to corrosion issues, and is not recommended.[4, 14, 15] This is particularly likely in large buildings, which often have specifications that require the use of copper pipe for smaller diameters (e.g. below 2 inches or 5.1 cm), but allow use of steel and galvanized steel for larger diameters.[16] Galvanized steel is commonly substituted for copper to cut costs when large diameter pipes are needed,[16] leading to mixed-metal systems with a high potential for deposition corrosion and associated failures. For example, a recent case of deposition corrosion in the field was uncovered when a large new building constructed with galvanized steel plumbing began to experience failures just two years after its construction, ultimately resulting in more than $10 million in replacement costs. Failures were most common in the hot water recirculating system, which contained both copper and galvanized steel pipe, contrary to long-standing recommendations.[4, 7] This is particularly concerning in light of recent trends, under which hot water recirculating systems will be encouraged[17] or even required[18] in new construction to promote water conservation and control pathogens.

Emerging Deposition Corrosion Issues. Due to increasing concern over lead release to water, partial lead service line replacements with copper have been conducted in several cities with lead service lines,[19] a practice which places copper ahead of lead, as well as any galvanized steel premise plumbing, in the flow sequence, creating potential for deposition corrosion.[19-21] Furthermore, the antimicrobial properties of silver, a highly noble metal, have led to dosing of ionic silver in hospitals for *Legionella* control,[13, 22] with adverse implications for steel and copper pipe infrastructure within the building. Finally, innovations in disinfection[23] and water

treatment[24] involving silver, gold, or carbon nanomaterials have been proposed that would provide yet another source of noble ions and colloids upstream of vulnerable potable water infrastructure.[25] In order to eventually address the current and pending concerns associated with deposition corrosion, an ability to replicate and reproduce circumstances of past deposition corrosion failures is needed.

Theory of Deposition Corrosion. Deposition corrosion proceeds in two distinct phases: the plating phase and the corrosion phase (Figure 4-1). Although the corrosion phase can be described using galvanic corrosion theory,[26-28] little is known about the circumstances under which plating can occur in potable water systems. The thermodynamic driving force for plating to occur can be expressed in terms of the reduction potential (E) for the conversion of copper ions to copper metal; standard threshold potentials are 520 mV for the reduction of Cu(I) and 340 mV for the reduction of Cu(II) relative to the Normal Hydrogen Electrode (NHE).[29] Thermodynamically, plating is only possible when the potential of the surface to be plated is less (more negative) than the reduction potential.[30] Deliberate plating of copper can be accomplished by electrically fixing the potential of the surface to provide the necessary driving force for the reaction, with the resulting current flow (I) providing a direct measure of the plating reaction rate. In addition to traditional electroplating methods, "electroless" plating processes now exist in which addition of reducing agents to the plating solution allows plating to occur spontaneously.[30] Previous work in boiler systems has demonstrated that spontaneous, environmental plating of copper corrosion products on downstream iron tubing can occur via both displacement reactions with iron and disproportionation reactions of copper(I) species.[31, 32]

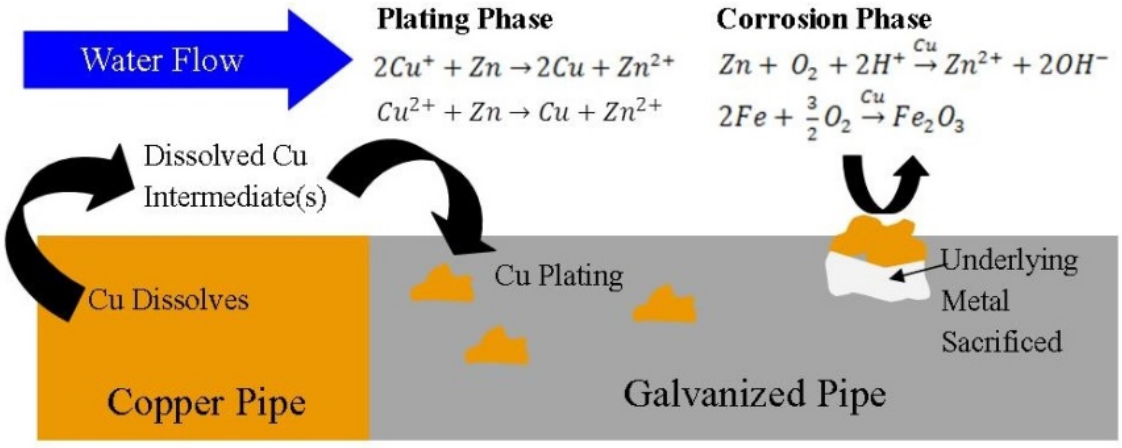

Figure 4-1. Mechanistic Diagram of Deposition Corrosion

Plating can be predicted by comparing the measured surface potential of a pipe material to the threshold value for copper deposition from the literature, as modified by temperature, pH, ionic strength, complexing ions, and the presence of other oxidizing and reducing agents. For copper, determination of the true plating potential is complicated by the participation of copper (I) species, since electroplating from a copper (II) solution is thought to proceed through a copper (I) intermediate.[33, 34] Hence, when copper (I) is present, which can occur in potable water, especially in waters with ammonia when dissolved oxygen is low,[35] it is expected to plate more efficiently than copper (II). For all of these reasons, empirical determination of the plating

potential using standard voltammetry techniques[36, 37] in a given environment can provide useful insights.[30]

The spontaneous plating of copper on the surface of a less noble metal (e.g. zinc, iron), is eventually self-limiting in nature. As copper plates on the metal surface, the surface potential becomes increasingly positive, decreasing the driving force for further copper deposition. Consequently, achievable depths of metallic copper via displacement reactions such as the reduction of copper by zinc metal (Figure 4-1) are less than 1 μm in depth.[30] The thin, non-uniform nature of these deposits presents serious challenges for detection of the pure deposits by most analytical methods, as most techniques (e.g. EDS, XRF) quantify all metals present at depths several times greater than the expected 1 μm deposit thickness.[38]

Previous Work. Most prior research on deposition corrosion in drinking water distribution systems has focused on the effect of dissolved copper on the corrosion of galvanized steel pipes, and early studies reported that a concentration of 0.3 mg/L doubled the corrosion rate.[6, 7] One previous analysis of eight case studies showed a correlation between the amount of copper deposited on the surface and the corrosion rate of galvanized steel pipe,[4] supporting the hypothesis that these failures were a result of deposition corrosion. Despite the strong field data demonstrating problems, attempts to study deposition corrosion at the bench and pilot scale have led to inconsistent results (Table 4-1). In some cases, the addition of dissolved copper has increased corrosion of galvanized steel or lead pipes, but in other cases dissolved copper has little effect. This discrepancy is interesting, and implies that some lab studies have been unable to reproduce the key elements of the deposition corrosion phenomenon as it occurs in practice or that changes in water chemistry might eliminate deposition corrosion issues.

Key Factors in Deposition Corrosion. Examination of corrosion mechanisms identified several key factors likely to impact deposition corrosion. A key thermodynamic controlling factor is the potential of the iron surface, which is affected by water chemistry; copper will plate only if the surface potential is below the threshold for plating. Another potentially important factor is the oxidation state of copper. Based on expectations from both thermodynamic and mechanistic experience reported by the plating industry,[33, 34] Cu(I) species are expected to plate more readily than Cu(II) species. However, the concentration of soluble copper readily available at the surface for plating is also expected to be an important factor, and the relatively low solubility of Cu(I) species could override thermodynamic benefits. If copper solubility is a limiting factor, the presence of corrosion inhibitors, such as phosphates, could limit the extent of plating as shown in previous work.[6]

In the corrosion phase, the supply of oxidants (e.g. oxygen, disinfectant) is critical to observing differences in the corrosion rate. During stagnation, the limited supply of these oxidants will limit corrosion; however, during flow, fresh oxidant is continuously supplied, allowing high corrosion rates at the micro-galvanic sites. The importance of flow pattern may explain some of the discrepancies in previous results (Table 4-1); one early study cited the "batch nature" of their tests as a likely reason for discrepancies between lab and field results,[6] and a few studies that tested both stagnant and flowing conditions found more dramatic deposition corrosion results with flow.[5, 21]

Table 4-1. Prior Research on Deposition Corrosion in Drinking Water at the Bench or Pilot Scale

Reference	Cu Level	Cu Source	Relevant Findings for Galvanized and Lead Pipe
(Kenworthy 1943)	0.5 – 1.5 mg/L	UNKN	Bench scale tests in stagnant water: Weight loss and Cu dose are correlated.
(Kenworthy 1943)	Various up to 0.3 mg/L	Cu Pipe	In bench scale hot water recirculating tests, Cu level is controlled by changing length of Cu pipe in the recirculating system. Increasing weight loss and penetration depth correlated to higher Cu doses.
(Hatch 1955)	Various up to 10 mg/L	UNKN	Agitated batch tests at 35 °C. Increasing weight loss is correlated with increasing Cu concentration, but results are not as dramatic as the authors expected based on field experience.
(Fox et al. 1986)	2 mg/L	$CuSO_4$; azurite	Bench scale tests in constant 60 °C baths: "The addition of copper sulfate . . . did not have an obvious corrosion impact." Addition of azurite crystals showed some acceleration of Zn corrosion
(Fox et al. 1986)	0.05 – 5 mg/L	$CuSO_4$	Pilot scale tests at 50 °C with Cu dosing 4 days/month under both stagnant and realistic flow regimes: Up to 5X increase in scale formation at highest Cu dose of 5 mg/L, but no deep pitting (localized corrosion).
(Hu et al. 2012)	0.3 – 5 mg/L	Cu^{2+}	For Pb pipe under stagnant conditions, Pb release increased by 2X for lowest Cu dose compared to control, with no significant differences between Cu doses.
(Hu et al. 2012)	5 mg/L	Cu^{2+}	For Pb pipe under continuously recirculating conditions, Pb release was 5X-7X higher with 5 mg/L Cu^{2+} addition than the control.

Objectives. The primary goal of this work was to verify the key factors expected to control the severity of deposition corrosion including the effects of soluble copper concentration, copper speciation, and flow pattern (stagnant versus recirculating). The second goal of this work was to use surface analysis techniques to examine metallic copper deposits on the surfaces of both field and laboratory pipes to better understand the nature of deposition corrosion and provide a basis for forensically identifying such problems in the field.

MATERIALS AND METHODS

Scanning Potential Plating Tests. Scanning potential tests were conducted with a potentiostat (Gamry PCI4) using linear sweep voltammetry (LSV).[29] The working and counter electrodes were platinum wires with areas of approximately 1 cm^2, and the reference electrode was silver / silver chloride (Ag/AgCl). The test solution consisted of 450 mL of synthetic tap water (Table

4-2) with 100 mg/L of copper added as copper (II) chloride and a pH of 6.00 ± 0.05. The solution was purged with nitrogen before and during each test to eliminate oxygen, and stirred at 300 rpm throughout. During the test, the potential was scanned from +800 to -800 mV at a rate of 5 mV/s. Each test was carried out in triplicate and background-corrected using a set of triplicate scans taken in a copper-free control solution. To study the effect of phosphate, dibasic sodium phosphate (Na_2HPO_4) was added in varying amounts up to 25 mg/L as P. To determine the soluble copper and phosphate concentrations, samples were filtered using a 0.45 μm syringe filter. To determine the mass of copper plated on the surface, the working electrode was cleaned in a known amount of concentrated nitric acid, then diluted 1:20 for analysis. All metal concentrations were determined by inductively coupled plasma – mass spectrometry (ICP-MS; Thermo Scientific Thermo Electric X Series) using Standard Method 3125B.[39]

Table 4-2. Key water quality parameters of test waters used for all experiments

	Synthetic Water	Blacksburg Water	Case Study Water[c]
pH	Multiple[a]	7.8	7.8
Disinfectant	Multiple[b]	3 mg/L Chloramines	1.6-1.7 mg/L Chloramines
Alkalinity (as $CaCO_3$)	15 mg/L	40 mg/L	212 mg/L
Chloride-to-Sulfate Mass Ratio (CSMR)	16.0	3.0	1.0
Corrosion Inhibitor	None	Zinc Orthophosphate	none

[a] pH = 6.00 for plating tests, pH = 8.00 for dump-and-fill and recirculating tests
[b] no disinfectant for plating tests, 4 mg/L chloramines for dump-and-fill and recirculating tests
[c] The case study water was used in both before and after ion exchange softening; the initial hardness was 300 mg/L as $CaCO_3$

Constant Potential Plating Tests. Constant potential tests were carried out using the same electrode setup, test solution volume, and stir rate as above. For these experiments, the same synthetic water was used (Table 4-2), but with a more realistic concentration of copper (500 μg/L), and oxygen was not excluded. During each test, a fixed potential was applied for 24 hours. At the end of each test, the copper plated on the working electrode was dissolved in a known volume of 50% nitric acid, which was diluted for analysis by ICP-MS as above.

Dump-and-Fill Testing. Bench scale tests were carried out using a dump-and-fill protocol in two real tap waters and one synthetic tap water (Table 4-2; Figure 4-2). For the tests in Blacksburg water, triplicate ¾-in (1.9 cm) diameter, 4-in (10.2 cm) long galvanized steel pipes with and without copper were used and water was changed three times per week. To test the effect of copper on unlined iron mains, small iron coupons were embedded in stoppers and placed in PVC pipes with the same dimensions as the galvanized steel pipes. In these tests, copper was dosed as copper (II) sulfate ($CuSO_4$) at 0.2 mg/L Cu throughout the experiment; magnesium sulfate ($MgSO_4$) was added to the controls to give the same ionic strength for both conditions. The case study tests also used triplicate ¾-in (1.9 cm) diameter pipes, but pipe sections were 12-in (30.5 cm) in length and water was changed only twice per week; copper was dosed at 0.5 mg/L Cu

using $CuSO_4$. In the synthetic water tests, five replicate 12-in (30.5 cm) pipe nipples and a much higher copper level of 10 mg/L were used, with water changes three times per week, but dosing occurring only once/week (on Fridays) for the first eight weeks of the 24-week experiment. Three different copper oxidation states were tested in this experiment; the copper (0) condition was dosed as powdered copper metal, the copper (I) condition as copper (I) chloride (CuCl), and the copper (II) condition as copper (II) chloride ($CuCl_2$). The concentration of sodium chloride (NaCl) in the synthetic water was adjusted to give the same chloride concentration for all conditions. In all three tests, the entire volume was collected from the pipe as a weekly composite and acidified to 2% in the sampling bottle with nitric acid, thoroughly shaken, and allowed to digest for 48 hours before analysis by ICP-MS as above.

Flow Testing. Two different experiments were conducted using a recirculating setup with a reservoir volume of 15.5 L (Figure 4-2). The first experiment was an extension of the synthetic cold water dump-and-fill study above. Two of the five pipe nipples from the cold water Control, Cu(I), and Cu(II) conditions were selected and placed into a recirculating loop with no additional copper dosing. Synthetic water *without* copper, but with otherwise the same water chemistry as the previous test (Table 4-2) was changed in the reservoir once/week for eleven weeks. The second experiment started with new galvanized steel pipe nipples for the same three conditions (Control, Cu(I), Cu(II)) using the same synthetic base water (Table 4-2; Figure 4-2). For the first two weeks of the second experiment, copper was dosed at a concentration of 10 mg/L to the reservoir; for the remaining weeks, the control water was used for all conditions. At the end of eleven weeks, a 3-in (7.6 cm) section was cut from the inlet of each pipe for analysis and results were compared with the two-phase test. To gain insight into longer-term effects, the remaining 9-in (22.9 cm) of pipe were returned to the recirculating setup and supplied with control water for six additional months. For both experiments, measurements of dissolved oxygen (optical probe, Hamilton), total chlorine (Hach colorimetric method), and pH were made at the beginning and end of the week. At the beginning of the week when the water was fresh, the corrosion potential (E_{corr}) was also measured using a reference electrode (Ag/AgCl) and a digital multimeter (RadioShack 22-811). To allow for more accurate measurement of total metals, the entire volume of the reservoir was acidified to pH 2 with nitric acid at the end of each week and allowed to sit a minimum of 24 hours before sampling for analysis by ICP-MS.

Surface Analysis. For case study pipe sections, the percentage of the area covered with visible rust deposits was used as one indicator of corrosion activity, and was determined using ImageJ software (NIH). To determine the copper concentration in these scales, sections of scale were removed and digested using a mixture of nitric acid and hydroxylamine hydrochloride. For laboratory pipes, the concentration of copper on the surface of the galvanized steel pipes was measured using a handheld x-ray fluorescence (XRF) analyzer (Innov-X Alpha 800 LZX). Small (approximately 1-in (2.5 cm) square) sections of both field and laboratory pipe samples were imaged using an FEI Quanta 600 FEG environmental scanning electron microscope (ESEM) equipped with an energy-dispersive spectrometer for elemental analysis (EDS; Bruker). All samples were sputtered with gold/palladium before analysis, and an accelerating voltage of 20 kV was used. Both secondary electron (ETD) and backscatter (BSED) images were taken during this work.

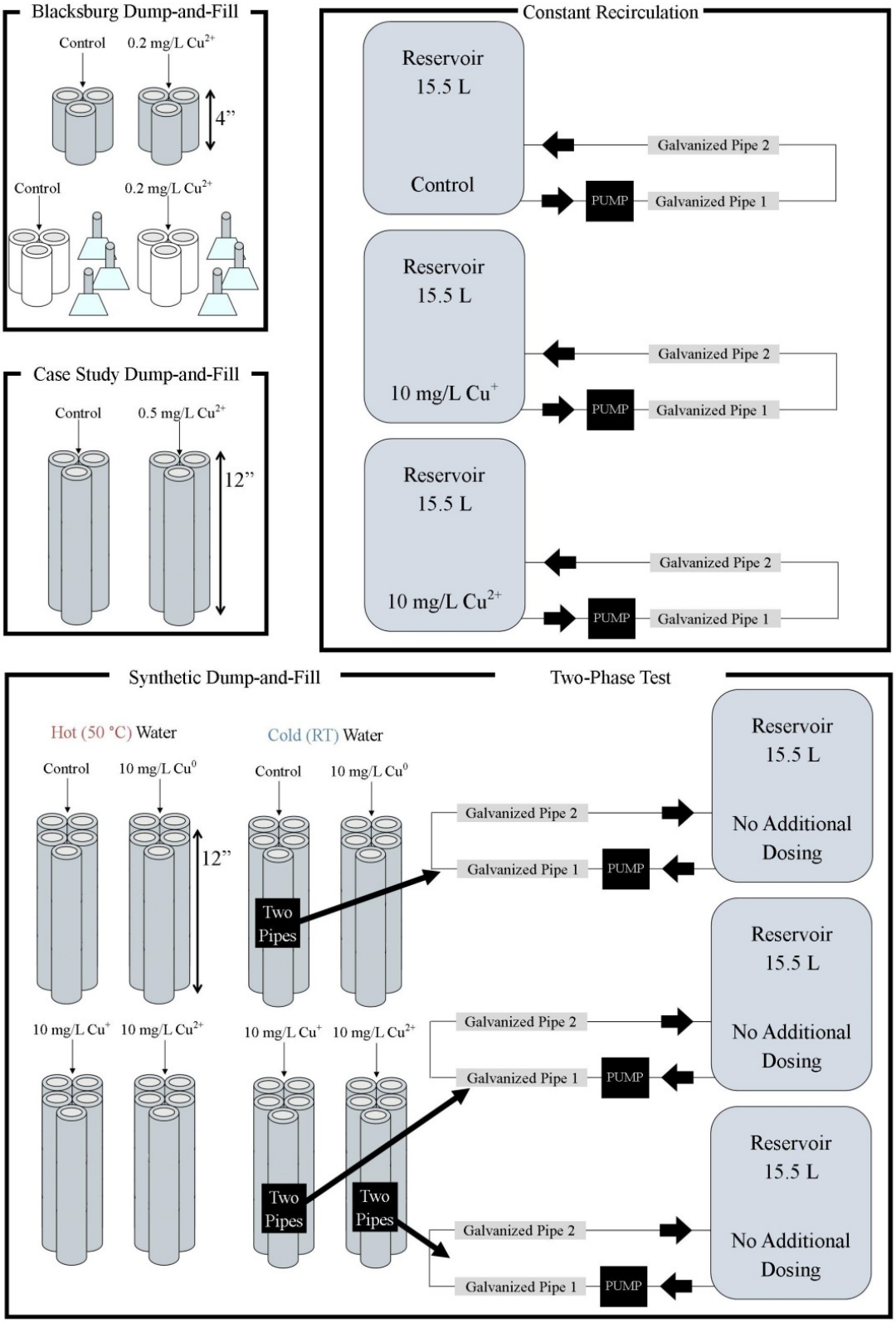

Figure 4-2. Illustration of all laboratory studies including dump-and-fill tests in three different waters (Blacksburg water, case study water, and synthetic water) and both the “two-phase” recirculating test and the “constant recirculation” test.

RESULTS AND DISCUSSION

After examining the mechanisms and practical electrochemistry of copper plating kinetics under conditions relevant to potable water, a variety of laboratory and field studies were undertaken to quantify impacts of deposition corrosion under an array of copper concentrations and flow conditions. Both pipes harvested from the case study building and samples generated during the laboratory studies were then examined by surface analysis techniques to establish a basis for forensic evaluations of pipe failures observed in practice.

Effect of Soluble Copper Concentration on the Plating Phase. LSV scans at different added phosphate concentrations demonstrated that the extent of plating generally decreased as higher concentrations of phosphate were added to the copper plating solution (Figure 4-3[a]). To put the reported phosphate values in practical context, at the lowest total phosphate dose (1 mg/L), 90% of the original copper remained soluble and the residual phosphate concentration was low (0.04 mg/L as P). However, at the highest total phosphate dose (25 mg/L), only 4% of the original copper was soluble and the residual phosphate concentration was nearly 8 mg/L. Negative currents (indicative of copper plating reactions) increased slightly for the lowest dose of phosphate compared to the control without phosphate, suggesting that a small amount of phosphate could actually increase the extent of copper plating. In general, however, the extent of plating, as measured by both the maximum current (i.e., the plating rate) and the total mass of copper plated on the platinum working electrode, was strongly correlated to the soluble copper concentration (Figure 4-3[b]). In order to estimate the mass of copper plated on the surface during the scanning potential tests, the current/time curves (Figure 4-3[a]) were integrated, assuming a two-electron transfer (Cu^{2+} to Cu^{0}). The resulting estimated mass was in reasonable agreement with the mass measured by dissolution of the plated copper, with an average relative percent difference (RPD) of only 26% (Figure 4-4[a]).

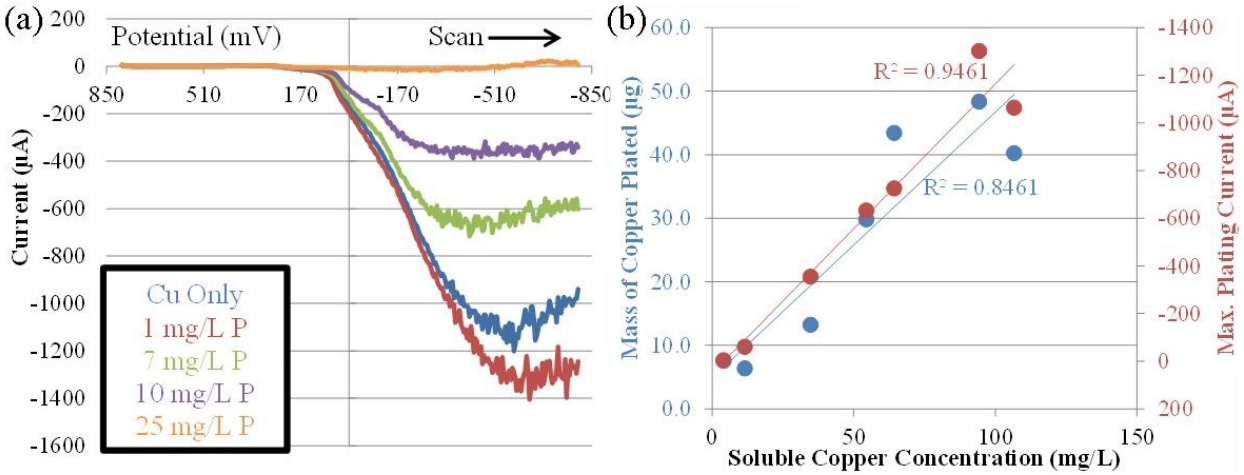

Figure 4-3. Results of LSV tests showing (a) current as a function of potential during an LSV scan at varying levels of added phosphate; (b) a strong correlation between the soluble copper concentration and both the mass of copper plated during the test (blue) and the maximum plating current (I_{max}; red)

Fixed potential tests at several different applied potentials between -800 and +800 mV (versus Ag/AgCl) showed the expected sharp drop in the mass of copper plated between 0 and 100 mV, with as much as 80 µg of copper plated below 0 mV, no significant plating occurring above 100 mV, and an intermediate amount of plating at 50 mV (Figure 4-4[b]). Therefore, the plating threshold for copper under the conditions used in this study is between 0 – 100 mV Ag/AgCl, which is much more positive than the surface potential expected for galvanized steel pipe under these conditions (-500 to -800 mV), demonstrating that copper plating is generally thermodynamically favorable in aerated potable water.

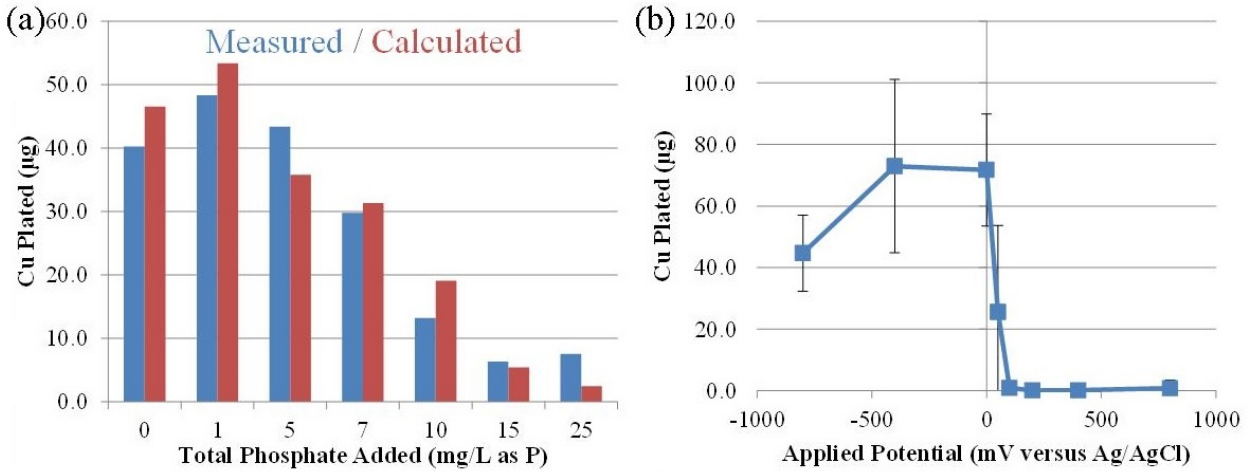

Figure 4-4. Mass of copper plated on the platinum electrode during (a) LSV tests comparing the actual copper measured by dissolution in nitric acid (blue) with the theoretical mass calculated by integrating the curves in Figure 4-2a (red); (b) fixed potential tests showing the effect of applied potential on copper plating, and revealing a threshold for copper plating between 0 – 100 mV (versus Ag/AgCl).

Dump-and-Fill Testing: Results and Limitations. In general, the dump-and-fill experiments showed only a small effect on corrosion rate of iron and galvanized steel as the concentration of copper increased (Table 4-3). In the Blacksburg water experiments, which had the longest duration but the lowest copper dose (0.2 mg/L), no significant difference in iron or zinc release was ever observed for galvanized steel pipe when copper was added, and a small but statistically significant 1.5X increase in unlined iron corrosion was observed with added copper (Table 4-3). It is also important to note that the Blacksburg test water used phosphate as a corrosion inhibitor, which plating tests indicated could lower the concentration of soluble copper to the point that plating does not occur in the short term. Tests in the case study tap water demonstrated larger, but less consistent effects; increases in zinc release of 2X and iron release of 3X were observed with 0.5 mg/L added copper, but were erratic and not always statistically significant (Table 4-3). In a final attempt to capture deposition corrosion effects using a dump-and-fill method, high copper doses of 10 mg/L and a larger number of replicates (5) were used in a synthetic water, which gave much more consistent water quality than possible in real tap waters. For three different species of copper (Cu^0, Cu^+, and Cu^{2+}) and both hot and cold water, effects of added copper on metal release from galvanized steel pipe remained relatively small (on the order of 2X increases in both Zn and Fe release) but statistically significant (Table 4-3). The mismatch between the relatively benign results of the dump-and-fill tests and the dramatic deposition corrosion failures observed in the field indicated that simple batch tests were unlikely to reproduce the failures.

Table 4-3. Summary of Dump-and-Fill Deposition Corrosion Experiments

Material, Water Type	Copper Dosing	Time Frame	Metal Release Compared to Control
Galvanized Pipe, Blacksburg Water	0.2 mg/L Cu(II)	8 months (always dosing)	No Diff. Zn (p = 0.41) No Diff. Fe (p = 0.85)
Iron Coupons, Blacksburg Water	0.2 mg/L Cu(II)	8 months (always dosing)	1.5X Fe (p = 9E-12)
Galvanized Pipe, Case Study Water	0.5 mg/L Cu(II)	3 months (always dosing)	No Diff. Zn (p = 0.14) 3.3X Fe (p = 0.03)
Galvanized Pipe, Case Study Softened	0.5 mg/L Cu(II)	3 months (always dosing)	2.1X Zn (p = 0.02) No Diff Fe (p = 0.35)
Galvanized Pipe, **COLD**[a] Synth Water	10 mg/L Cu(0)	6 months (dosing 2 months)	1.4X Zn (p = 1E-4) No Diff. Fe (p = 0.22)
Galvanized Pipe, **COLD**[a] Synth Water	10 mg/L Cu(I)	6 months (dosing 2 months)	1.7X Zn (p = 5E-11) No Diff. Fe (p = 0.42)
Galvanized Pipe, **COLD**[a] Synth Water	10 mg/L Cu(II)	6 months (dosing 2 months)	1.3X Zn (p = 0.002) No Diff. Fe (p = 0.23)
Galvanized Pipe, **HOT**[a] Synth Water	10 mg/L Cu(0)	6 months (dosing 2 months)	1.3X Zn (p = 0.02) No Diff. Fe (p = 0.42)
Galvanized Pipe, **HOT**[a] Synth Water	10 mg/L Cu(I)	6 months (dosing 2 months)	2.4X Zn (p = 4E-6) 1.7X Fe (p = 0.04)
Galvanized Pipe, **HOT**[a] Synth Water	10 mg/L Cu(II)	6 months (dosing 2 months)	2.0X Zn (p = 2E-9) 1.6X Fe (p = 0.03)

[a] COLD = room temperature; HOT = 50 °C

Flow Testing. To test the hypothesis that frequent or continuous flow was necessary to drive deposition corrosion, pipes from the synthetic water dump-and-fill test (Figure 4-2, Table 4-3) – two each from the cold water Control, cold water Cu(I), and cold water Cu(II) conditions – were placed into a recirculating flow setup with *no additional copper dosing*. Despite the fact that no additional copper was added, the Cu(I) condition exhibited cumulative zinc release 4.6X higher and iron release 29X higher than the control during eleven weeks of recirculation (Table 4-4, "Two-Phase"). The Cu(II) condition had a similar, but less dramatic result, with 2.5X higher zinc and 4X higher iron (Table 4-4). The conditions with copper also exhibited other markers of accelerated corrosion rate including lower final dissolved oxygen, higher chlorine consumption, and higher final pH than the controls, some of which were statistically significant for the Cu(I) condition when a t-test paired by sampling date was used (Table 4-4). The sudden increase in corrosion rate when switching the same pipes from stagnant to recirculating conditions provides support for the hypothesis that mass transport of oxidants was a limiting factor in earlier tests during the corrosion phase. Moreover, this test showed that even when the plating phase occurred largely during stagnation events, it had a very persistent and devastating impact on the long-term corrosion behavior once flow resumed.

Table 4-4. Comparison of Constant Recirculation to "Two-Phase" Testing at 11 Weeks

	Two-Phase[a]	Constant Recirculation[b]
Cumulative Zn Release	Cu(I) 4.6X Higher than Ctrl Cu(II) 2.5X Higher than Ctrl	Cu(I) 5.2X Higher than Ctrl Cu(II) 7.7X Higher than Ctrl
Cumulative Fe Release	Cu(I) 29X Higher than Ctrl Cu(II) 4X Higher than Ctrl	Cu(I) 41X Higher than Ctrl Cu(II) 55X Higher than Ctrl
Final DO (Week 1)	Ctrl 6.45, Cu(I) 6.85, Cu(II) 8.96	Ctrl 7.26, Cu(I) 6.63, Cu(II) 6.59
Final DO (Week 11)	Ctrl 7.30, Cu(I) 6.63, Cu(II) 6.96	Ctrl 7.24, Cu(I) 7.08, Cu(II) 7.18
Significant Diff. in DO?[c]	**NO** Cu(I) (p = 0.64) **NO** Cu(II) (p = 0.19)	**YES** Cu(I) (p = 0.0004) **YES** Cu(II) (p = 0.006)
% Cl_2 Consumed (Wk 1)	Ctrl 99%, Cu(I) 98%, Cu(II) 92%	Ctrl 34%, Cu(I) 59%, Cu(II) 28%
% Cl_2 Consumed (Wk 11)	Ctrl 86%, Cu(I) 98%, Cu(II) 98%	Ctrl 49%, Cu(I) 66%, Cu(II) 59%
Significant Diff. in Cl_2?[c]	**YES** Cu(I) (p = 0.0008) **NO** Cu(II) (p = 0.37)	**YES** Cu(I) (p = 0.008) **YES** Cu(II) (p = 0.004)
Final pH (Week 1)	Ctrl 8.05, Cu(I) 9.58, Cu(II) 9.63	Ctrl 7.51, Cu(I) 8.45, Cu(II) 8.28
Final pH (Week 11)	Ctrl 7.69, Cu(I) 7.92, Cu(II) 7.71	Ctrl 7.59, Cu(I) 7.67, Cu(II) 7.75
Significant Diff. in pH?[c]	**YES** Cu(I) (p = 0.003) **NO** Cu(II) (p = 0.13)	**YES** Cu(I) (p = 0.007) **YES** Cu(II) (p = 0.001)

[a]At the end of the dump-and-fill experiments with synthetic cold water (Table 4-2), two pipes were placed into a recirculating loop with no additional dosing.
[b]Pipes placed under constant recirculation and dosed for two weeks, then run for nine additional weeks with no dosing.
[c]Paired t-tests (by sampling date) for weekly measurements (n = 11); 95% confidence level

To determine whether mass transport of copper to the surface was also a limiting factor in the dump-and-fill studies, an additional test was conducted in which both the plating phase and the corrosion phase occurred under flowing conditions. After eleven weeks, results were even more dramatic than those observed in the previous test, with cumulative zinc release 5X-7X higher and cumulative iron release 41X-55X higher than the control (Table 4-4, Figure 4-5[a]). In this test, the decrease in dissolved oxygen, increase in chlorine demand, and increase in pH compared to the control were all statistically significant for both the Cu(I) and Cu(II) conditions (Table 4-4). This result implied that deposition corrosion impacts are most devastating when high copper concentrations are present under constant flowing conditions, as occurs in hot water recirculating systems.

Measurements of the corrosion potential (E_{corr}) in this study also supported the hypothesis that deposition corrosion was occurring (Figure 4-5[b]). When copper was added, the E_{corr} shifted positively by as much as 300 mV, which would be expected if copper, which has a much more positive corrosion potential than zinc or iron, was progressively plating on the surface. In contrast, for the control, E_{corr} remained relatively constant (within 30 mV) throughout the first 11 weeks. Interestingly, the deposition corrosion effect was much more pronounced on the first pipe in flow than on the second pipe, which was odd, given that the copper concentration was the

same throughout the solution, and might be due to a turbulent flow (entry) effect, which has been documented in the literature.[40]

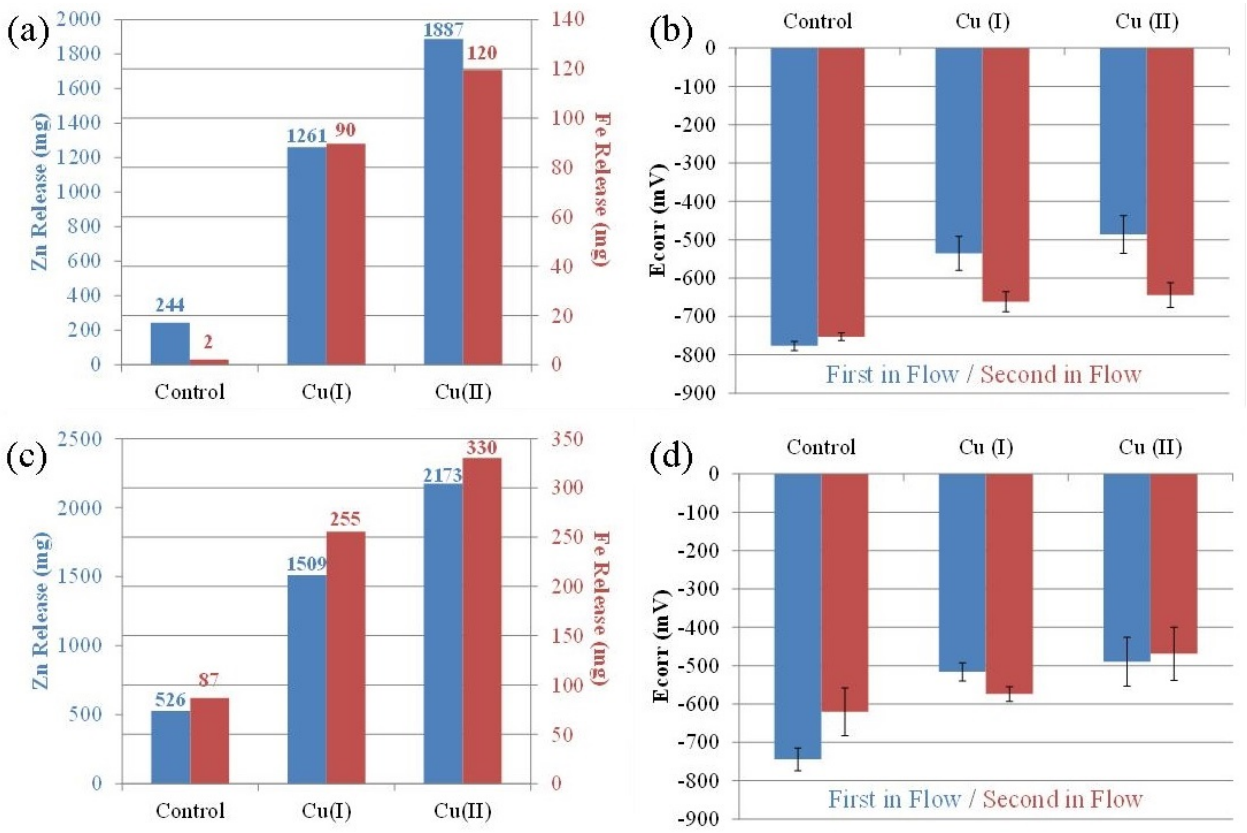

Figure 4-5. Results from laboratory deposition corrosion test with constant recirculation including (a) cumulative mass of zinc (blue) and iron (red) released after the first 11 weeks; (b) average corrosion potential (E_{corr}) for the first 11 weeks in the first (blue) and second (red) pipes in flow for each condition; (c) update to the data in (a) after an additional 6 months; (d) update to the data in (b) after an additional 6 months

As the test continued without additional copper dosing, the differences between the control and copper-dosed conditions lessened, but did not disappear (Figure 4-5[c],[d]). Even more than six months after the initial exposure to copper, zinc and iron levels remained 3X-4X higher than the control (Figure 4-5[c]), and E_{corr} remained more than 200 mV positive-shifted (Figure 4-5[d]). Clearly, even short-term exposure to high levels of copper, such as when a new copper pipe or brass fitting is installed upstream, can have a lasting impact on the corrosion rate and lifetime of galvanized steel pipe.

Comparing Laboratory Experience with Case Study Analysis. Both the samples generated in the constant recirculation study and pipes harvested from the case study building were examined for evidence of pure copper deposits.

For the case study building described in the introduction, investigation of removed pipe sections revealed evidence of attack consistent with deposition corrosion, especially in the hot water recirculating system, as expected based on previous work.[4, 7] Localized attack was visually

obvious (Figure 4-6[a]), with severity increasing from the entrance of the building (no copper present in water) to the cold water system (small amounts of copper present in water) to the hot water system (high copper levels present in water due to recirculation). This observation was quantified as the percent of the surface covered with scale in the samples received from the site (Figure 4-6[b]). To determine whether deposition corrosion was occurring, small pieces of pipe scale from each location were dissolved and analyzed using ICP-MS for copper content (Figure 4-6[c]). As expected for deposition corrosion, as the percentage of copper in the scale increased, so did the severity of attack. In the hot water recirculating system, percent levels (2-3%) of copper were measured on the surface.

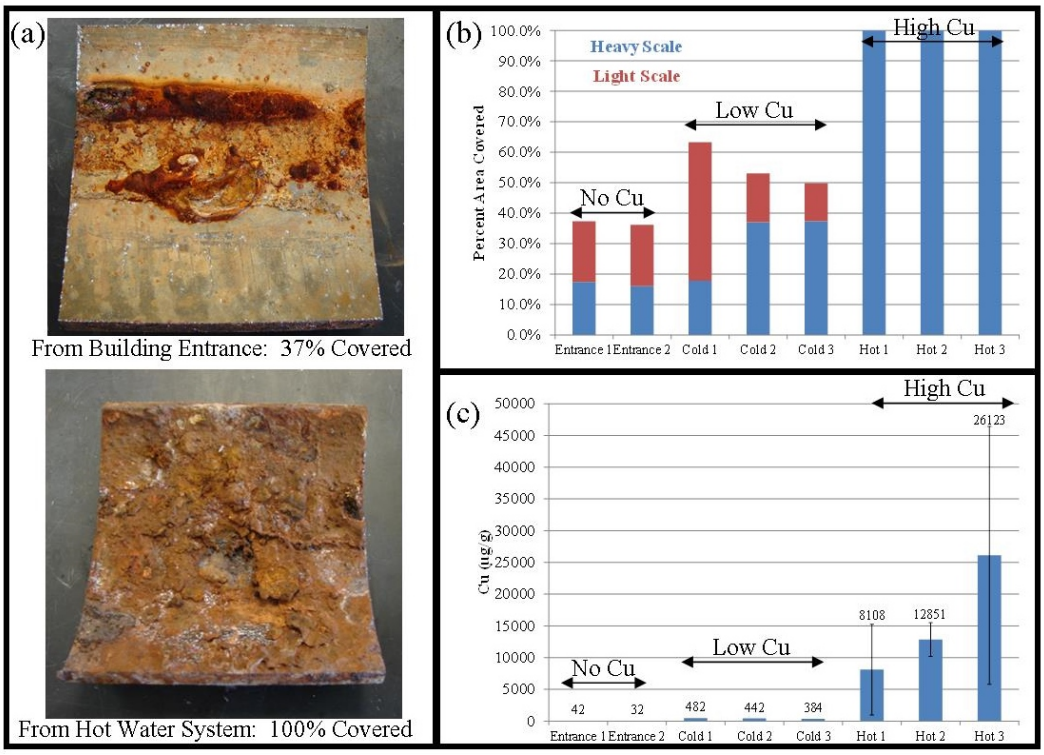

Figure 4-6. Analysis of pipe samples from case study location including (a) photos of pipe samples from building entrance (top) and hot water system (bottom); (b) percent area covered with scale for when no, low, or high Cu is present in water; (c) concentration of copper in scale for measured for the pipe sections in (b)

In the constant recirculation laboratory test, a similarly dramatic result was achieved (Figure 4-7). Again, the difference between the control and the conditions with copper was visually obvious (Figure 4-7[a]), with some visual evidence of the initiation of localized corrosion in the first pipe section after only eleven weeks. The percentage of copper on the surface was also similar to that in the case study (Figure 4-7[b]), with levels as high as 3% observed on the first pipe section and lower levels on the second pipe section. This is also consistent with the earlier E_{corr} results (Figure 4-5[b]), which showed a more dramatic positive shift in these early pipe sections.

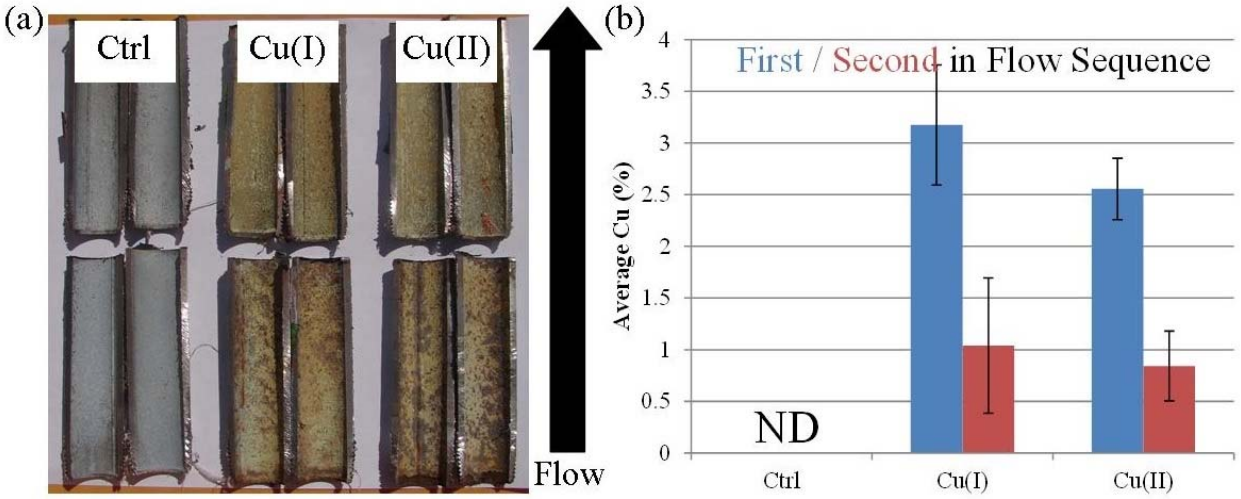

Figure 4-7. Analysis of pipe samples from laboratory deposition corrosion tests after 11 weeks including (a) a photo of the interior pipe surfaces and (b) concentration of copper in the scale by XRF. Values reported are averages of four different points on the pipe surface; error bars represent 95% confidence intervals. ND = non-detect.

In order to determine whether the surface deposits were present as discrete "islands" of pure copper, as expected for deposition corrosion, a combination of SEM and EDS was used. Although EDS cannot determine oxidation state, it was hypothesized that the copper to oxygen atomic ratio could provide insight into the copper oxidation state. Ideally, copper (II) oxide (CuO) would have a copper:oxygen ratio of 1, copper (I) oxide (Cu_2O) would have a copper:oxygen ratio of 2, and pure copper would have no oxygen present. In reality, surface oxidation of pure copper leads to a detectable oxygen signal; in this work, a pure copper sheet gave a copper:oxygen ratio of 2.8-3.0. However, although analysis of newly purchased Cu_2O particles gave an average copper:oxygen ratio of 1.9, close to the expected ratio of 2.0, over a large area, the copper:oxygen ratio in the sample ranged from 1.8 to 5.5, depending on particle size. Based on these results, it is not possible to distinguish reliably between true Cu^0 deposits and copper oxides using EDS.

Despite the limitations of the technique, SEM/EDS analysis of both laboratory (Figure 4-8[a],[b]) and field (Figure 4-8[c],[d]) pipes did reveal discrete "islands" of copper on the surface consistent with a deposition corrosion mechanism. Comparison of electron images from field and laboratory samples (Figure 4-8[a],[c]) indicates that the two types of samples have a similar copper deposit morphology.

For the laboratory sample, the copper-rich deposits can be clearly identified using EDS mapping, which colors the image based on the relative elemental composition at each pixel (Figure 4-8[b]). In this image, copper-rich regions are shown in red. Quantitative analysis of the EDS signal gave a copper:oxygen ratio of 2.3, which could be consistent with pure copper, but is not definitive evidence of pure copper, as explained above. However, despite their similar morphology, copper-rich deposits on field samples gave less dramatic EDS maps (Figure 4-8[d]) and had a much lower copper:oxygen ratio of 0.4. Differences are likely due to many factors including smaller visible copper deposits, resulting in lower overall signal within the deposit,

increased exposure to air during harvesting, shipping, and storage, and the more complex water chemistry and interactions present in real water systems compared to the laboratory study.

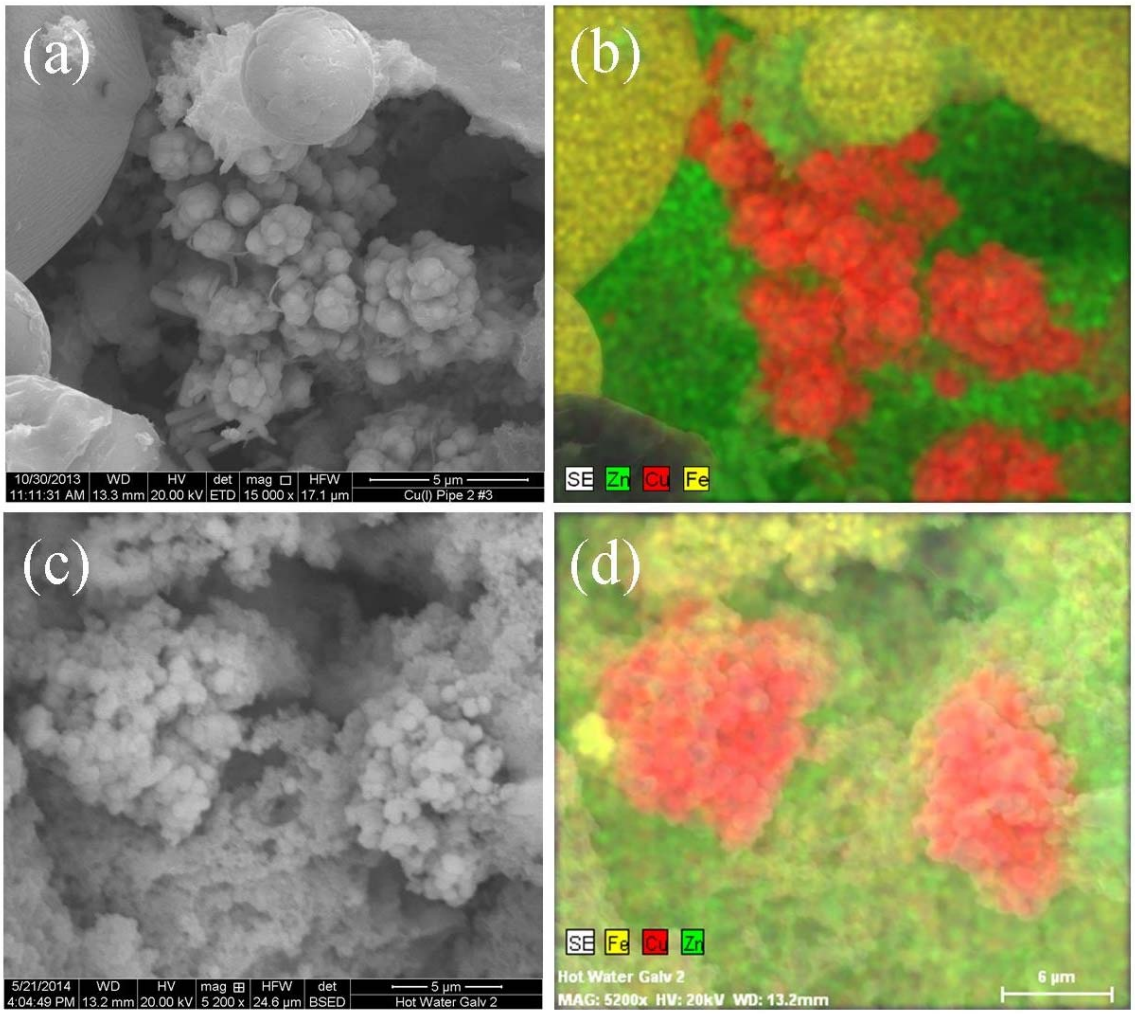

Figure 4-8. ESEM images showing Cu deposits on the surface of (a,b) lab and (c,d) field samples. (a) shows an electron image of copper deposits on a galvanized pipe sample from the laboratory recirculating tests; (b) shows an EDS element map for the same area. The red area represents copper and has the composition 62% Cu, 27% O, 4% Fe, 7% Zn. (c) shows an electron image of copper deposits on a galvanized pipe sample from the case study field site; (d) shows an EDS map for the same area. Again, the red area represents copper, this time with the composition 19% Cu, 52% O, 2.5% Fe, 11.5% Zn, 14% Cl.

CONCLUSIONS

Mechanistically-based potentiostat experiments for copper plating, bench-scale corrosion tests with copper, and surface analysis of both field and laboratory samples for copper deposits yielded the following conclusions:

- LSV tests on platinum electrodes in the presence of copper solutions with and without phosphate demonstrated that both the plating rate and mass of copper plated are strongly

correlated with the soluble copper concentration in solution, and implied that the addition of phosphate corrosion inhibitors can provide some protection against deposition corrosion.

- Fixed potential tests at copper concentrations more representative of real systems determined a threshold plating potential between 0-100 mV versus Ag/AgCl (222-322 mV versus SHE) under the conditions used for the laboratory experiments.
- Dump-and-fill experiments using multiple tap water chemistries were unable to reproduce the devastating increases in corrosion rate expected from field experiences with deposition corrosion, but had measurable average increases in metal release of 2-3 times when copper was added.
- Recirculating tests were much more successful than dump-and-fill experiments in reproducing deposition corrosion effects, with up to a 7X increase in zinc and 55X increase in iron release with copper compared to the control. Dramatic increases in metal release were also present when pipes were plated in dump-and-fill tests and switched to a recirculating setup for corrosion testing, implying that the increased mass transport of oxidants to the surface was a key factor in the corrosion phase.
- Taken together, the results of the laboratory tests suggest that recirculating systems represent a worst-case scenario for deposition corrosion. This is concerning, given recent trends in large building construction, in which hot water recirculating systems are being required to further water conservation and pathogen control efforts.
- Copper-rich "islands" were successfully identified on the surface of both field and laboratory pipes using SEM-EDS. Due to limitations of the technique, it was impossible to distinguish whether these deposits were plated copper metal or copper (I) oxides; however, the presence of these deposits does provide strong circumstantial evidence of a deposition corrosion mechanism.

ACKNOWLEDGEMENTS

The authors acknowledge the financial support of the National Science Foundation under NSF CBET SusChEM GOALI 1336616 and the Graduate Research Fellowship Program (GRFP), as well as the support of the American Water Works Association through the Abel Wolman Fellowship. Opinions and findings expressed herein are those of the authors and do not necessarily reflect the views of the NSF or AWWA. The authors would also like to acknowledge the Virginia Tech ICTAS Nanoscale Characterization and Fabrication Laboratory (NCFL) for use of the ESEM.

REFERENCES

1. M. Edwards, "Controlling Corrosion in Drinking Water Distribution Systems: A Grand Challenge for the 21st Century," *Water Science and Technology* 49, 2 (2004): p. 1-8.
2. L.S. McNeill and M. Edwards, "Iron Pipe Corrosion in Distribution Systems," *Journal AWWA* 93, 7 (2001): p. 88-100.

3. American Water Works Association. "Buried No Longer: Confronting America's Water Infrastructure Challenge," 2012, http://www.awwa.org/Portals/0/files/legreg/documents/BuriedNoLonger.pdf;
4. H. Cruse, "Dissolved-Copper Effect on Iron Pipe," *Journal AWWA* 63, 2 (1971): p. 79-81.
5. K.P. Fox, C.H. Tate, G.P. Treweek, R.R. Trussel, A.E. Bowers, M.J. McGuire, and D.D. Newkirk, "Copper-Induced Corrosion of Galvanized Steel Pipe." 1986.
6. G.B. Hatch, "Control of Couples Developed in Water Systems," *Corrosion* 11, 1 (1955): p. 15-22.
7. L. Kenworthy, "The Problem of Copper and Galvanized Iron in the Same Water System," *The Journal of the Institute of Metals* 69, (1943).
8. C.B. Muchmore, "Algae Control in Water-Supply Reservoirs," *Journal AWWA* 70, 5 (1978): p. 273-279.
9. H.K. Hudnell, "The state of U.S. freshwater harmful algal blooms assessments, policy and legislation," *Toxicon* 55, 5 (2010): p. 1024-1034.
10. C.L. Murray-Gulde, J.E. Heatley, A.L. Schwartzman, and J.J.H. Rodgers, "Algicidal Effectiveness of Clearigate, Cutrine-Plus, and Copper Sulfate and Margins of Safety Associated with Their Use," *Archives of Environmental Contamination and Toxicology* 43, 1 (2002): p. 19-27.
11. W. Bishop, B. Willis, and C.T. Horton, "Affinity and Efficacy of Copper Following an Algicide Exposure: Application of the Critical Burden Concept for Lyngbya wollei Control in Lay Lake, AL," *Environmental Management*, (2014): p. 1-8.
12. W. Zhan, A. Sathasivan, C. Joll, G. Wai, A. Heitz, and I. Kristiana, "Impact of NOM character on copper adsorption by trace ferric hydroxide from iron corrosion in water supply system," *Chemical Engineering Journal* 200, (2012): p. 122-132.
13. J.E. Stout and V.L. Yu, "Experiences of the first 16 hospitals using copper-silver ionization for Legionella control: implications for the evaluation of other disinfection modalities," *Infection Control and Hospital Epidemiology* 24, 8 (2003): p. 563-568.
14. American Water Works Association, *Corrosion Control for Operators* (Denver, CO: American Water Works Association, 1986).
15. NACE, *Prevention & Control of Water-Caused Problems in Building Potable Water Systems* 2nd ed (Houston: NACE International, 1995).
16. C. Noble, "Corrosion of Galvanized Piping in Domestic Water Systems," *The Conduit (M&M Engineering Associates, Inc.)* 13, 1 (2013): p. 1-3.
17. American Society of Heating Refrigerating and Air-conditioning Engineers Inc. (ASHRAE). "Proposed New Standard 188: Prevention of Legionellosis Associated with Building Water Systems. BSR/ASHRAE Public Review Draft," 2011, https://osr.ashrae.org/;
18. R.H. Brazeau and M.A. Edwards, "Role of Hot Water System Design on Factors Influential to Pathogen Regrowth: Temperature, Chlorine Residual, Hydrogen Evolution, and Sediment," *Environmental Engineering Science* 30, 10 (2013): p. 617-627.
19. S. Triantafyllidou and M. Edwards, "Galvanic Corrosion After Simulated Small-Scale Partial Lead Service Line Replacements," *Journal AWWA* 103, 9 (2011): p. 85-99.
20. C. Cartier, R.B. Arnold Jr, S. Triantafyllidou, M. Prévost, and M. Edwards, "Effect of Flow Rate and Lead/Copper Pipe Sequence on Lead Release from Service Lines," *Water Research* 46, 13 (2012): p. 4142-4152.

21. J. Hu, F. Gan, S. Triantafyllidou, C.K. Nguyen, and M. Edwards, "Copper-Induced Metal Release from Lead Pipe into Drinking Water," *Corrosion* 68, 11 (2012): p. 1037-48.
22. B.R. Kim, J.E. Anderson, S.A. Mueller, W.A. Gaines, and A.M. Kendall, "Literature Review -- Efficacy of Various Disinfectants Against *Legionella* in Water Systems," *Water Research* 36, (2002): p. 4433-44.
23. Q. Li, S. Mahendra, D.Y. Lyon, L. Brunet, M.V. Liga, D. Li, and P.J.J. Alvarez, "Antimicrobial nanomaterials for water disinfection and microbial control: Potential applications and implications," *Water Research* 42, 18 (2008): p. 4591-4602.
24. J.-Y. Bottero, J. Rose, and M.R. Wiesner, "Nanotechnologies: Tools for sustainability in a new wave of water treatment processes," *Integrated Environmental Assessment and Management* 2, 4 (2006): p. 391-395.
25. X. Qu, P.J.J. Alvarez, and Q. Li, "Applications of nanotechnology in water and wastewater treatment," *Water Research* 47, 12 (2013): p. 3931-3946.
26. H.P. Hack, *Galvanic Corrosion Test Methods* Corrosion Testing Made Easy, ed. B.C. Syrett(Houston, TX: NACE International, 1993).
27. H.P. Hack, ed. *Galvanic Corrosion* (Philadelphia, PA: ASTM, 1988).
28. D.A. Jones, *Principles and prevention of corrosion* 2nd ed (Englewood Cliffs, NJ: Prentice Hall, 1996), xvi, 572 p.
29. A.J. Bard and L.R. Faulkner, *Electrochemical Methods: Fundamentals and Applications (2nd Ed.)* 2nd ed (New York, NY: John Wiley & Sons, Inc., 2001).
30. N. Kanani, ed. *Electroplating and Electroless Plating of Copper & its Alloys* (Materials Park, OH: ASM International, 2003).
31. R.E. Hargrave, "Unusual Failures Involving Copper Deposition in Boiler Tubing," *Corrosion* 47, 7 (1991): p. 555-567.
32. S.C. Bose, S.V. Reddy, and K. Singh, "Interdependence of On-Load Corrosion, Creep-Rupture, and Copper Deposit in Augmenting Failure Processes of Boiler Tubes," *Corrosion* 56, 11 (2000): p. 1158-1169.
33. E. Mattsson and J.O.M. Bockris, "Galvanostatic studies of the kinetics of deposition and dissolution in the copper + copper sulphate system," *Transactions of the Faraday Society* 55, 0 (1959): p. 1586-1601.
34. P.M. Vereecken, R.A. Binstead, H. Deligianni, and P.C. Andricacos, "The Chemistry of Additivies in Damascene Copper Plating," *IBM Journal of Research and Development* 49, 1 (2005): p. 3-18.
35. American Water Works Association, *Internal corrosion of water distribution systems*: American Water Works Association, 1996).
36. J.P. Healy, D. Pletcher, and M. Goodenough, "The chemistry of the additives in an acid copper electroplating bath: Part I. Polyethylene glycol and chloride ion," *Journal of Electroanalytical Chemistry* 338, 1–2 (1992): p. 155-165.
37. J.P. Healy, D. Pletcher, and M. Goodenough, "The chemistry of the additives in an acid copper electroplating bath: Part II. The instability 4,5-dithiaoctane-1,8-disulphonic acid in the bath on open circuit," *Journal of Electroanalytical Chemistry* 338, 1–2 (1992): p. 167-177.
38. J.I. Goldstein, D.E. Newbury, P. Echlin, D.C. Joy, C.E. Lyman, E. Lifshin, L. Sawyer, and J.R. Michael, *Scanning Electron Microscopy and X-Ray Microanalysis (3rd Ed.)* (New York: Springer, 2003).

39. APHA, *Standard Methods for the Examination of Water and Wastewater* 20th ed: APHA, AWWA, WEF, 1998).
40. F.P. Berger and K.F.F.L. Hau, "Mass transfer in turbulent pipe flow measured by the electrochemical method," *International Journal of Heat and Mass Transfer* 20, 11 (1977): p. 1185-1194.

CHAPTER 5. COPPER DEPOSITION CORROSION ELEVATES LEAD RELEASE TO POTABLE WATER

Brandi Clark[a], Justin St. Clair[b], and Marc Edwards[a]

[a]Virginia Polytechnic Institute and State University, Blacksburg, Va.
[b] Apptech Solutions, Salem, Va.

ABSTRACT

Deposition corrosion has been identified as a possible factor contributing to consumer exposure to elevated lead in water after partial lead service line replacements (PLSLRs). Dump and fill tests in two different waters showed very different results, with one showing a substantial increase in lead leaching (approximately 3X) and the other showing little effect when copper was added compared to the control. These differences were consistent with expected trends based on copper solubility and the amount of copper deposited on the pipe. Detailed analysis of lead pipes from both laboratory studies and field tests were consistent with pure metallic copper deposits on the pipe surface, especially near the galvanic junction with copper, supporting a significant deposition corrosion mechanism.

This chapter is currently under review for publication in *Journal American Water Works Association*

INTRODUCTION

The practice of partial lead service line replacement (PLSLR), in which an existing lead service line is partially replaced with new copper pipe, has recently fallen into disfavor due to evidence that this practice leads to elevated lead in water in both the short and long term (American Academy of Pediatrics 2011; EPA National Drinking Water Advisory Council 2011; Triantafyllidou and Edwards 2011; United States Environmental Protection Agency 2011), potentially elevating blood lead and creating adverse health outcomes (Brown et al. 2011; Brown and Margolis 2012; Edwards 2013). Longer-term problems with elevated lead from PLSLRs can be due to two related mechanisms: galvanic corrosion and deposition corrosion (Britton and Richards 1981; Triantafyllidou and Edwards 2011; United States Environmental Protection Agency 2011). Galvanic corrosion arises from electrical contact between lead and copper, sacrificing lead and accelerating its corrosion rate (Dudi 2004). In deposition corrosion, copper dissolves from the new upstream pipe and re-deposits downstream on the lead pipe, potentially creating a large number of micro-galvanic cells over the lead pipe surface (Britton and Richards 1981; Dudi 2004; Triantafyllidou and Edwards 2011).

Although deposition corrosion has been acknowledged as a contributing factor to elevated lead in water in several studies (Britton and Richards 1981; Triantafyllidou and Edwards 2011; Cartier et al. 2012; Giammar et al. 2012; St. Clair 2012), the majority of recent work on PLSLRs has focused on the effect of water chemistry on galvanic current (Triantafyllidou and Edwards 2011; Zhou 2013), flow rate and pattern (Arnold and Edwards 2012; Cartier et al. 2012; St. Clair 2012), and connection practices (Clark et al. 2013; Wang et al. 2013). Based on a review of the data available, the EPA Science Advisory Board (SAB) recommended the installation of dielectrics to eliminate the increased lead risks associated with galvanic corrosion, but acknowledged that this would not eliminate deposition corrosion, and that the relative contribution of deposition corrosion compared to galvanic corrosion in elevated lead release after PLSLR was unknown (United States Environmental Protection Agency 2011).

Copper Upstream of Iron or Lead: A "Disastrous" Flow Sequence. Most previous work on deposition corrosion in potable water systems has focused on copper-induced corrosion of galvanized steel (Kenworthy 1943; Hatch 1955; Cruse 1971; Fox et al. 1986); however, the "disastrous" increase in corrosion rate observed in the field for galvanized steel (Cruse 1971) led to general recommendations against ever installing noble metals (e.g. copper) upstream of less noble metals (e.g. lead) (Copper Development Association 1999). The importance of flow sequence leads to two different scenarios for lead/copper galvanic connections with potentially different lead release behavior. For lead upstream of copper, such as a lead service line connected to copper premise plumbing, galvanic corrosion might be expected to be the dominant mechanism, with deposition corrosion being limited to the area near the joint due to migration of copper ions upstream during stagnation (Figure 5-1a). However, for lead downstream of copper, such as in PLSLRs, deposition corrosion can occur over the entire surface due to continuous transport of the released copper with flow, and the relative importance of deposition corrosion compared to galvanic corrosion may increase substantially (Figure 5-1b). Furthermore, it has been hypothesized that the relative importance of these two mechanisms shifts over time, with deposition corrosion becoming more pronounced with time as copper deposits continue to form on the lead pipe surface (Dudi 2004). This hypothesis is consistent with previous results in a

long-term pilot study, which found that while the lead concentration at high flow rate decreased with time for both pure lead pipe and lead upstream of copper, it increased with time for lead pipe downstream of copper (St. Clair 2012).

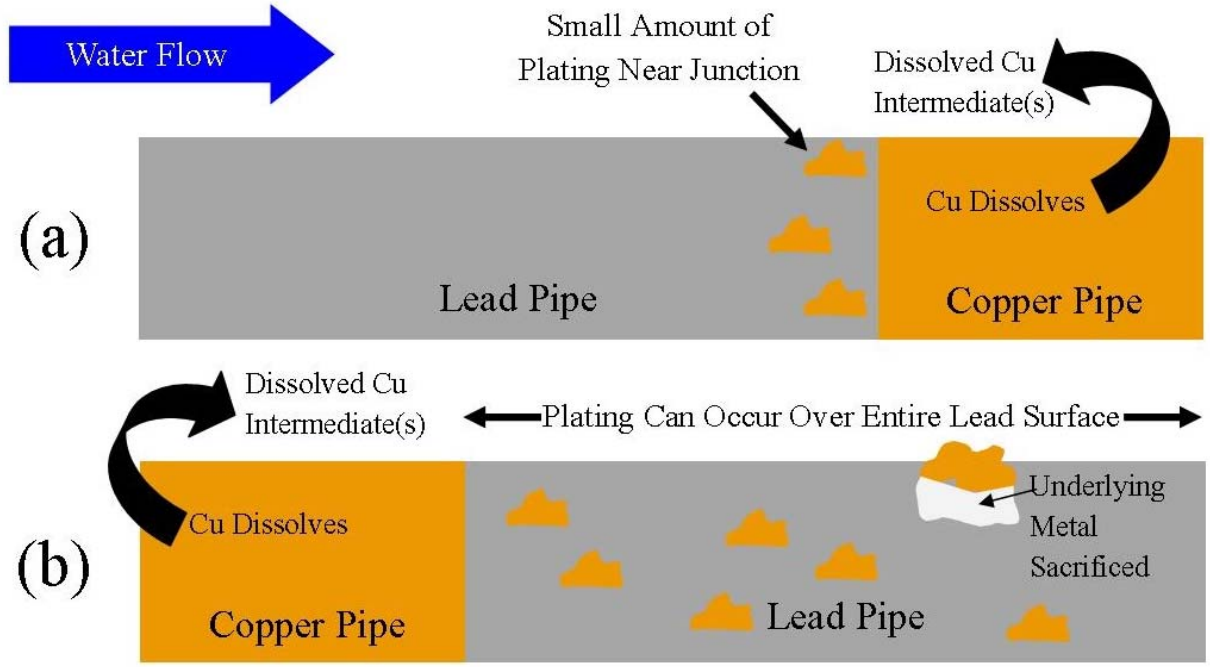

Figure 5-1. Diagram illustrating two different lead-copper configurations and their potential for deposition corrosion; (a) represents the case in which copper pipe is located *downstream* of lead (premise plumbing with lead service line), resulting in little potential for deposition corrosion; (b) represents the case in which copper is located *upstream* of lead pipe (PLSLR), potentially allowing deposition to occur over the whole lead pipe surface.

Previous Work. Only one recent study has explicitly investigated the effects of dissolved copper ions on lead corrosion (Hu et al. 2012). Under flowing conditions, lead release increased 5-7 times with the addition of 5 mg/L copper compared to the control (Hu et al. 2012). However, in stagnant tests, the same concentration of copper was associated with smaller increases in lead release, up to 2 times (Hu et al. 2012). This is consistent with previous work for galvanized steel, which found more dramatic effects at the same copper dose in flow-through tests compared to batch tests (Fox et al. 1986). However, despite documenting a link between copper dose and increased lead corrosion rate, this previous study did not determine whether deposits on the lead pipe surface were consistent with metallic copper and a deposition corrosion mechanism (Hu et al. 2012).

One important but little-studied aspect of deposition corrosion is the effect of water chemistry on the extent of copper plating. Based on expectations from both thermodynamic and mechanistic experience reported by the plating industry (Mattsson and Bockris 1959; Vereecken et al. 2005), the speciation of copper is expected to be important, with soluble copper (I) species expected to plate much more readily than soluble copper (II) species. Changes in water chemistry that affect copper solubility, such as increased pH and the addition of orthophosphate inhibitors provide a possible mitigation strategy for deposition corrosion effects regardless of speciation (Chapter 4).

Objectives. In this work, the extent to which deposition corrosion can occur in PLSLRs was investigated through bench scale experiments in two waters using three different copper species: copper metal, copper (I), and copper (II). Moreover, surface analyses were undertaken of lead pipes from previous laboratory tests as well as lead pipes harvested from the field in an attempt to identify metallic copper deposits, which would support the hypothesis that deposition corrosion is a contributing mechanism to higher lead in water sometimes observed after PLSLR.

MATERIALS AND METHODS

Bench Scale Testing. Bench scale tests were carried out using a dump-and-fill protocol in both Blacksburg tap water and synthetic tap water (Table 5-1). In both cases, triplicate lead pipes (3/4" ID, 1" OD) were used and water was changed three times per week on Mondays, Wednesdays, and Fridays. For the tests in Blacksburg water, 4" long pipes were used and copper was dosed as copper (II) sulfate ($CuSO_4$) in varying concentrations up to 200 ppb throughout the experiment; magnesium sulfate ($MgSO_4$) was added as needed to give the same ionic strength for all conditions. In the synthetic water tests, longer pipes (12") and a much higher copper level of 10 mg/L were used, with dosing occurring only once/week (on Fridays) for the first eight weeks of the 24-week experiment. Three different copper oxidation states were tested in this experiment; the copper (0) condition was dosed as powdered copper metal, the copper (I) condition as copper (I) chloride (CuCl), and the copper (II) condition as copper (II) chloride ($CuCl_2$). The concentration of NaCl in the synthetic water was adjusted to give the same chloride concentration for all conditions. In both tests, the entire volume of water was collected from the pipe as a weekly composite and acidified to 2% in the sampling bottle with nitric acid, thoroughly shaken, and allowed to digest for 48 hours before analysis. Metal concentrations were determined by inductively coupled plasma – mass spectrometry (ICP-MS; Thermo Scientific Thermo Electric X Series) using Standard Method 3125B (APHA 1998).

Table 5-1. Key water quality parameters of synthetic and Blacksburg drinking waters used for dump-and-fill tests

	Synthetic Tap Water	Blacksburg Water
pH	8.0	7.8
Disinfectant	Chloramines, 4 mg/L	Chloramines, 3 mg/L
Alkalinity (as $CaCO_3$)	15 mg/L	40 mg/L
Chloride-to-Sulfate Mass Ratio (CSMR)	16.0	3.0
Corrosion Inhibitor	None	Zinc Orthophosphate

Source of Lead Pipes. Surface analyses were conducted on lead pipe sections from four different sources (Table 5-2):

1. New lead pipes that had been galvanically connected to varying lengths of copper and exposed to varying water chemistries for more than 2 years using a dump-and-fill protocol (Triantafyllidou and Edwards 2011).
2. The one-inch section closest to the galvanic junction harvested from new lead pipes connected to lead or copper using various connectors during realistic-flow pilot-scale tests in Blacksburg water for 4.5 years (Cartier et al. 2012; St. Clair 2012).
3. A section of lead pipe harvested from a home in Washington, D.C. The lead pipe section was located at the entrance to the home and soldered into a brass fitting, which was then threaded into the copper premise plumbing.
4. Lead pipe harvested from the distribution system in Washington, D.C. after approximately 100 years in service, then connected to copper in pilot-scale loops testing galvanic corrosion with copper for up to one year (Welter et al. 2013).

Table 5-2. Summary of lead pipes used for various surface analyses

Pipe Source	Original Results Reported in:	Analyses Conducted
Dump and Fill	(Triantafyllidou and Edwards 2011)	XRF, SEM/EDS, XPS
Blacksburg Pilot	(Cartier et al. 2012; St. Clair 2012)	XRF, SEM/EDS
Washington, D.C. Pilot	(Welter et al. 2013)	XRF
Field	NA (no previous study)	XRF

Surface Analysis. Before analysis, all pipe sections were cut in half lengthwise to allow examination of the interior pipe surface. The concentration of copper on the interior pipe surface was measured using a handheld x-ray fluorescence (XRF) analyzer (Innov-X Alpha 800 LZX). The measurement time for each XRF reading was 45 seconds. After completing the XRF analysis, small (approximately 1" square) sections of selected pipes were imaged using an FEI Quanta 600 FEG environmental scanning electron microscope (ESEM) equipped with an energy-dispersive spectrometer for elemental analysis (EDS; Bruker). All samples were sputtered with gold/palladium before analysis, and an accelerating voltage of 20 kV was used. Both secondary electron (ETD) and backscatter (BSED) images were taken during this work; more detailed microscope conditions are listed at the bottom of each image. X-ray Photoelectron Spectroscopy (XPS) was carried out on a PHI Quantera SXM.

RESULTS AND DISCUSSION

Bench Scale Testing. Dump and fill tests in synthetic water at a high copper concentration of 10 mg/L demonstrated an increase in lead leaching of 2.5-3.5 times in the presence of copper compared to the copper-free control (Figure 5-2a). No statistically significant difference in lead leaching was observed between the three different copper species, implying that plating kinetics and speciation are not a controlling factor in deposition corrosion, at least in this oxygenated and chloraminated water (Figure 5-2a). One possible limiting factor is the mass transport of copper

to the pipe surface; previous studies have shown that flowing tests are more successful at reproducing deposition corrosion than stagnant tests (Hu et al. 2012).

Tests at lower copper concentrations in Blacksburg water gave much lower concentrations of lead overall (Figure 5-2b), and conditions with copper dosing gave *lower* concentrations of lead than the control; in some cases more than a 50% decrease in lead concentration was observed when copper was added. One possible explanation for this is that the "control" was not copper-free due to copper alloys upstream in the building plumbing system; despite extensive pre-flushing (10 minutes) the background concentration of copper in the water used for the test was 18 ppb on average.

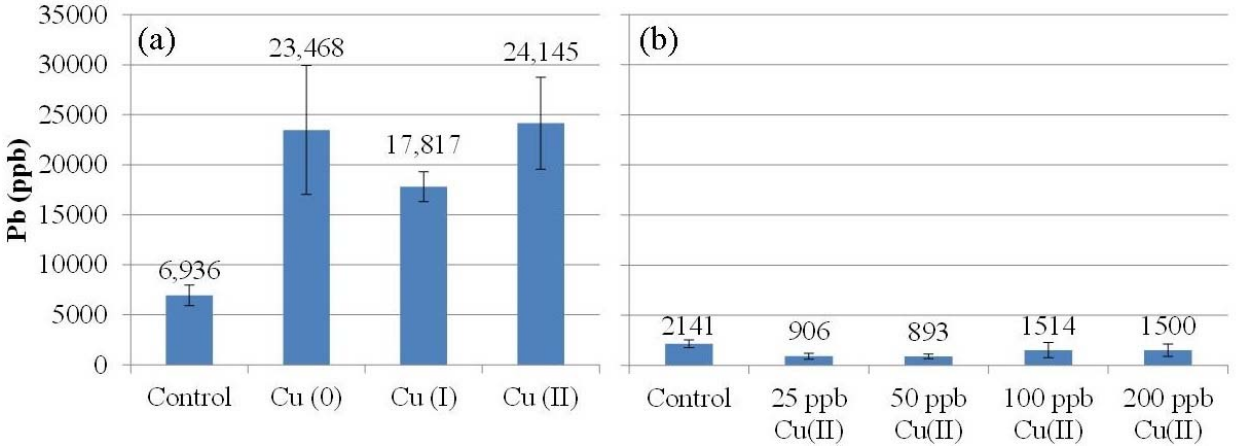

Figure 5-2. Average lead release from water dump-and-fill tests in (a) synthetic water, pooled over 24 weeks (dosing occurred during the first 8 weeks only) and (b) Blacksburg water, pooled over the first 24 weeks (dosing occurred in all weeks). Error bars represent 95% confidence.

The differences between the levels of deposition corrosion observed in the two dump-and-fill tests emphasize the possible importance of copper concentration, particularly soluble copper concentration. Previous work that explicitly examined the effect of soluble copper concentration on the extent of copper plating found a strong positive correlation between soluble copper and the mass of copper plated (Chapter 4). In Blacksburg water, the solubility of copper (II), as estimated using MINEQL+, was 8 ppb, while in the synthetic water it was 114 ppb, more than 14 times higher. In both cases, the solubility was controlled by pH, which was lower in the synthetic water after copper dosing. As expected, the measured extent of copper deposition on the surface for these two conditions (calculated by mass balance using the initial and final copper concentrations during each water change) trended with copper solubility. Specifically, the mass of copper plated was 2.9 mg/cm^2 for Blacksburg water and 29.5 mg/cm^2 for synthetic water, a difference of more than 10 times. Consistent with the deposition corrosion mechanism, this difference in the mass of copper deposited on the surface was also similar in magnitude to the difference in lead release, with the pipes exposed to synthetic water releasing 16X more lead than those exposed to Blacksburg water.

Examining the "Dissolved Copper Effect" in Previous Research. Surface analysis of lead pipes used in bench-scale simulated PLSLR experiments (Table 5-2, "Dump and Fill") revealed elevated copper concentrations throughout the lead pipe surface, with the average copper concentration on the surface ranging from 0.24 – 0.47% (Figure 5-3a). Copper concentrations

tended to be highest close to the galvanic junction; values as high as 1.36% were measured in the area nearest the copper pipe (Figure 5-3a).

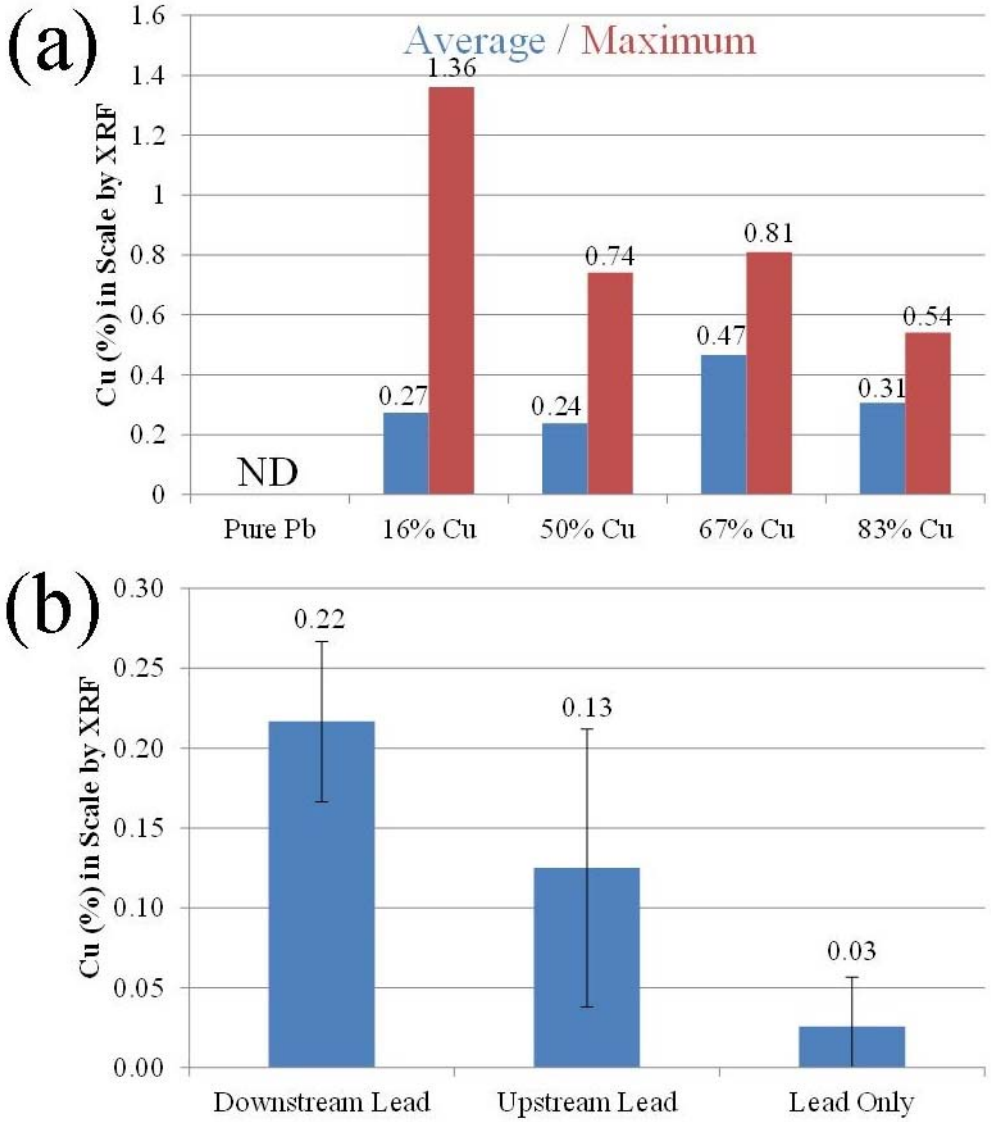

Figure 5-3. Percentage of copper detected in scale on new lead pipes by XRF (a) after more than 2 years of bench-scale dump-and-fill simulated partial lead service line experiments (Triantafyllidou and Edwards 2011) and (b) in the inch of pipe closest to the galvanic junction after 4.5 years of realistic-flow simulated partial lead service line experiments in Blacksburg water; error bars represent 95% confidence for triplicate pipes.

Based on the observation that the highest copper concentrations are typically found near the galvanic junction, one-inch sections were harvested from a 4.5-year long-term pilot-scale test of PLSLRs using various connectors (Table 5-2, "Blacksburg Pilot"). Pipes from this experiment could be separated into three categories: lead downstream of copper, lead upstream of copper, and pure lead pipe. As would be expected from deposition corrosion, surface analysis by XRF revealed that the downstream lead pipes had the highest copper concentrations, an average of 0.22% (Figure 5-3b). Although the copper concentration in the first one-inch section of the

upstream lead pipes was lower than in the downstream pipe on average (0.13%), the difference was not statistically significant (Figure 5-3b); this is consistent with the expectation that copper can migrate upstream to some extent during stagnation periods by convection or diffusion (e.g. Figure 5-1a). The pure lead pipes contained small, but detectable levels of copper, likely as a result of contact with copper-containing connectors or trace levels of copper present in the source water. For galvanized iron, trace amounts of copper as low as 10 ppb have been linked to deposition-corrosion-induced failures in the field (Cruse 1971), and the results herein indicate that even low levels of copper in the source water can have detrimental impacts on lead release in the long term.

SEM analysis of the dump-and-fill pipes (Table 5-2) identified a number of large, copper-rich deposits on the pipe surface (Figure 5-4). Deposits as large as 130 μm in diameter were identified (Figure 5-4a), and were readily visible when the instrument was operated in backscatter mode, which is dominated by contrast based on atomic number (Z), making lead (Z = 82) appear bright and copper (Z = 29) appear dark (Figure 5-4b). An even more dramatic contrast was possible using EDS mapping, in which copper-rich areas are shown in red and lead-rich areas are shown in green (Figure 5-4c). Although EDS cannot definitively determine oxidation state, the copper to oxygen atomic ratio provides some insight. Theoretically, copper (II) oxide (CuO) would give a copper:oxygen ratio of 1, copper (I) oxide (Cu_2O) would give a copper:oxygen ratio of 2, and pure copper would have no oxygen present. In practice, however, surface oxidation of the copper metal always leads to measurable oxygen concentrations. For example, EDS analysis of a pure copper sheet gave copper:oxygen ratios between 2.8-3.0. In comparison, quantification of EDS signal from the red area in Figure 5-4c gave atomic percentages of 86% copper and 14% oxygen, resulting in a copper:oxygen ratio of 6.1. This is strong evidence that at least some of the copper-rich deposit on the sampled pipes is composed of pure copper.

Although copper-rich deposits were also identified by SEM/EDS on the surface of the pipe sections harvested from the Blacksburg pilot study (Table 5-2; Figure 5-5), the results were much less definitive than for the dump-and-fill pipes above. Fewer, smaller deposits were present, with particle diameters on the order of 20 μm (Figure 5-5a), and quantification of the EDS signal from the red area in Figure 5-5b revealed Cu:O ratios ranging from 0.6 to 0.8, although the morphology of the deposit was similar to that for the dump-and-fill pipes (Figure 5-4d).

XPS analysis was carried out using a small section from the same dump-and-fill pipe used for ESEM, with hope of determining oxidation state by detecting small shifts in binding energy (Skoog et al. 2007). However, focusing on the copper deposits gave an average copper concentration of 1.3% while the average lead concentration was approximately 12%, indicating that the deposits were smaller than the area sampled by the instrument. The remaining >80% of the signal was composed of carbon and oxygen due to the very shallow (1-5 nm) penetration depth and surface oxides/contamination (Skoog et al. 2007). Attempts to remove the surface contamination by ion sputtering did increase the relative signal available from copper, but it also affects the oxidation state by reducing copper, and would bias the results of a high resolution scan, potentially causing a false positive for metallic copper. Hence, the XPS results were inconclusive.

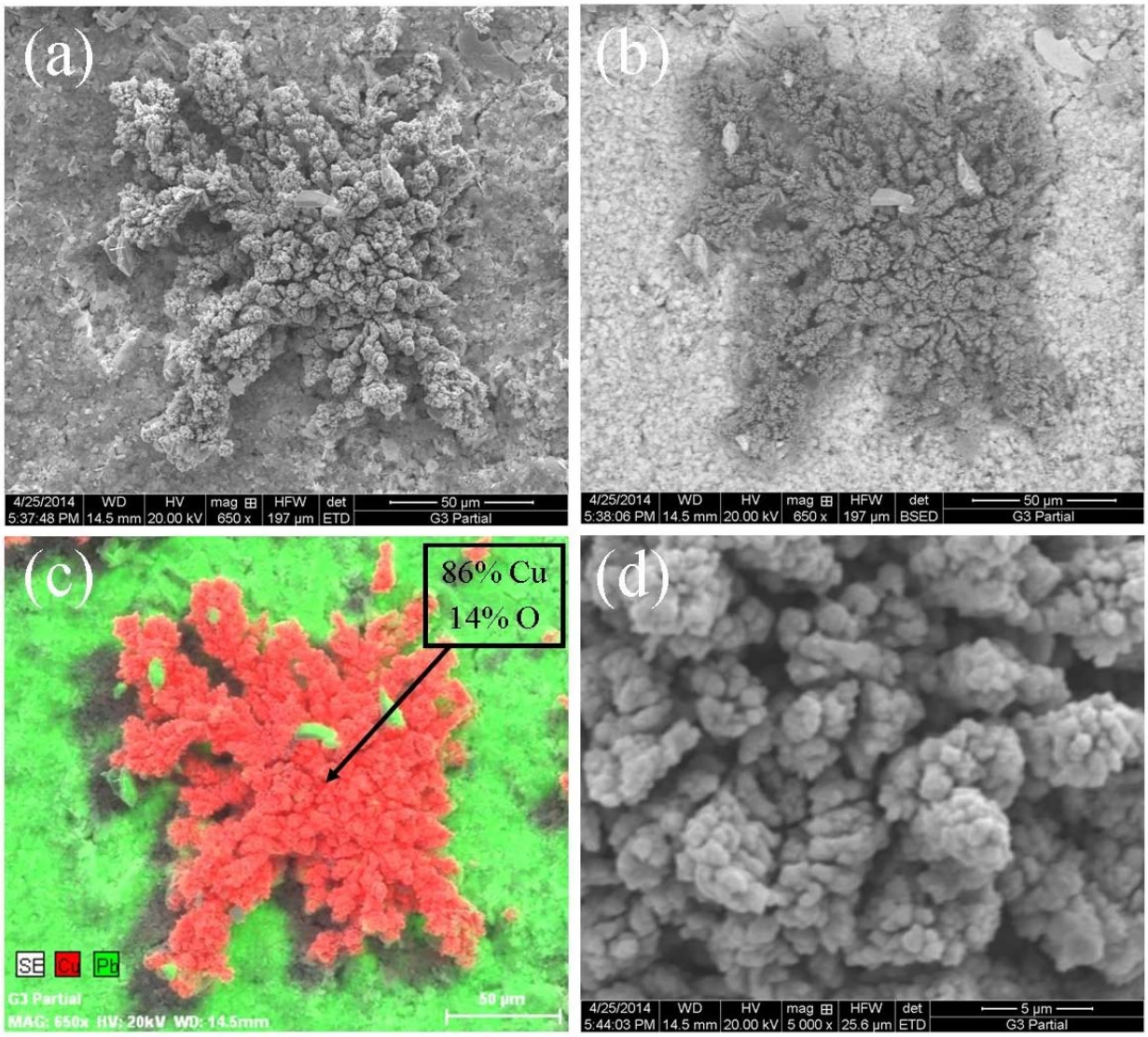

Figure 5-4. Scanning electron microscope images showing a copper deposit on lead on one of the pipes from Figure 5-3a. (a) secondary electron image; (b) backscatter image of the same area (lighter areas = higher atomic number); (c) EDS map with copper-rich areas shown in red and lead-rich areas shown in green; (d) higher zoom secondary electron image showing morphology of copper deposits

Evidence of Deposition Corrosion in the Field. XRF analysis of pipes harvested from the field demonstrated that copper concentrations on the pipe surface were even higher for pipes exposed for decades than those exposed a few years in laboratory studies. For the upstream lead pipe section harvested from Washington, D.C. (Table 5-2, "Field"), the copper concentration on the lead surface near the galvanic junction was more than 20% by weight, then fell off rapidly as distance from the junction increased (Figure 5-6); this trend is consistent with copper migration slightly upstream during stagnation and a relatively small area of lead potentially affected by deposition corrosion.

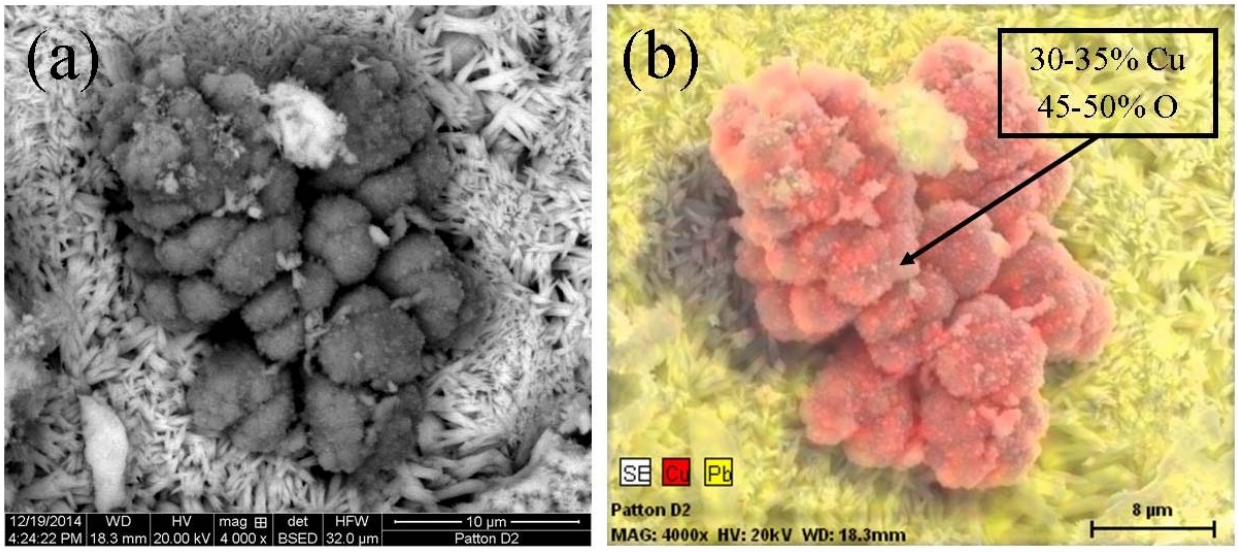

Figure 5-5. Scanning electron microscope images showing a copper deposit on lead on one of the pipes from Figure 3b; (a) backscatter image (lighter areas = higher atomic number); (b) EDS map with copper-rich areas shown in red and lead-rich areas shown in yellow; note the higher magnification compared to Figure 5-4.

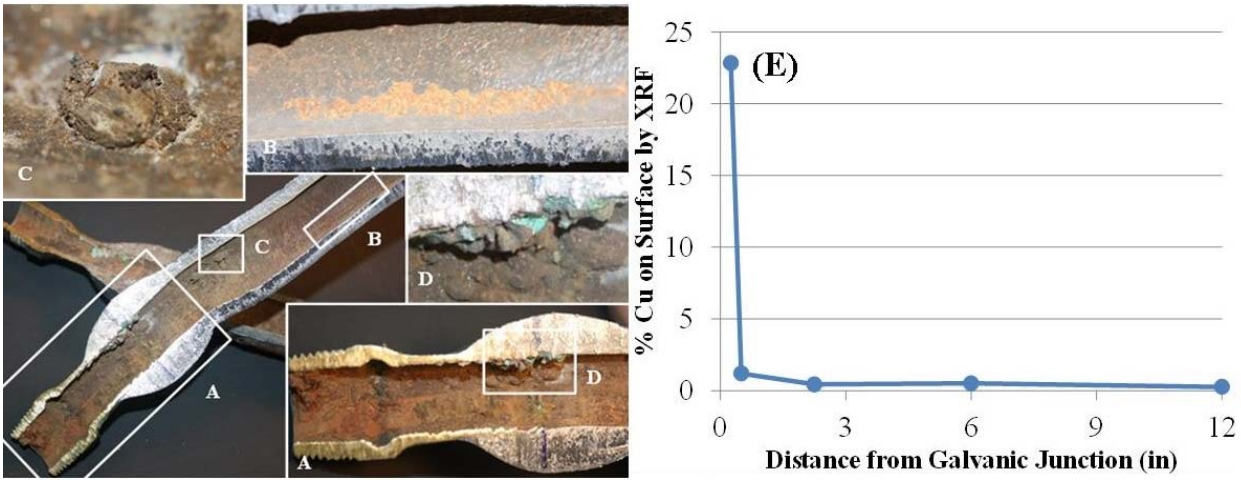

Figure 5-6. Lead pipe harvested from the entrance of a home with copper premise plumbing. The pipe was soldered to brass; photos taken from a section near the junction. Large accumulations of rust are present at the galvanic connection (A) while visually there is much less rust present away from the junction (B). Large tubercles exist at both the galvanic connection (D) and away from the junction (C). A profile of the copper concentration on the surface versus the distance from the galvanic junction (E) shows a dramatic drop in copper concentration moving away from the junction

Deposition Corrosion as a Confounding Factor. A recent pilot study in Washington, D.C. constructed to examine galvanic corrosion effects, including connection type, on lead release after PLSLR led to perplexing results (Welter et al. 2013). In contrast with laboratory studies with both new and harvested lead pipes (Clark et al. 2013; Wang et al. 2013), the authors found no significant difference in total lead release between different pipe connectors, even when using plastic connectors that eliminated galvanic corrosion (Welter et al. 2013). This result led the authors to conclude that "the galvanic corrosion contribution, if it was present, was dwarfed by

the other factors," and the authors hypothesized that differences in the composition of the interior pipe scale could be responsible for the variability (Welter et al. 2013).

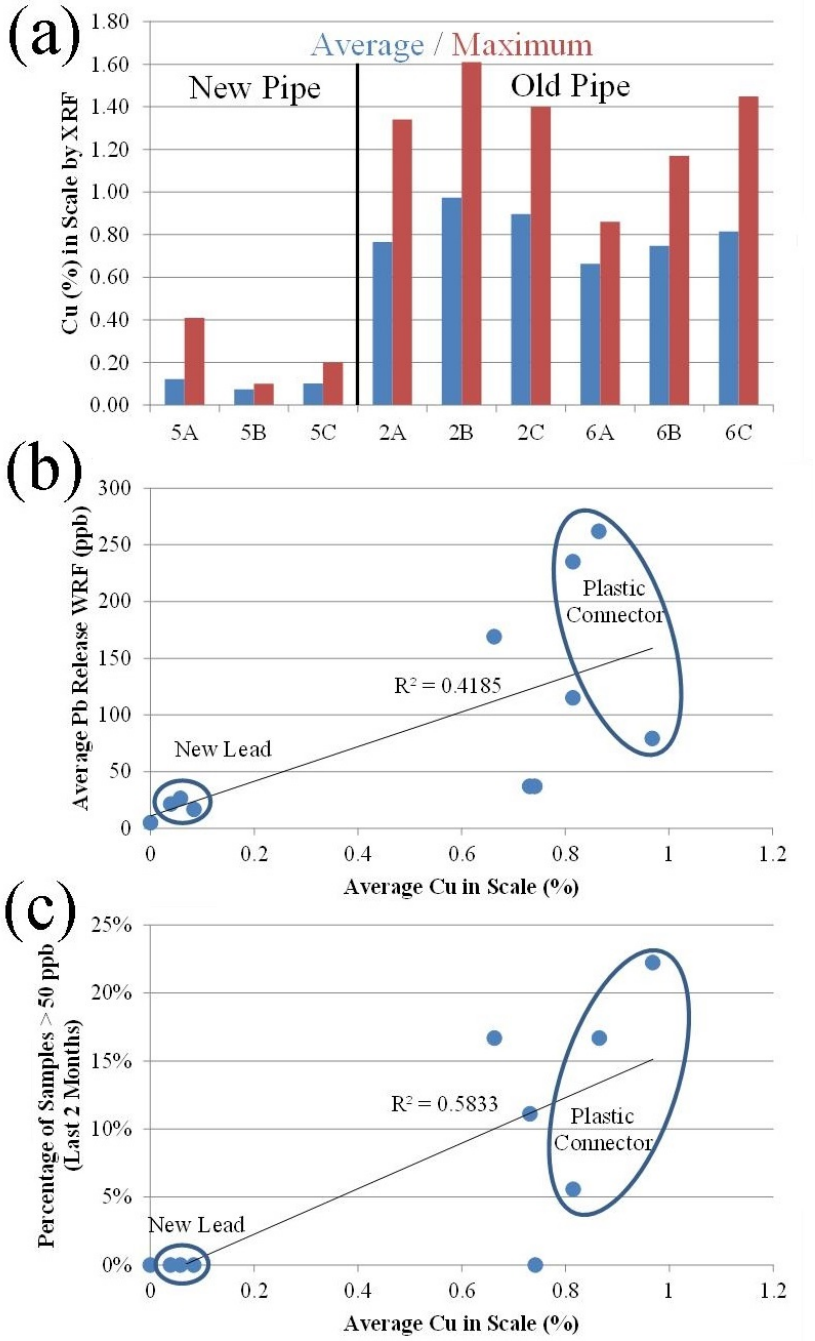

Figure 5-7. (a) Percentage of copper detected in scale on lead pipes from Washington, D.C. by XRF after 1 year of pipe loop experiments connected to copper (Welter et al. 2013). Pipes 5A – 5C were new pipes at the start of the experiments; Pipes 2A-2C and 6A-6C were harvested from the distribution system after approximately 100 years in service; Correlation between the average copper concentration on the lead pipe surface measured by XRF (from (a)) and (b) the average lead concentrations and (c) the percentage of samples > 50 ppb during the last two months reported for the Washington, D.C. pipe loop testing (Welter et al. 2013)

To investigate this, the copper concentrations on the interior surfaces of the lead pipes used in the D.C. pilot were measured using XRF, which revealed average copper concentrations ranging from 0.66% to 0.97%, with copper concentrations as high as 1.61% present in some locations on the pipe (Figure 5-7a). In contrast, the new lead pipes used in the pilot experiments had much lower average surface copper concentrations of approximately 0.1% (Figure 5-7a). This difference between new and harvested pipes implies that either (1) copper deposits already existed on the lead pipes before the experiments took place or (2) copper deposition/adsorption occurred more readily on the older pipe surfaces than on new lead.

To determine whether the relatively high copper concentrations identified in these pipes influenced the pilot results, total lead data reported for the pilot experiments (Welter et al. 2013) were compared to the copper data obtained by XRF. Although no data were reported in the pilot for lead corrosion in the absence of copper, data were available for a control pipe loop in the same facility, which was constructed with harvested lead pipe without copper. In this pipe loop, the lead concentration never exceeded 15 ppb, and the average lead concentration was approximately 5 ppb. For the purpose of this analysis, the control loop was assumed to have a copper surface concentration of 0. When the average total lead concentrations reported for the pilot were plotted as a function of the copper content on the pipe surface measured by XRF (Figure 5-7b), a slight positive correlation ($R^2 = 0.42$) was identified. Furthermore, when the percentage of samples with lead greater than 50 ppb (a measurement of the spike frequency) during the last two months of the pilot was plotted against the surface copper concentration, an even stronger correlation resulted (Figure 5-7c; $R^2 = 0.58$). This is consistent with previous work that found that lead placed downstream of copper (and therefore prone to copper deposition) had more high-lead spikes than lead placed upstream of copper (Cartier et al. 2012; St. Clair 2012), and highlights the importance of considering deposition corrosion as a contributing factor to lead release.

CONCLUSIONS

- Dump-and-fill tests in an aggressive synthetic water with high levels (10 mg/L) of copper resulted in approximately three times more lead release than the same water without copper.
- Dump-and-fill tests in Blacksburg water did not reveal an increase in lead corrosion when copper was added compared to the control. For the condition with the highest copper doses, the difference in corrosion rate compared to the synthetic water was comparable to differences in both copper solubility and the mass of copper attached to the pipe surface per unit area.
- XRF analysis of lead pipes previously connected to copper pipes in laboratory experiments revealed copper concentrations on the surface as high as 1.36% by weight, implying that deposition corrosion was occurring in these systems.
- SEM/EDS analysis of the pipes above revealed that copper was deposited on the surface in discrete “islands” with copper compositions by EDS as high as 86% (atomic), compared to a value of 78% obtained for a pure copper sheet, providing strong circumstantial evidence for deposition corrosion as a contributing mechanism.

- XRF analysis of harvested lead service lines from Washington, D.C. revealed average copper concentrations of 0.66% to 0.97%, which was higher than that measured on pipes from laboratory studies, implying that deposition corrosion over decades of exposure in the field might be at least as serious as that quantified under laboratory conditions.
- When lead service lines are harvested from the distribution system for use in corrosion experiments, the presence of existing copper on the surface can be a confounding factor for total lead release and should be accounted for in experiment design and data interpretation.

ACKNOWLEDGEMENTS

The authors acknowledge the financial support of the National Science Foundation under NSF CBET SusChEM GOALI 1336616 and the Graduate Research Fellowship Program (GRFP). The authors would also like to acknowledge the financial support of the Robert Wood Johnson Foundation (RWJF) under the Public Health Law Research program and the Abel Wolman Fellowship (American Water Works Association). Opinions and findings expressed herein are those of the authors and do not necessarily reflect the views of the NSF, RWJF, or AWWA. The authors would further like to thank Yanna Lambrinidou at Parents for Nontoxic Alternatives (PNA) and Greg Welter at O'Brien & Gere for providing lead pipe samples for surface analysis, as well as the Virginia Tech ICTAS Nanoscale Characterization and Fabrication Laboratory (NCFL) for use of the ESEM and for their assistance in carrying out the XPS analysis.

REFERENCES

American Academy of Pediatrics, 2011. Letter to EPA Science Advisory Board Recommending Immediate Moratorium on Partial Lead Service Line Replacements. from http://yosemite.epa.gov/sab/sabproduct.nsf/177871EFC7607CD08525785C0050AAB1/$File/aapcomments.PDF.

APHA, 1998. *Standard Methods for the Examination of Water and Wastewater*, APHA, AWWA, WEF.

Arnold, R. B. and M. Edwards, 2012. Potential Reversal and the Effects of Flow Pattern on Galvanic Corrosion of Lead. *Environmental Science & Technology* 46:20:10941-10947.

Britton, A. and W. N. Richards, 1981. Factors Influencing Plumbosolvency in Scotland. *J. Inst. Water Eng. Scient.* 35:349-364.

Brown, M. J. and S. Margolis, 2012. Lead in Drinking Water and Human Blood Lead Levels in the United States. *Morbidity and Mortality Weekly Report (MMWR) Supplements* 61:4.

Brown, M. J., J. Raymond, D. Homa, C. Kennedy and T. Sinks, 2011. Association between children's blood lead levels, lead service lines, and water disinfection, Washington, DC, 1998–2006. *Environmental Research* 111:1:67-74.

Cartier, C., R. B. Arnold Jr, S. Triantafyllidou, M. Prévost and M. Edwards, 2012. Effect of Flow Rate and Lead/Copper Pipe Sequence on Lead Release from Service Lines. *Water Research* 46:13:4142-4152.

Clark, B., C. Cartier, J. S. CLAIR, S. Triantafyllidou, M. Prevost and M. Edwards, 2013. Effect of connection type on galvanic corrosion between lead and copper pipes. *Journal AWWA* 105:10.

Copper Development Association, 1999. Copper Tube in Domestic Water Services Design and Installation (Pub 33). from http://www.copper.co.za/downloads/library/33-Copper-Tube-in-Domestic-Water-Services.pdf.

Cruse, H., 1971. Dissolved-Copper Effect on Iron Pipe. *Journal AWWA* 63:2:79-81.

Dudi, A., 2004. Reconsidering Lead Corrosion in Drinking Water: Product Testing, Direct Chloramines Attack, and Galvanic Corrosion. Department of Civil and Environmental Engineering, Virginia Tech. M.S.

Edwards, M., 2013. Fetal Death and Reduced Birth Rates Associated with Exposure to Lead-Contaminated Drinking Water. *Environmental Science & Technology* 48:1:739-746.

EPA National Drinking Water Advisory Council, 2011. Letter to EPA Administrator on Revised Lead and Copper Rule. from http://water.epa.gov/drink/ndwac/upload/ndwaclettertoepadec2011.pdf.

Fox, K. P., C. H. Tate, G. P. Treweek, R. R. Trussel, A. E. Bowers, M. J. McGuire and D. D. Newkirk, 1986. Copper-Induced Corrosion of Galvanized Steel Pipe.

Giammar, D. E., G. J. Welter and A. Cantor, 2012. Review of Previous Water Research Foundation Projects on Galvanic Corrosion. Accessed online July 2012 at http://www.waterrf.org/ProjectsReports/ProjectPapers/Lists/PublicProjectPapers/Attachments/3/4349_LiteratureReview.pdf.

Hatch, G. B., 1955. Control of Couples Developed in Water Systems. *Corrosion* 11:1:15-22.

Hu, J., F. Gan, S. Triantafyllidou, C. K. Nguyen and M. Edwards, 2012. Copper-Induced Metal Release from Lead Pipe into Drinking Water. *Corrosion* 68:11.

Kenworthy, L., 1943. The Problem of Copper and Galvanized Iron in the Same Water System. *The Journal of the Institute of Metals* 69.

Mattsson, E. and J. O. M. Bockris, 1959. Galvanostatic studies of the kinetics of deposition and dissolution in the copper + copper sulphate system. *Transactions of the Faraday Society* 55:0:1586-1601.

Skoog, D. A., F. J. Holler and S. R. Crouch, 2007. *Principles of Instrumental Analysis*. Belmont, CA, Thomson Brooks/Cole.

St. Clair, J., 2012. Practical Impacts of Galvanic Corrosion in Water Service Lines and Premise Plumbing. Department of Civil and Environmental Engineering. Blacksburg, VA, Virginia Tech. M.S.

Triantafyllidou, S. and M. Edwards, 2011. Galvanic Corrosion After Simulated Small-Scale Partial Lead Service Line Replacements. *Journal AWWA* 103:9:85-99.

United States Environmental Protection Agency, 2011. SAB Evaluation of the Effectiveness of Partial Lead Service Line Replacements (EPA-SAB-11-015).

Vereecken, P. M., R. A. Binstead, H. Deligianni and P. C. Andricacos, 2005. The Chemistry of Additivies in Damascene Copper Plating. *IBM Journal of Research and Development* 49:1:3-18.

Wang, Y., V. Mehta, G. J. Welter and D. E. Giammar, 2013. Effect of connection methods on lead release from galvanic corrosion (PDF). *Journal-American Water Works Association* 105:7:E337-E351.

Welter, G., D. E. Giammar, Y. Wang and A. Cantor, 2013. Water Research Foundation Report #4349: Galvanic Corrosion Following Partial Lead Service Line Replacement.

Zhou, E. M., 2013. Impact of Galvanic Corrosion on Lead Release after Partial Lead Service Line Replacement. Graduate Department of Civil Engineering, University of Toronto. MASc.

CHAPTER 6. PRELIMINARY EVALUATION OF NANOMATERIAL IMPACTS ON CORROSION OF DRINKING WATER DISTRIBUTION SYSTEM INFRASTRUCTURE

Brandi Clark, Casey Murray, Marc Edwards

[a]Virginia Polytechnic Institute and State University, Blacksburg, Va.
[b]O'Brien & Gere, Bowie, Md.

ABSTRACT

Although nanotechnology has been proposed as a solution to many water treatment problems from trace contaminant removal to disinfection, little is known about its effect on new or aging potable water infrastructure. A matrix of bench-scale tests examined the effect of three nanomaterials on the corrosion rate of four common pipe materials, as tracked by metal release to water, electrochemistry, and corrosion morphology. In waters with and without a chlorine disinfectant, as measured by metal release carbon nanomaterials had no effect, whereas silver nanoparticles had some marginal and some potentially dramatic effects on corrosion rate (32-fold increase in iron release from stainless steel compared to the control). For stainless steel, some evidence of localized corrosion was present when silver nanoparticles were added, with a pitting rate as high as 1.2 mm/y, which has potentially serious consequences for stainless steel performance. Continuous flow recirculating tests revealed a small but statistically significant increase in metal release of 14% when copper pipes were exposed to silver nanoparticles compared to the control, but no difference in metal release for stainless steel pipes exposed to silver nanoparticles. Subsequent tests were consistent with the hypothesis that silver ion is the active species with respect to corrosion, and that increases in corrosion rate proceed through a deposition corrosion mechanism.

INTRODUCTION

In order to meet the growing challenge of providing clean, affordable drinking water in the 21st century, nanomaterial-based water purification strategies are receiving increased attention and may eventually play a role in future water treatment (U.S. Environmental Protection Agency 2007; Shannon et al. 2008). Potential applications for nanomaterials in this area are diverse, and include adsorption of organic and heavy metal contaminants, use in membranes to prevent-biofouling or aid in removal, photocatalysis for contaminant breakdown, and novel disinfection methods (Lisha et al. 2009; Wong et al. 2009; Qu et al. 2013; Dankovich and Smith 2014). In a few cases, these technologies have already been commercialized for point-of-use water treatment, including metal oxide nanoparticles for arsenic removal, nano-titanium-dioxide-based photocatalysis for removal of organics, and silver nanoparticles for disinfection (Li et al. 2008; Qu et al. 2013). While it has been acknowledged that these applications could release nanomaterials and noble metal ions to drinking water (Li et al. 2008; Dankovich and Smith 2014), and some concerns about the potential human health and environmental ecosystem impacts have been raised (Alvarez 2006; U.S. Environmental Protection Agency 2007; Li et al. 2008; Qu et al. 2013), no consideration has been given to the impact these nanomaterials could have on aging drinking water distribution system assets.

Adverse Consequences Can Be Expected. It is expected that the addition of nanoparticles to the drinking water distribution system could affect the corrosion of a wide range of pipe materials (Table 6-1). For example, copper nanoparticles have been proposed as a novel disinfectant, potentially replacing silver nanoparticles as a cost-effective alternative (Dankovich and Smith 2014). However, it is well-known that the presence of dissolved copper ions in drinking water can cause an increase in the corrosion rate of galvanized steel and lead pipes by a deposition corrosion mechanism, in which copper is plated on the surface of the less noble pipe materials to create micro-galvanic cells (Kenworthy 1943; Hatch 1955; Cruse 1971; Hu et al. 2012). For both silver and copper nanoparticles, whose antimicrobial properties are dependent on the release of metal ions (Qu et al. 2013; Dankovich and Smith 2014), a deposition corrosion mechanism is also possible (Figure 6-1a). Silver ion (Ag^+), for example, can undergo displacement plating reactions with all common metal pipe materials, including copper (Figure 6-1a), leaving small "islands" of silver dispersed throughout the pipe surface. These silver deposits can then catalyze the corrosion of the underlying pipe wall, with the potential for rapid pipe failures due to non-uniform corrosion. This mechanism may be even more pronounced when silver is added directly as Ag^+, rather than as silver nanoparticles (AgNPs); direct addition of Ag^+ has been used in some hospitals to control pathogens, such as *Legionella* (Kim et al. 2002; Stout and Yu 2003).

In theory, un-oxidized nanoparticles may also be able to undergo a similar process (Figure 6-1b), in which attractive forces between the nanoparticle surface and the pipe surface allow the particle to adhere to the pipe wall directly, causing a similar acceleration in corrosion. If this second mechanism is active for gold, palladium, and carbon nanomaterials used for water treatment (Table 6-1), as expected based on the fact that they even more noble than silver (Davis 2000), it is expected they would accelerate pipe corrosion of most materials via deposition corrosion effects. Carbon, for example, is nearly as noble as gold (Davis 2000), and galvanic connection with carbon was shown to accelerate the corrosion of 316L stainless steel in medical implant testing (Thompson et al. 1979).

Table 6-1. Possible Detrimental Effects of Nanoparticles and Noble Metal Ions on Distribution System Infrastructure

Contaminant	Possible Sources	Pipe Materials Affected*
Copper Nanoparticles	Novel disinfection methods[a]	Galvanized Steel (S/P) Uncoated Iron / Steel (M) Lead (S)
Copper Ions	Oxidation of copper nanoparticles (above), copper pipe corrosion, dosing to prevent nitrification,[b] dosing for algal bloom prevention,[c] in-building dosing for *Legionella* control[d]	Galvanized Steel[e] (S/P) Uncoated Iron / Steel[e] (M) Lead[f] (S)
Silver Nanoparticles	Anti-biofouling membrane technologies,[g] novel full-scale disinfection methods,[g] point-of-use disinfection[g]	Galvanized Steel (S/P) Uncoated Iron / Steel (M) Lead (S) Copper (S/P) / Brass & Bronze (P) Stainless Steel (P)
Silver Ions	Oxidation of silver nanoparticles (above), in-building dosing for *Legionella* control[d]	All of the Above
Carbon Nanomaterials	Contaminant adsorption,[g] photocatalysis for contaminant breakdown or solar disinfection,[g] sampling/monitoring applications[g]	All of the Above
Gold Nanoparticles	Mercury removal,[h] organics removal as bimetallic with palladium[i]	All of the Above
Palladium Nanoparticles	organics removal as bimetallic with gold[i]	All of the Above

*M = water main material; S = service line material; P = premise plumbing material
[a]Dankovich and Smith 2014 [b]Zhan et al. 2012 [c]e.g. Muchmore 1978
[d]Stout and Yu 2003 [e]e.g. Kenworthy 1943, Hatch 1955, Cruse 1971
[f]Hu et al. 2012 [g]Qu et al 2013 [h]Lisha et al. 2009
[i]Wong et al. 2009

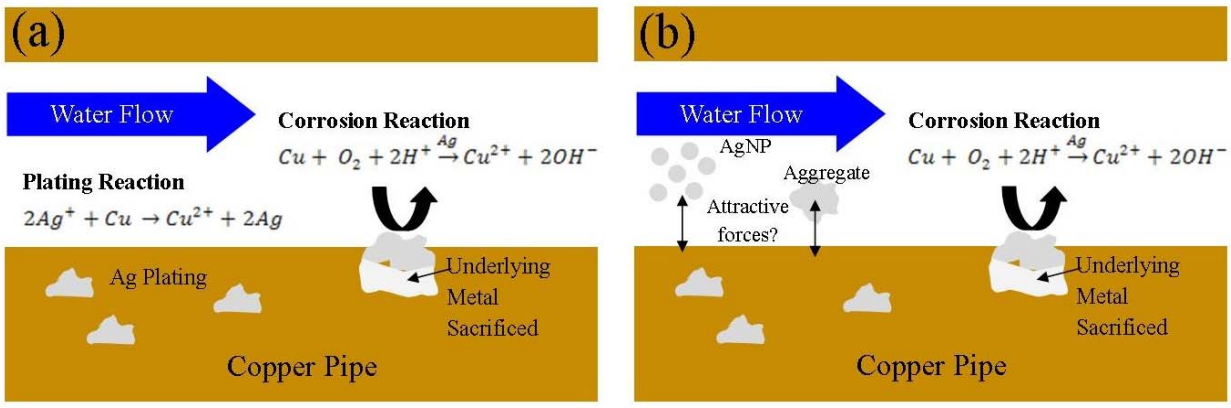

Figure 6-1. Illustration of hypothesized mechanism for deposition corrosion of copper in the presence of (a) silver ions or (b) silver nanoparticles

Objectives. The primary goal of this work was to conduct preliminary experiments to screen for possible impacts of nanomaterials on drinking water infrastructure by comparing the metal release, surface potential, and corrosion morphology of four common pipe materials in the presence of three common nanomaterials. A secondary goal of this work was to compare the corrosion impact of noble nanomaterials to the corresponding noble metal ion, in this case AgNP and Ag^+. Finally, after exposure, surfaces were examined for non-uniform corrosion trends, which have serious implications for material lifetime.

MATERIALS AND METHODS

Source of Nanomaterials. Fullerene (C_{60}; Acros Organics 99.9%+; catalog # AC295010010) and carbon nanotubes (CNT; multi-walled; ~140 nm diameter; ~7 micron length; Strem Chemical, Inc.; catalog # 06-0470) were purchased from Fisher Scientific and used as-received. On each dosing day in the nanomaterials screening experiment (below), 5 mg of nanoparticles were suspended in 20 mL of distilled and deionized water using sonication to disperse, then immediately added to each bottle. Silver nanoparticles were synthesized using the citrate method (Lee and Meisel 1982). Just before dosing in the screening experiment (below), AgNP were purified by centrifuging at 5000 rpm for 5 minutes, then re-suspended in distilled water for dosing. Analysis of the suspended nanoparticles using dynamic light scattering (Malvern NanoZS Zetasizer) gave an average diameter of approximately 70 nm and a polydispersity index of 0.28.

Nanomaterials Screening Experiment. Jar tests were conducted using a dump-and-fill protocol to determine the effect of the three nanomaterials above on four different pipe materials – iron, copper, 304L stainless steel, and 316L stainless steel (Figure 6-2a). Test coupons were made by cutting metal sheets of 0.7 mm thickness for copper and 1.3 mm thickness for stainless steel into 1 by 2 inch coupons. To create iron test coupons, sections of 2 mm diameter wire were cut to 2 inches in length. Each condition was tested in triplicate using a synthetic tap water (Table 6-2) both without disinfectant and with 4 mg/L of free chlorine, giving a total of 24 jars for each material (as in Figure 6-2b). The water volume in each jar was approximately 125 mL, and water was changed three times per week on a Monday-Wednesday- Friday schedule for approximately five months for iron, nine months for copper, and eleven months for stainless steel. Between water changes, samples were stored in a box to minimize light exposure and placed on a shaker table at low speed. For the first six weeks, nanomaterials were added each Friday at a concentration of approximately 1 mg/L. For the first eight weeks, the corrosion potential (E_{corr}) was measured weekly versus silver / silver chloride (Ag/AgCl); for the remainder of the study, E_{corr} was measured monthly. Samples were collected as weekly composites. Copper and stainless steel samples were acidified to 2% with nitric acid and allowed to digest for 72 hours before sampling. Iron samples underwent a more rigorous digestion with the addition of 2% nitric acid and 0.1% hydroxylamine hydrochloride, and were then allowed to digest for one week at 50 °C before sampling. All metal concentrations were determined by inductively coupled plasma – mass spectrometry (ICP-MS; Thermo Scientific Thermo Electric X Series) using Standard Method 3125B (APHA 1998).

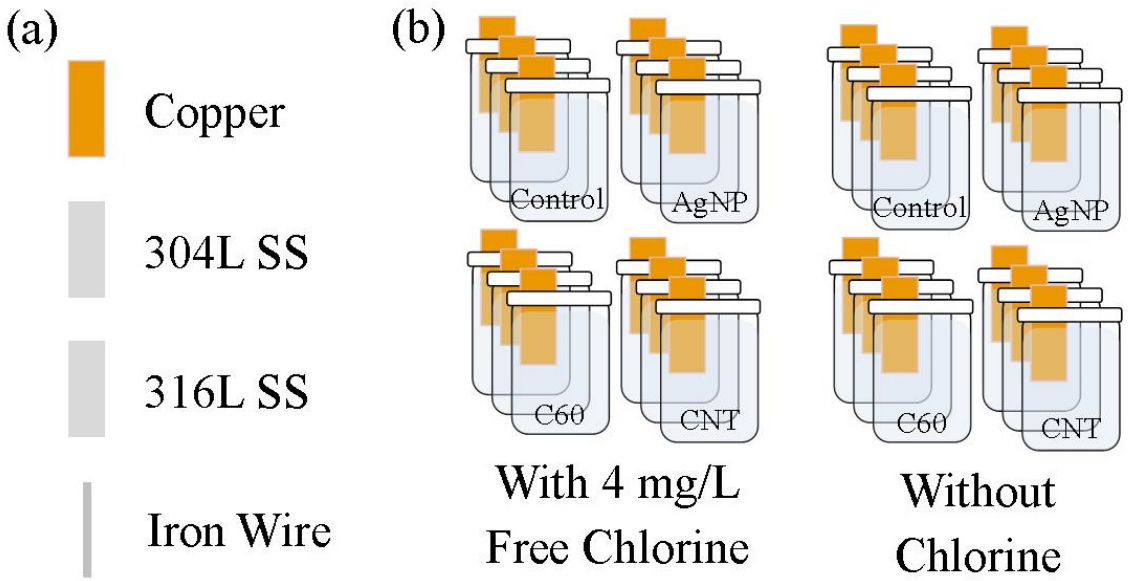

Figure 6-2. Illustration of the nanomaterials screening study showing (a) the four metals tested; (b) the conditions tested for each metal, using copper as an example.

Continuous Flow Comparison of Silver Ions and Nanoparticles. Three recirculating rigs were constructed using two 6-inch long, ¾" diameter copper pipe sections each attached to a 15.5 L reservoir. By insulating the reservoirs, temperature was maintained at a level consistent with a hot water recirculating system (50 °C). During the first phase (6 weeks total), water with the same chemistry as in the screening test above (Table 6-2) was changed in the reservoirs once per week. One rig served as the control, one was dosed with silver nanoparticles (AgNP) at a concentration of 1 mg/L, and one was dosed with silver ions (Ag^+) at a concentration of 1 mg/L. During the second phase (8 months), no additional silver dosing occurred, water was changed in the reservoirs every four weeks, and disinfectant was added back to 4 mg/L weekly. Fresh water E_{corr} was measured immediately after the water change each week during Phase 1 and each month during Phase 2. To determine total copper release, the entire reservoir was removed at the end of each water change cycle and acidified to 1% with nitric acid and allowed to sit at least one week before sampling for ICP-MS as above.

Additional Testing with Silver Ions. Additional tests were conducted in which silver ion (as silver nitrate) was dosed at 100 ppb in two different waters.

In one study, both dump-and-fill and recirculating tests were conducted over 11 weeks in pure (distilled and deionized) water. One foot sections of both new ¾" copper pipes and ¾" copper pipes that had been previously exposed to the same water for 18 months were used in these experiments, for a total of four rigs: a new copper control, new copper with silver dosing, an aged copper control, and aged copper with silver dosing. In the dump and fill tests, the same four conditions were tested with water changes twice per week. Samples were collected as weekly composites and acidified to 2% with nitric acid. The recirculating experiment had the a similar setup to the comparison test described above, but used longer copper pipes (1-ft) and room temperature water. Water was changed once/week and the entire reservoir was separated

from the rig and acidified to pH 2 at the end of each week. Total copper was determined by ICP-MS as above.

Table 6-2. Key water quality parameters of synthetic and Blacksburg tap waters.

	Synthetic Tap Water	Blacksburg Tap Water
pH	7.5	7.8
Disinfectant	Free Chlorine, 4 mg/L	Chloramines, 3 mg/L
Alkalinity (as $CaCO_3$)	15 mg/L	40 mg/L
Chloride-to-Sulfate Mass Ratio (CSMR)	16.0	3.0
Corrosion Inhibitor	None	Zinc Orthophosphate

Dump and fill tests in Blacksburg tap water (Table 6-2) were conducted in triplicate for both galvanized steel and copper pipes (¾" diameter, 4" long) with and without silver dosing. Water was changed three times per week, and samples were collected as weekly composites. The experiment continued for 26 weeks for galvanized pipe and 33 weeks for copper pipe. As above, all samples were digested by adding 2% nitric acid before sampling and analysis by ICP-MS.

Surface Analysis. Before analysis, pipe sections from the 9-month copper recirculating experiment were cut in half lengthwise to allow examination of the interior pipe surface. The concentration of silver on the interior pipe surface was measured using a handheld x-ray fluorescence (XRF) analyzer (Innov-X Alpha 800 LZX). After completing the XRF analysis, small (approximately 1" square) sections of selected pipes were imaged using an FEI Quanta 600 FEG environmental scanning electron microscope (ESEM) equipped with an energy-dispersive spectrometer for elemental analysis (EDS; Bruker). All samples were sputtered with gold/palladium before analysis, and an accelerating voltage of 20 kV was used. When capturing SEM images, backscatter mode (BSED) was used to provide atomic number (Z) contrast, allowing silver deposits (Z = 47) to appear relatively bright compared to copper (Z = 29). Stainless steel coupons from the nanomaterials screening experiment were not sputtered with gold/palladium but were otherwise analyzed using the same ESEM conditions.

RESULTS AND DISCUSSION

Nanomaterial Screening Test Results. Dump-and-fill tests with different nanomaterials in synthetic tap water with and without chlorine generally showed little difference in metal release when nanomaterials were added compared to the control (Figure 6-3). For iron wire, increases in metal release of 10-20% were observed with AgNP compared to the corresponding controls with and without chlorine (Figure 6-3a). In contrast, *decreases* in metal release (of 5-20%) were observed for both C_{60} and CNT. For C_{60}, decreases occurred both with and without chlorine, and for CNT occurred only with chlorine. Throughout the study, all iron wires dosed with nanomaterials had E_{corr} values that were slightly positive shifted compared to the control (40-70

mV with chlorine and 10-30 mV without chlorine), which is consistent with the deposition of a more noble material on the metal surface and possible acceleration of corrosion. These shifts were statistically significant at 95% confidence for all nanomaterials with chlorine and for only CNTs without chlorine. After only five months of exposure, the iron condition was stopped due to the complete severing of some wires via non-uniform corrosion when exposed to AgNP (Figure 6-4). For the wires with chlorine (Figure 6-4a), 2 of 3 wires exposed to silver were severed by corrosion during the test (Figure 6-4b). For wires without chlorine (Figure 6-4c), 1 of 3 wires exposed to silver were severed (Figure 6-4d).

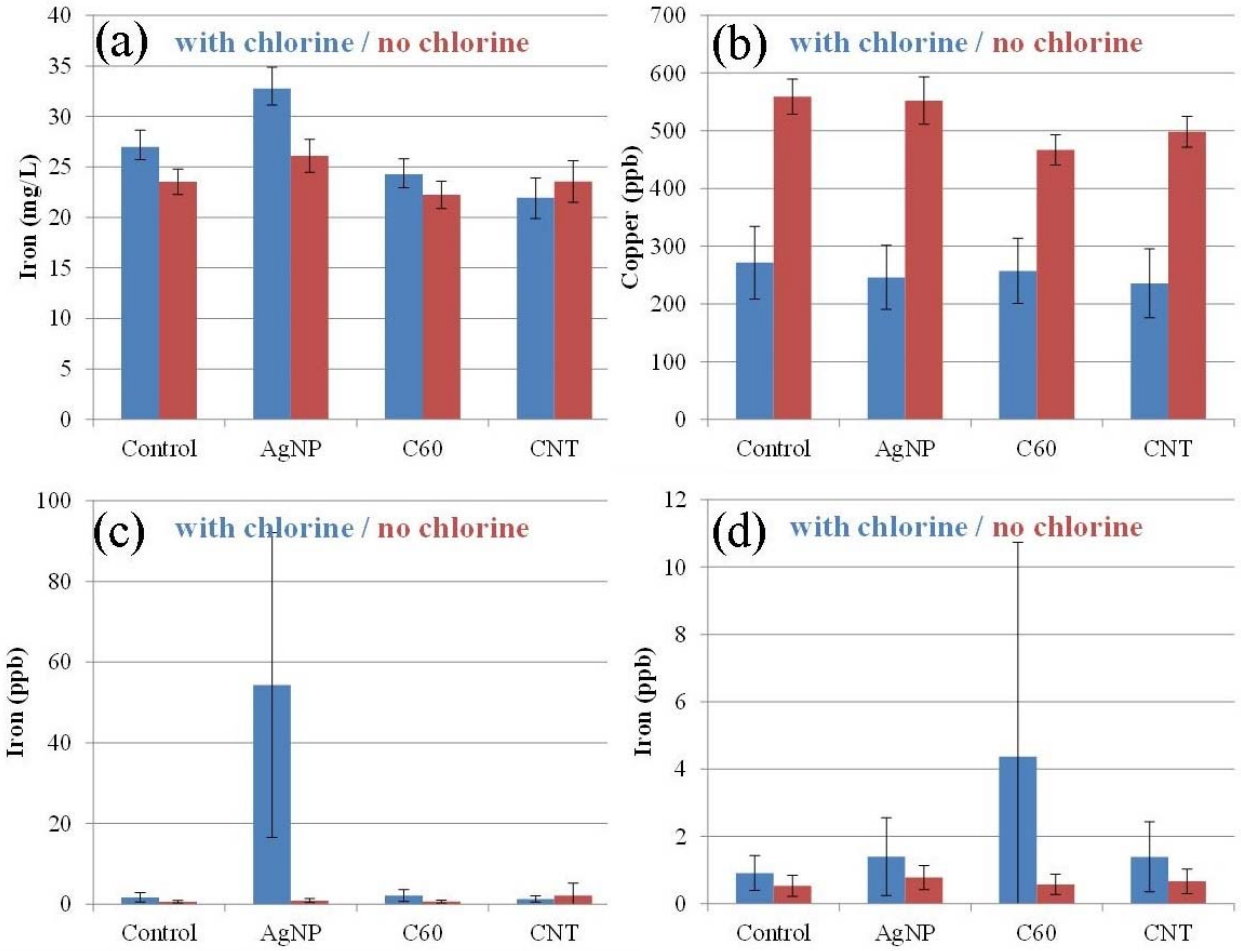

Figure 6-3. Average metal release for the nanomaterials screening test with error bars representing 95% confidence. (a) iron release from iron wire, showing a small but statistically significant increase for silver nanoparticles (AgNP) both with and without chlorine and small decreases for both carbon nanomaterials; (b) copper release from copper, showing no significant increases, but a slight decrease in metal leaching with fullerene (C60) without chlorine and carbon nanotubes (CNT) both with and without chlorine; (c) iron release from 304L stainless steel with an increase of 32X with AgNP and chlorine and no significant difference for any other condition; (d) 316L stainless steel showing no significant difference for any condition.

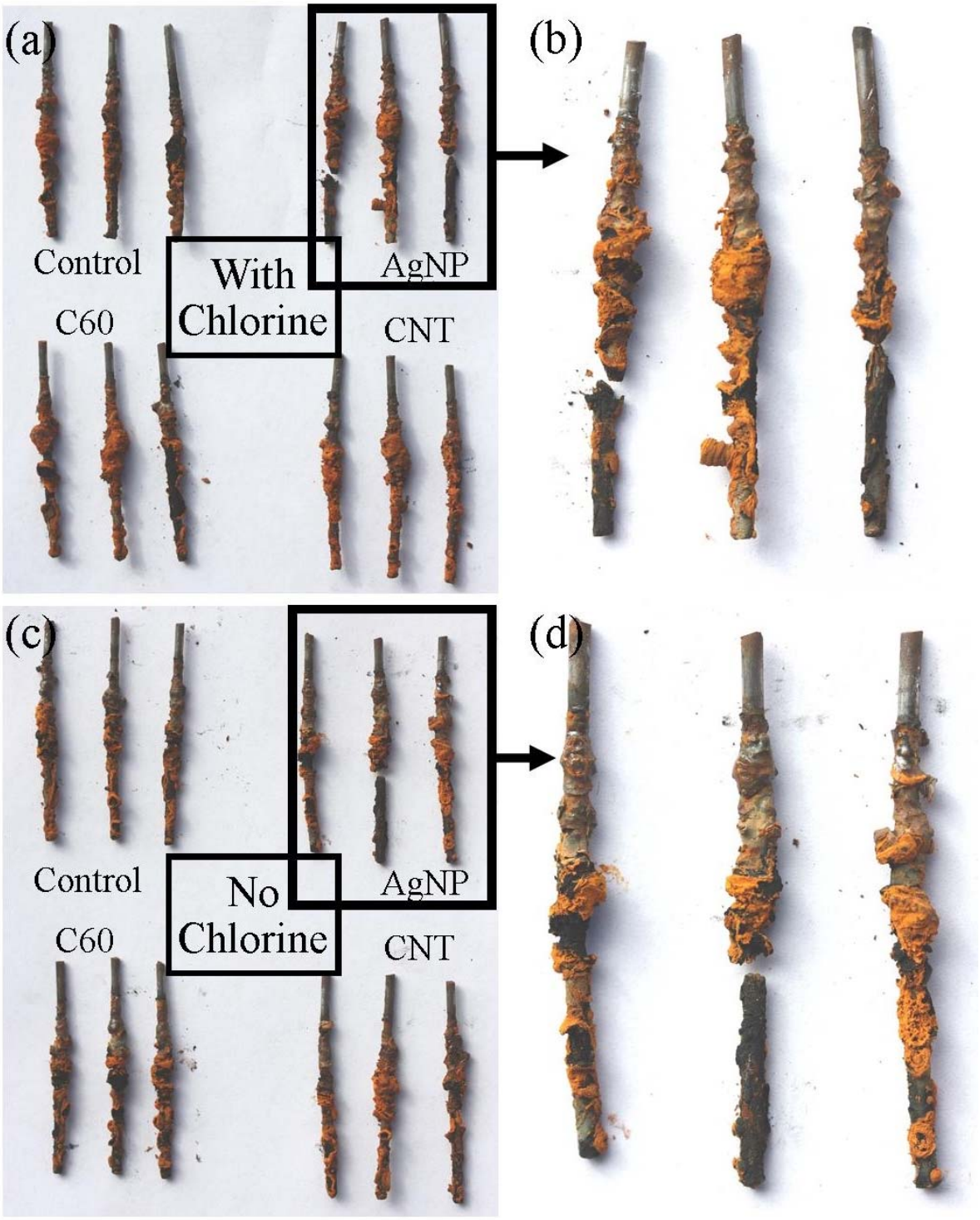

Figure 6-4. Photos of the iron wires used in the nanomaterials screening tests. (a) all wires exposed to chlorine disinfectant; (b) close-up view of the wires exposed to silver and chlorine; (c) all wires from the conditions without disinfectant; (d) close-up view of the wires exposed to silver in the absence of chlorine.

For copper, no significant increases in metal release were observed with the addition of nanoparticles (Figure 6-3b); however, as with iron, a small but statistically significant decrease in metal release (of 10-15%) was observed when C_{60} was added to water without chlorine and when CNT was added to water both with and without chlorine compared to the control. No statistically significant shift in E_{corr} was observed for any copper condition. Thus, there is no evidence copper was adversely affected by nanoparticles in these short term experiments.
For one type of stainless steel (304L), AgNPs were associated with a dramatic increase in iron release of 32 times compared to the control in the presence of chlorine (Figure 6-3c), but carbon nanomaterials and AgNPs without chlorine showed no significant change in metal release compared to the control. However, for the other type of stainless steel tested (316L), no significant changes in metal release were associated with any nanomaterial (Figure 6-3d). In the absence of chlorine, AgNPs were associated with a statistically significant *positive* shift in E_{corr} of 45-65 mV, implying silver deposition and/or an increase in corrosion rate is occurring. However, the presence of AgNPs + chlorine was associated with a statistically significant *negative* shift in E_{corr} of 60-70 mV, implying an overall decrease in the uniform corrosion rate, contrary to metal release results.

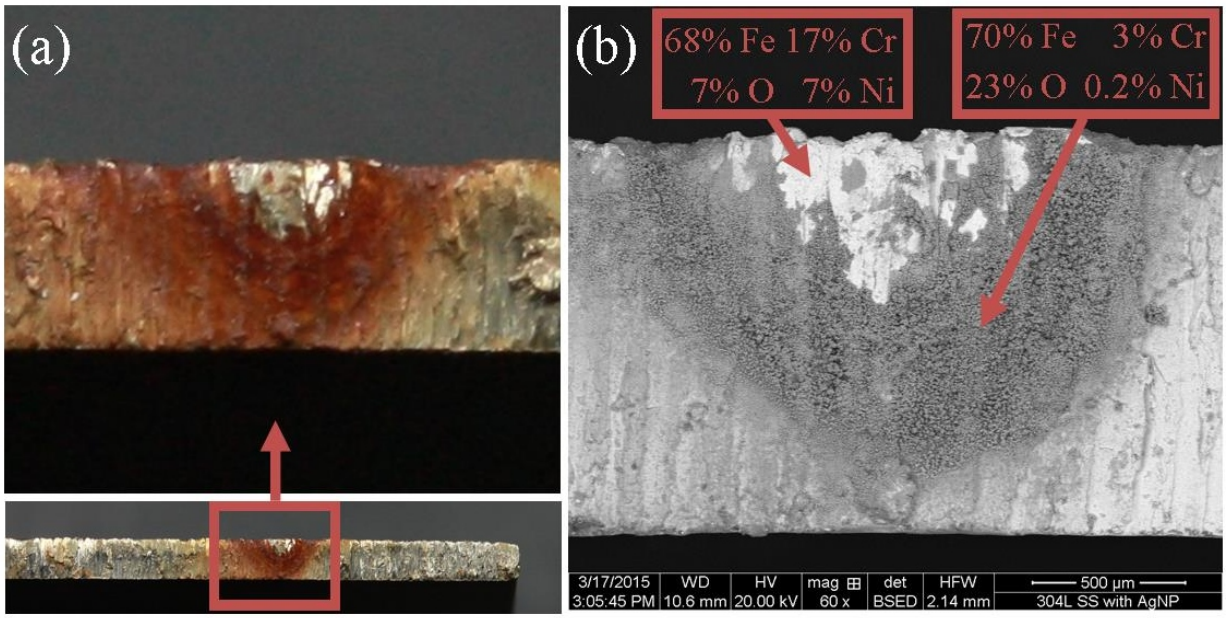

Figure 6-5. Images of localized corrosion on a 304L stainless steel coupon exposed to silver nanoparticles including (a) photos and (b) electron microscope image (backscatter detector) showing the elemental composition of both the bright metal area and the oxide layer (mass percentages)

One possible explanation for the discrepancy between metal release and E_{corr} is severe localized, rather than uniform, corrosion effects. Examination of the 304L stainless steel surfaces exposed to AgNPs with chlorine at the end of the experiment revealed visual evidence of severe localized corrosion along the cut edges of one test coupon (Figure 6-5a). Further examination using SEM/EDS confirmed the penetration depth of the oxidized area, but did not reveal any evidence of deposited silver (Figure 6-5b). One possible explanation is loss of the silver-containing corrosion product before the end of the experiment. However, approximately 65% of the total of 0.75 mg of silver added during the study was unaccounted for in a mass balance based on the measured silver release to water. Therefore, another possible explanation is that the remaining

silver is distributed in small deposits across the surface, leading to levels lower than can be reliably detected using EDS. As measured on the SEM image (Figure 6-5b), the penetration depth of the pit is 1.1 mm, giving an overall pitting rate of 1.2 mm/y. To put this pitting rate into context, a ¾" diameter, schedule 80 pipe of standard wall thickness pitting at this rate would experience failure in just 3.3 years (ASTM 2015).

Overall, in this water, carbon nanomaterials had a beneficial or at least no negative effect on metal release, implying that their presence did not cause a substantial increase in corrosion rate. AgNPs, on the other hand, were associated with increases in metal release that were sometimes dramatic, as in the case of 304L stainless steel, and were singled out for further study.

Mechanistic Implications. One possible explanation for the detrimental effects of AgNP is that deposition corrosion involving silver ions (Ag^+, as in Figure 6-1b), can occur in this system in addition to any effect of the nanoparticle alone. The conversion of AgNP to Ag^+ is known to occur rapidly, in some cases within minutes, under the oxidizing conditions caused by chlorine disinfectant (Tugulea et al. 2014), and dominance of ion-induced deposition corrosion may explain why silver has more dramatic impacts when chlorine is present than when it is absent. To estimate the persistence of AgNP in the test water, AgNP were added to glass jars containing the test water with and without chlorine and monitored by measuring absorbance at 430 nm at various intervals (Figure 6-6). When chlorine was present at the level used in the screening test above (4 mg/L), AgNPs began to disappear immediately, and were reduced to 40% after 30 minutes (Figure 6-6). In the absence of chlorine, however, nanoparticles were relatively stable, with measureable concentrations remaining at least one month later (Figure 6-6).

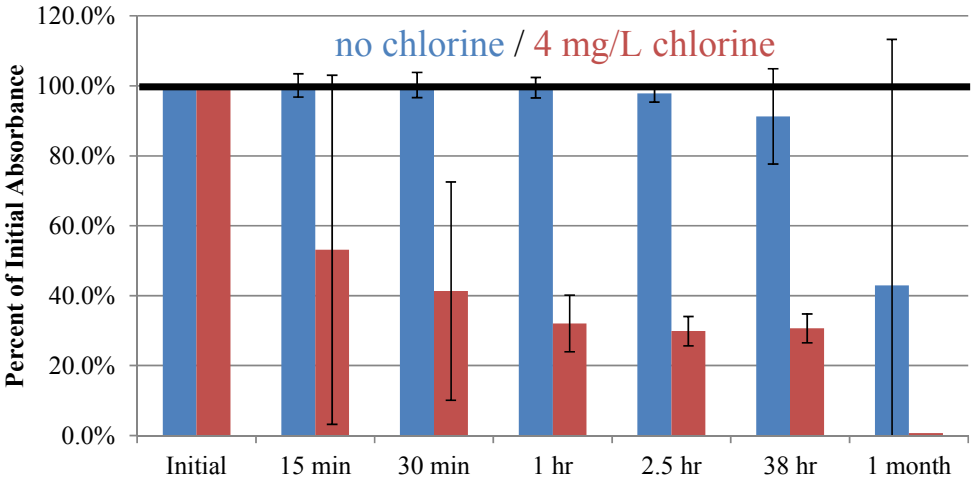

Figure 6-6. Conversion of silver nanoparticles (AgNP) to silver ion (Ag^+) as measured by change in absorbance at 430 nm both in the presence (red) and absence (blue) of chlorine disinfectant.

Comparing Silver Nanoparticles to Silver Ions. Recirculating tests with copper pipe allowed a direct comparison of the effects of AgNP and Ag^+ compared to a silver-free control (Figure 6-7). Over the nine month test, the total mass of copper released to water was 14% higher for AgNPs and 63% with Ag^+ compared to the control (Figure 6-7a). If monthly samples for total copper are compared using a paired t test (by sampling date), the difference between the control and AgNP was statistically significant at 95% confidence ($p = 0.03$); however, the difference

between the control and Ag^+ was not significant (p = 0.08). As expected, the total mass of copper lost throughout the test followed a similar trend, with AgNP losing 9% more mass than the control and Ag^+ losing 40% more mass than the control (Figure 6-7b). This trend is consistent with the hypothesis that deposition corrosion via Ag^+ has a greater impact on corrosion rate; because under these conditions, only some fraction of AgNP would undergo conversion to Ag^+ and subsequent plating. Measurements of E_{corr} during the dosing period were also consistent with deposition corrosion, with both conditions with silver demonstrating statistically significant positive shifts in E_{corr} of 60-90 mV compared to the control. However, this shift in E_{corr} did not remain statistically significant for months after silver addition was halted.

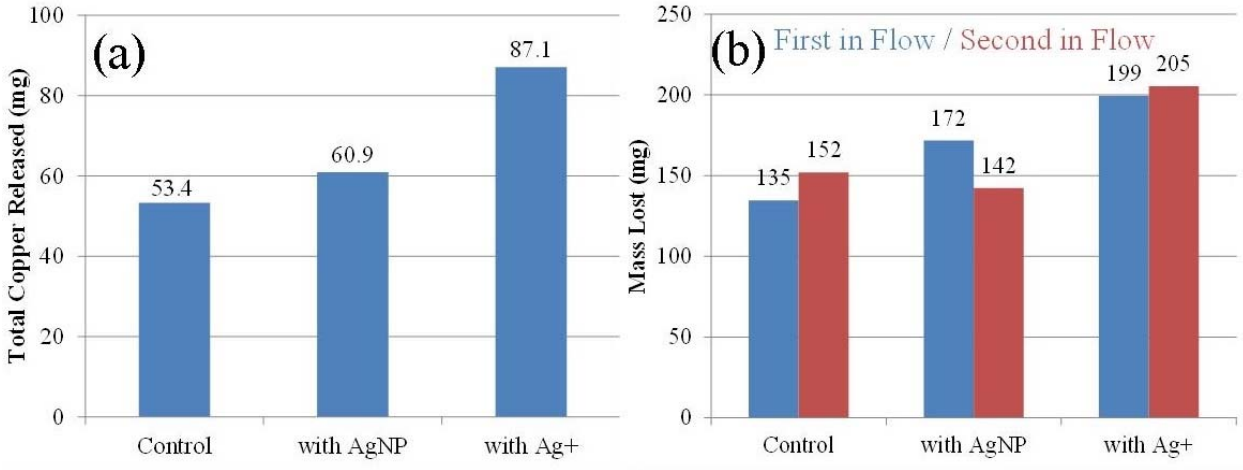

Figure 6-7. Comparison of control, silver nanoparticle (with AgNP), and silver ion (with Ag+) in terms of (a) cumulative mass of copper released to water and (b) copper pipe mass lost during the test. Difference between control and AgNP is statistically significant (p = 0.03); difference between control and Ag^+ is not (p = 0.08)

Surface analysis of copper pipes by XRF revealed concentrations of silver ranging from 0.33% to 1.48% for AgNP and from non-detect to 2.05% for Ag^+, with the highest concentrations at the inlet of each pipe and the lowest concentrations at the outlet. Sections taken from the inlet section with the highest silver concentration for each condition were used to obtain SEM images of silver deposits on the copper pipe surface for both AgNP (Figure 6-8a,b) and Ag^+ (Figure 6-8c,d). For AgNP, silver deposits of varying size were located throughout the pipe section (Figure 6-8a). A map of elemental composition generated using EDS revealed that these deposits were mostly composed of silver (60%), with the remainder of the signal coming from chlorine and oxygen (Figure 6-8b). The presence of chlorine is consistent with a mechanism involving reduction of AgNP with chlorine disinfectant, which would produce chloride ions. However, not all deposits contained chlorine (Figure 6-8b), implying that multiple deposition mechanisms occurred under these conditions. In comparison, deposits formed from silver ion were of similar size (Figure 6-8c), but had no associated chlorine (Figure 6-8d).

Similar tests comparing AgNP and Ag^+ were also conducted for 304L stainless steel. The setup was similar to the recirculating rigs for copper, but with a few changes intended to create a worst-case corrosion scenario for stainless steel. These changes included using three parallel pipes with small diameter (¼") rather than ¾" diameter pipes to increase the surface area to

volume ratio and the daily addition of chlorine dioxide disinfectant at the MRL of 0.8 mg/L to represent in-building disinfection. However, despite the dramatic results for 304L stainless steel in the dump-and-fill screening test, the 16 week recirculating experiment showed no significant differences in metal release, weight loss, or visual evidence of pitting corrosion for either form of silver.

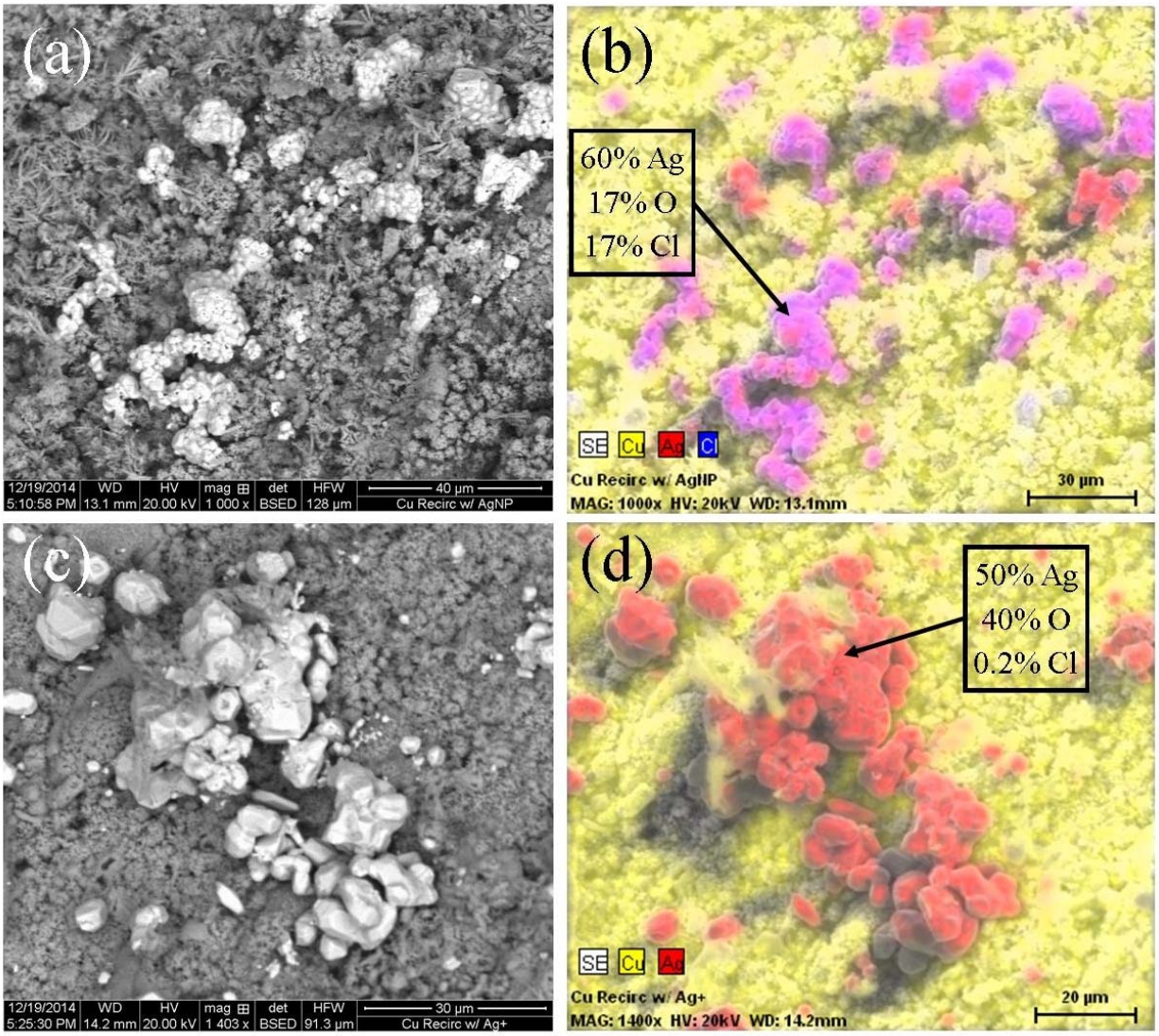

Figure 6-8. (a) Backscattered electron image of the AgNP condition (silver = bright, copper= dark); (b) EDS map of the same area as in (a) with Cu in yellow, Ag in red, and Cl in blue. (c) Backscattered electron image of the Ag^+ condition (silver = bright; copper = dark); (d) EDS map of the same area with Cu in yellow and Ag in red.

Effect of Silver Ions. To determine whether Ag^+ could have an effect in other waters at the US EPA lifetime health advisory level of 0.1 mg/L (U.S. Environmental Protection Agency 2012), which has been used as a guideline for silver dosing (Kim et al. 2002), additional tests were carried out for both copper and galvanized steel pipes. For both Blacksburg water and distilled water, the differences in metal release between conditions with silver addition and the control

were small or nonexistent; the greatest statistically significant increase in metal release was a 33% increase observed in Blacksburg water (Table 6-3). In distilled water, although the differences in metal release were not statistically significant, the steady state dissolved oxygen concentration, as measured at the end of the water change week, was approximately 0.2 mg/L lower in the conditions with silver with high statistical confidence (Table 6-3). In addition, measurable concentrations of silver of 0.3-0.4% and some visual evidence of the initiation of localized corrosion were present on the copper pipe surface, indicating that longer-term problems cannot be ruled out based on the results of this relatively short recirculating test.

Table 6-3. Summary of Experiments with Silver Ion (Ag^+)

Material, Water Type	Silver Dosing	Flow Pattern (Time Frame)	Metal Release Compared to Control[a]	Other Corrosion Indicators
Copper, Synthetic Water	1000 ppb (1st 6 wks)	Recirculating (9 months)	No Significant Diff. (p = 0.08)	+70-90 mV E_{corr} versus control 40% more mass loss than control
Copper, DI Water	100 ppb	Dump-and-Fill (11 weeks)	No Diff. New (p = 0.29) 5.8% Inc Old Pipe (p = 0.001)	Not Measured
Copper, DI Water	100 ppb	Recirculating (11 weeks)	No Diff. New (p = 0.15) No Diff. Old (p = 0.07)	Steady state dissolved oxygen drop of 0.2 mg/L w/ Ag v. control[b]
Copper, Blacksburg Water	100 ppb	Dump-and-Fill (33 weeks)	33% Inc (p = 0.001)	Not Measured
Galvanized Steel, Blacksburg Water	100 ppb	Dump-and-Fill (26 weeks)	No Diff. Zn (p = 0.20) No Diff. Fe (p = 0.59)	Not Measured

[a]All metal release t-tests are paired by sampling date
[b]statistically significant with t-test paired on sampling date (N = 11); p = 2.4E-7 for new pipe and p = 5.3E-5 for old pipe

CONCLUSIONS

Dump and fill tests, recirculating tests, and surface analysis of several common pipe materials exposed to nanomaterials yielded the following conclusions:

- When copper, iron, and two types of stainless steel were exposed to water with and without chlorine containing carbon nanomaterials (CNTs or C_{60}), metal release either did not change or decreased slightly, implying that carbon nanomaterials did not cause an increase in corrosion rate in this water.
- When the same pipe materials were exposed to AgNP, however, metal release increased for both iron and 304L stainless steel. For stainless steel, the increase was dramatic, with average iron release more than 30 times higher with AgNP than in the control.
- The presence of AgNP was also associated with localized corrosion effects for both iron and stainless steel. For iron, 2 mm wires exposed to water containing AgNP were

completely severed after five months of exposure; for stainless steel, a rapid pitting rate of 1.2 mm/y was associated with AgNP exposure. These localized effects have potentially serious consequences for the lifetime of iron and stainless steel pipe infrastructure exposed to distribution system nanomaterials.

- A comparison of the effect of AgNP and Ag^+ on copper pipes revealed small increases in metal release and copper pipe weight loss in both cases. Copper pipes exposed to AgNP lost 9% more mass than the control, while copper pipes exposed to Ag^+ lost 40% more mass than the control.
- Surface analysis by SEM/EDS demonstrated silver-rich "islands" on the surfaces of both pipe materials. However, the deposits from AgNP often contained chlorine, while the deposits from Ag^+ contained only silver and oxygen, implying different deposition mechanisms for AgNP compared to Ag^+.
- When the Ag^+ concentration was reduced to 0.1 mg/L and tested in two other waters for both galvanized steel and copper pipe, a similar trend was observed, with small increases in metal release, if any, when Ag^+ was added compared to the control.

ACKNOWLEDGEMENTS

The authors acknowledge the financial support of the National Science Foundation under NSF CBET SusChEM GOALI 1336616 and the Graduate Research Fellowship Program (GRFP), as well as the support of the American Water Works Association through the Abel Wolman Fellowship. Opinions and findings expressed herein are those of the authors and do not necessarily reflect the views of the NSF or AWWA. The authors would also like to acknowledge the Virginia Tech ICTAS Nanoscale Characterization and Fabrication Laboratory (NCFL) for use of the ESEM.

REFERENCES

Alvarez, P. J., 2006. Nanotechnology in the Environment—The Good, the Bad, and the Ugly. *Journal of Environmental Engineering* 132:1233.

APHA, 1998. *Standard Methods for the Examination of Water and Wastewater*, APHA, AWWA, WEF.

ASTM, 2015. ASTM Standard A312M-15, "Standard Specification for Seamless, Welded, and Heavily Cold Work Austenitic Stainless Steel Pipes". West Conshohocken, PA, ASTM International.

Cruse, H., 1971. Dissolved-Copper Effect on Iron Pipe. *Journal AWWA* 63:2:79-81.

Dankovich, T. A. and J. A. Smith, 2014. Incorporation of copper nanoparticles into paper for point-of-use water purification. *Water Research* 63:0:245-251.

Davis, J. R., Ed. 2000. *Corrosion: Understanding the Basics*. Materials Park, OH, ASM International.

Hatch, G. B., 1955. Control of Couples Developed in Water Systems. *Corrosion* 11:1:15-22.

Hu, J., F. Gan, S. Triantafyllidou, C. K. Nguyen and M. Edwards, 2012. Copper-Induced Metal Release from Lead Pipe into Drinking Water. *Corrosion* 68:11:1037-1048.

Kenworthy, L., 1943. The Problem of Copper and Galvanized Iron in the Same Water System. *The Journal of the Institute of Metals* 69.

Kim, B. R., J. E. Anderson, S. A. Mueller, W. A. Gaines and A. M. Kendall, 2002. Literature Review -- Efficacy of Various Disinfectants Against *Legionella* in Water Systems. *Water Research* 36:4433-4444.

Lee, P. C. and D. Meisel, 1982. Adsorption and Surface-Enhanced Raman of Dyes on Silver and Gold Sols. *J. Phys. Chem.* 86:3391-3395.

Li, Q., S. Mahendra, D. Y. Lyon, L. Brunet, M. V. Liga, D. Li and P. J. J. Alvarez, 2008. Antimicrobial nanomaterials for water disinfection and microbial control: Potential applications and implications. *Water Research* 42:18:4591-4602.

Lisha, K. P., Anshup and T. Pradeep, 2009. Towards a practical solution for removing inorganic mercury from drinking water using gold nanoparticles. *Gold Bulletin* 42:2:144-152.

Muchmore, C. B., 1978. Algae Control in Water-Supply Reservoirs. Journal AWWA 70:5:273-279.

Qu, X., P. J. J. Alvarez and Q. Li, 2013. Applications of nanotechnology in water and wastewater treatment. *Water Research* 47:12:3931-3946.

Shannon, M. A., P. W. Bohn, M. Elimelech, J. G. Georgiadis, B. J. Marinas and A. M. Mayes, 2008. Science and technology for water purification in the coming decades. *Nature* 452:7185:301-310.

Stout, J. E. and V. L. Yu, 2003. Experiences of the first 16 hospitals using copper-silver ionization for Legionella control: implications for the evaluation of other disinfection modalities. *Infection Control and Hospital Epidemiology* 24:8:563-568.

Thompson, N. G., R. A. Buchanan and J. E. Lemons, 1979. In vitro corrosion of Ti-6Al-4V and type 316L stainless steel when galvanically coupled with carbon. *Journal of Biomedical Materials Research* 13:1:35-44.

Tugulea, A. M., D. Bérubé, M. Giddings, F. Lemieux, J. Hnatiw, J. Priem and M. L. Avramescu, 2014. Nano-silver in drinking water and drinking water sources: stability and influences on disinfection by-product formation. *Environmental Science and Pollution Research* 21:20:11823-11831.

U.S. Environmental Protection Agency, 2007. Nanotechnology White Paper (EPA 100/B-07/001).

U.S. Environmental Protection Agency, 2012. 2012 Edition of the Drinking Water Standards and Health Advisories (EPA 822-S-12-001). from http://water.epa.gov/action/advisories/drinking/upload/dwstandards2012.pdf.

Wong, M. S., P. J. J. Alvarez, Y.-l. Fang, N. Akçin, M. O. Nutt, J. T. Miller and K. N. Heck, 2009. Cleaner water using bimetallic nanoparticle catalysts. *Journal of Chemical Technology & Biotechnology* 84:2:158-166.

Zhan, W., A. Sathasivan, C. Joll, G. Wai, A. Heitz and I. Kristiana, 2012. Impact of NOM character on copper adsorption by trace ferric hydroxide from iron corrosion in water supply system. Chemical Engineering Journal 200:122-132.

APPENDIX A. SUPPORTING INFORMATION FOR CHAPTER 2

PROFILE SAMPLING TO CHARACTERIZE PARTICULATE LEAD RISKS IN POTABLE WATER

Brandi Clark[a], Sheldon Masters[a], and Marc Edwards[a]

[a]Virginia Polytechnic Institute and State University, Blacksburg, Va.

Summary of Figures and Tables

Table A-1. Detailed site information listed by site number, including the risk category (A-D), city (Washington, D.C. or Providence, RI), service line type (full, partially replaced, or unknown), and site-specific flow rate at which samples were collected for the samples referred to in the text as low, medium, and high flow (in L/min).

Site #	Risk Cat.	City	Service Type	Low	Medium	High
1	A	Washington	Unknown	1.9	7.3	NA*
2	A	Washington	Unknown	5.2	7.7	NA*
3	A	Washington	Unknown	1.2	6.3	4.1
4	C	Washington	Unknown	1.3	4.9	8.0
5	A	Washington	Unknown	0.8	5.2	6.4
6	A	Providence	Partial	1.4	5.8	3.8
7	B	Providence	Partial	0.8	7.1	4.5
8	B	Providence	Partial	1.6	7.2	10.3
9	B	Providence	Partial	1.1	5.3	6.8
10	C	Providence	Unknown	0.8	5.6	8.3
11	D	Providence	Partial	1.0	5.2	7.6
12	D	Providence	Full	0.8	6.5	12.8
13	D	Providence	Partial	1.3	10.5	14.2
14	A	Providence	Full	0.9	6.4	7.6
15	A	Providence	Unknown	0.9	3.4	4.3
16	D	Providence	Partial	1.0	5.6	6.5
17	D	Providence	Partial	1.4	7.3	5.6
18	C	Washington	Full	1.2	4.4	7.1
19	C	Washington	Full	1.0	9.2	10.3
20	C	Washington	Full	0.8	4.9	7.6
21	C	Washington	Partial	0.9	6.3	8.5
22	B	Washington	Full	1.2	6.7	7.3
23	B	Washington	Full	1.3	4.5	5.6
24	A	Washington	Full	1.4	4.4	4.9

*aerator not removable; no high flow samples without aerator could be collected

Table A-2. Lead concentrations in the aerator samples taken between the medium and high flow profiles at a flow rate of 1 L/min. Sample 1 was taken just after aerator removal; Sample 2 was taken after 3 minutes of flushing at 1 L/min. Values above 15 µg/L are shown in **bold**.

Site #	City	Sample 1 Pb (µg/L)	Sample 2 Pb (µg/L)
1	Washington	NA*	NA*
2	Washington	NA*	NA*
3	Washington	0.201	1.719
4	Washington	ND	ND
5	Washington	2.211	0.506
6	Providence	8.107	4.559
7	Providence	3.347	3.686
8	Providence	10.53	3.811
9	Providence	4.140	4.131
10	Providence	**10,800**	ND
11	Providence	**92.02**	3.916
12	Providence	9.673	4.165
13	Providence	**59.68**	11.23
14	Providence	**1618**	0.42
15	Providence	**15.21**	0.581
16	Providence	**72.7**	2.706
17	Providence	**90.88**	3.793
18	Washington	**131**	0.669
19	Washington	2.768	0.247
20	Washington	**7677**	2.775
21	Washington	11.96	1.781
22	Washington	0.274	ND
23	Washington	2.11	1.46
24	Washington	6.65	0.163

*aerator not removable; no aerator samples could be collected

The following figures illustrate the "general" (Figure A-1) and "detailed" (Figure A-2) sampling handling procedures described in the text. The general procedure was used for most samples, while the detailed procedure was used on the subset of samples that were both field-filtered (liters 3 and 5) and particle-containing (by visual screening) to generate Figure 3.

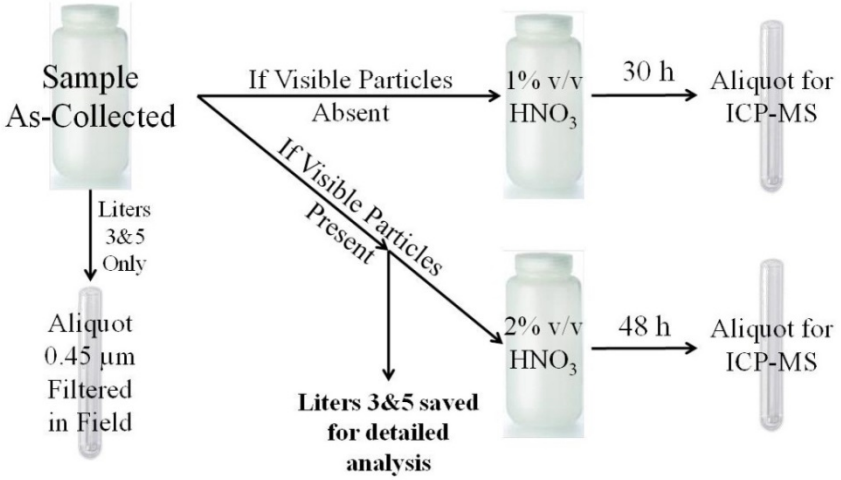

Figure A-1. Illustration of the *general* sample handling protocol. Samples are first screened for visible particles, then acidified to 1% v/v if particles are absent and 2% v/v if they are present.

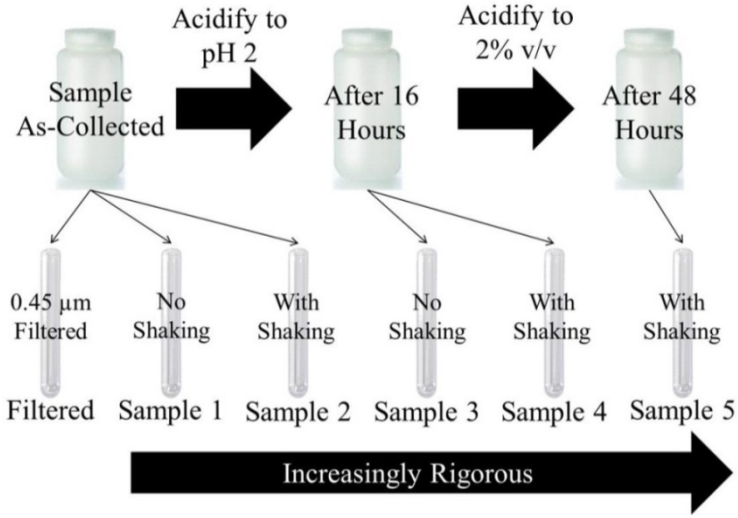

Figure A-2. Illustration of the *detailed* sample handling protocol used for a subset of the "3-D" profiling samples. An aliquot of each sample is filtered through a 0.45 µm filter in the field, then the remaining sample is subjected to increasingly rigorous digestion in the laboratory.

Table A-3. This accompanying table to Figure 3 in the body of the manuscript shows ninetieth percentile lead concentration (µg/L) for homes in each lead release category (A-D) comparing first draw samples to low, medium, and high flow samples. The highest concentration for each case is shown in **bold**.

	Case A	Case B	Case C	Case D	All Sites
# of Sites	8	5	6	5	24
First Draw	**4.9**	9.6	5.3	**104.7**	17.1
Low Flow	3.9	**28.0**	8.4	57.5	20.8
Medium Flow	1.3	7.9	6.0	49.8	14.1
High Flow	4.8	7.9	**165.4**	49.5	**70.9**
Overall	3.7	13.2	72.2	51.3	31.0

Tables A-4 and A-5 summarize the concentrations of other constituents for particle-containing samples with Pb concentrations greater than 15 µg/L. Table A-4 gives major ion concentrations including Na, Ca, Mg, K, Si, P, S, and Cl. Table A-5 gives trace metal concentrations including Al, Fe, Mn, Ni, Cu, Zn, Sn, and Pb.

Table A-4. Major ion concentrations (in mg/L) for samples with visible particulates and Pb concentrations greater than 15 µg/L. L = low flow, M = medium flow, and H = high flow.

Sample ID	Na (mg/L)	Ca (mg/L)	Mg (mg/L)	K (mg/L)	Si (mg/L)	P (mg/L)	S (mg/L)	Cl (mg/L)
Site 4 H 1	15.0	36.6	7.78	2.27	2.1	0.9	47.5	27.5
Site 4 H 2	13.8	34.1	7.25	2.12	1.9	0.9	42.1	25.0
Site 4 H 3	13.9	34.9	7.32	2.14	2.0	0.9	45.1	25.6
Site 4 H 4	14.1	34.5	7.34	2.13	2.0	0.9	45.6	25.9
Site 4 H 5	14.0	34.6	7.33	2.14	2.0	0.9	48.5	26.0
Site 4 H 6	14.1	35.4	7.41	2.18	2.0	0.9	43.9	26.4
Site 7 L 6	9.9	14.7	0.57	0.77	1.6	BDL	BDL	BDL
Site 7 L 7	9.8	14.5	0.57	0.77	1.6	BDL	BDL	BDL
Site 7 L 8	10.0	15.0	0.57	0.80	1.7	BDL	BDL	BDL
Site 8 L 5	10.3	14.9	0.58	0.72	1.7	BDL	BDL	BDL
Site 9 L 5	10.6	15.7	0.61	0.75	1.9	BDL	BDL	BDL
Site 10 H 1	10.7	16.0	0.61	0.75	1.9	BDL	BDL	BDL
Site 11 L 6	10.8	15.9	0.62	0.75	1.9	BDL	BDL	BDL
Site 11 H 1	10.8	15.8	0.62	0.75	2.0	BDL	BDL	BDL
Site 12 L 5	10.8	15.9	0.62	0.76	1.9	BDL	BDL	BDL
Site 12 M 2	10.9	15.9	0.62	0.75	1.9	BDL	BDL	BDL
Site 12 M 4	10.9	15.9	0.62	0.75	1.9	BDL	BDL	BDL

Sample ID	Na (mg/L)	Ca (mg/L)	Mg (mg/L)	K (mg/L)	Si (mg/L)	P (mg/L)	S (mg/L)	Cl (mg/L)
Site 12 M 5	10.8	15.9	0.62	0.76	1.9	BDL	BDL	BDL
Site 12 M 6	10.9	16.1	0.63	0.76	2.0	BDL	BDL	BDL
Site 12 M 7	10.7	15.7	0.62	0.75	1.9	BDL	BDL	BDL
Site 12 M 8	10.7	16.0	0.62	0.75	2.0	BDL	BDL	BDL
Site 12 M 9	10.5	15.7	0.62	0.74	2.1	BDL	BDL	BDL
Site 12 H 1	10.7	15.9	0.61	0.75	1.9	BDL	BDL	BDL
Site 12 H 2	10.9	16.1	0.62	0.76	1.9	BDL	BDL	BDL
Site 12 H 3	10.9	16.0	0.62	0.77	1.9	BDL	BDL	BDL
Site 12 H 4	10.7	15.8	0.61	0.76	1.9	BDL	BDL	BDL
Site 12 H 5	10.9	16.0	0.62	0.77	1.9	BDL	BDL	BDL
Site 12 H 6	10.9	16.1	0.62	0.77	1.9	BDL	BDL	BDL
Site 12 H 7	10.8	15.9	0.62	0.76	1.9	BDL	BDL	BDL
Site 12 H 8	10.7	15.9	0.61	0.76	1.9	BDL	BDL	BDL
Site 12 H 9	10.7	15.8	0.61	0.75	1.9	BDL	BDL	BDL
Site 13 L 1	10.5	17.3	0.62	0.85	1.9	BDL	BDL	BDL
Site 13 L 3	10.3	16.5	0.61	0.75	1.8	BDL	BDL	BDL
Site 13 L 5	10.2	16.8	0.60	0.76	1.8	BDL	BDL	BDL
Site 13 L 6	10.5	17.0	0.62	0.77	1.9	BDL	BDL	BDL
Site 13 L 7	10.5	17.1	0.62	0.77	1.8	BDL	BDL	BDL
Site 13 M 1	10.5	17.0	0.62	0.77	1.8	BDL	BDL	BDL
Site 13 M 2	10.5	17.1	0.62	0.77	1.8	BDL	BDL	BDL
Site 13 M 3	10.3	16.7	0.61	0.75	1.8	BDL	BDL	BDL
Site 13 M 4	10.4	17.3	0.62	0.77	1.8	BDL	BDL	BDL
Site 13 M 5	10.3	16.7	0.61	0.76	1.8	BDL	BDL	BDL
Site 13 H 1	10.3	16.7	0.61	0.75	1.8	BDL	BDL	BDL
Site 13 H 2	10.2	16.4	0.60	0.74	1.7	BDL	BDL	BDL
Site 13 H 3	10.4	16.6	0.61	0.75	1.8	BDL	BDL	BDL
Site 13 H 4	10.4	16.7	0.61	0.77	1.8	BDL	BDL	BDL
Site 13 H 5	10.3	16.7	0.61	0.76	1.8	BDL	BDL	BDL
Site 13 H 6	10.3	16.8	0.61	0.76	1.8	BDL	BDL	BDL
Site 13 H 7	10.3	17.0	0.61	0.76	1.8	BDL	BDL	BDL
Site 13 H 8	10.3	16.8	0.61	0.75	1.8	BDL	BDL	BDL
Site 13 H 9	10.3	16.8	0.61	0.75	1.8	BDL	BDL	BDL
Site 16 L 1	10.4	16.8	0.61	0.77	1.7	BDL	BDL	BDL
Site 16 M 1	10.3	16.9	0.60	0.76	1.9	BDL	BDL	BDL
Site 16 M 2	10.2	16.8	0.61	0.76	1.9	BDL	BDL	BDL
Site 16 M 3	10.1	16.6	0.60	0.77	1.9	BDL	BDL	BDL
Site 16 M 4	10.2	16.6	0.59	0.75	1.8	BDL	BDL	BDL
Site 16 M 5	10.1	16.4	0.60	0.79	1.9	BDL	BDL	BDL

Sample ID	Na (mg/L)	Ca (mg/L)	Mg (mg/L)	K (mg/L)	Si (mg/L)	P (mg/L)	S (mg/L)	Cl (mg/L)
Site 16 M 6	10.3	16.7	0.60	0.76	1.8	BDL	BDL	BDL
Site 16 M 7	10.2	16.6	0.60	0.75	1.8	BDL	BDL	BDL
Site 16 M 8	10.1	16.4	0.59	0.74	1.8	BDL	BDL	BDL
Site 16 M 9	10.1	16.5	0.59	0.75	1.8	BDL	BDL	BDL
Site 16 H 1	10.2	16.6	0.60	0.76	2.2	BDL	BDL	BDL
Site 16 H 2	10.2	16.6	0.60	0.75	2.0	BDL	BDL	BDL
Site 16 H 3	10.1	16.5	0.60	0.76	1.9	BDL	BDL	BDL
Site 16 H 4	10.2	16.5	0.61	0.75	1.9	BDL	BDL	BDL
Site 16 H 5	10.0	16.1	0.59	0.76	1.9	BDL	BDL	BDL
Site 16 H 6	10.2	16.6	0.60	0.75	1.9	BDL	BDL	BDL
Site 16 H 7	10.4	17.0	0.60	0.76	1.9	BDL	BDL	BDL
Site 16 H 8	10.2	16.4	0.60	0.75	1.9	BDL	BDL	BDL
Site 16 H 9	10.1	16.4	0.60	0.74	1.9	BDL	BDL	BDL
Site 17 M 5	10.0	16.7	0.59	0.78	1.8	BDL	BDL	BDL
Site 18 H 1	24.8	35.6	10.76	3.32	2.0	1.0	74.9	40.1
Site 18 H 2	24.7	35.4	10.87	3.28	2.0	1.4	74.1	39.8
Site 18 H 3	24.8	35.8	10.93	3.39	2.1	1.2	73.9	38.7
Site 18 H 4	24.7	35.5	10.83	3.31	2.0	1.0	74.3	40.0
Site 18 H 5	24.6	35.3	10.79	3.35	2.0	0.9	72.4	38.5
Site 18 H 6	24.7	35.4	10.76	3.31	2.0	0.8	74.6	40.1
Site 18 H 7	24.8	35.8	10.85	3.36	2.0	0.8	74.7	40.0
Site 18 H 8	24.8	35.3	10.83	3.33	2.0	0.8	75.7	40.2
Site 18 H 9	24.8	35.5	10.81	3.31	2.0	0.8	73.9	39.6
Site 19 H 1	20.4	33.2	8.64	2.99	2.1	2.2	54.0	33.9
Site 19 H 2	20.4	35.1	8.83	2.97	2.2	3.1	53.6	33.9
Site 19 H 3	20.4	34.8	8.83	3.00	2.2	2.7	51.8	32.7
Site 19 H 4	20.4	33.8	8.75	2.96	2.1	1.8	53.3	33.5
Site 19 H 5	20.4	33.2	8.71	3.03	2.2	1.3	55.2	33.6
Site 19 H 6	20.6	32.8	8.72	3.04	2.1	1.2	55.1	34.0
Site 19 H 7	20.7	33.3	8.74	3.09	2.2	1.1	55.3	34.3
Site 19 H 8	20.7	33.0	8.70	3.04	2.1	1.0	54.9	33.9
Site 20 H 1	24.2	33.5	10.44	3.19	1.9	1.2	70.7	40.5
Site 20 H 2	24.0	33.1	10.35	3.15	1.9	1.1	69.9	40.0
Site 20 H 3	23.8	33.7	10.34	3.25	1.9	1.4	70.4	40.9
Site 20 H 4	24.2	33.3	10.38	3.19	1.9	0.9	69.8	40.3
Site 20 H 5	23.7	33.1	10.24	3.24	1.9	0.9	69.9	40.8
Site 20 H 6	24.1	33.4	10.44	3.16	1.9	0.9	73.8	40.5
Site 20 H 7	24.1	33.7	10.36	3.18	1.9	0.8	70.4	40.8
Site 20 H 8	24.0	33.1	10.28	3.17	1.9	0.8	69.7	40.6

Sample ID	Na (mg/L)	Ca (mg/L)	Mg (mg/L)	K (mg/L)	Si (mg/L)	P (mg/L)	S (mg/L)	Cl (mg/L)
Site 20 H 9	24.0	33.6	10.36	3.17	1.9	0.8	73.9	41.0
Site 20 H 10	24.1	33.0	10.37	3.25	1.9	0.7	70.6	39.9
Site 21 H 1	23.4	30.5	9.44	3.10	2.0	0.9	65.8	37.7
Site 21 H 2	23.4	30.5	9.40	3.13	2.0	0.8	65.2	38.2
Site 21 H 3	23.3	30.7	9.41	3.17	2.0	0.8	66.8	39.5
Site 21 H 4	23.4	30.7	9.44	3.12	2.0	0.8	66.1	39.0
Site 21 H 5	23.2	30.4	9.33	3.13	1.9	0.8	65.5	38.9
Site 21 H 6	23.6	30.9	9.51	3.13	2.0	0.7	66.3	39.5
Site 21 H 7	23.5	30.8	9.53	3.13	2.0	0.7	66.5	39.4
Site 21 H 8	23.4	30.6	9.40	3.14	1.9	0.7	65.4	38.9
Site 21 H 9	23.3	30.6	9.42	3.13	2.0	0.7	69.1	39.5
Site 22 L 4	23.4	28.0	8.68	3.04	2.0	0.7	61.7	37.2
Site 22 L 5	18.2	29.0	6.99	3.06	2.2	0.6	49.4	32.5
Site 22 L 6	18.2	28.4	6.91	2.97	2.1	0.6	48.3	31.7

Table A-5. Trace metal concentrations (in µg/L) for samples with visible particulates and Pb concentrations greater than 15 µg/L. L = low flow, M = medium flow, and H = high flow.

Sample ID	Al (µg/L)	Fe (µg/L)	Mn (µg/L)	Ni (µg/L)	Cu (µg/L)	Zn (µg/L)	Sn (µg/L)	**Pb (µg/L)**
Site 4 H 1	105.4	630.5	11.76	1.904	61.46	84.23	BDL	**23.72**
Site 4 H 2	163.1	811.9	25.62	1.111	84.38	53.92	BDL	**35.74**
Site 4 H 3	168.5	770.6	27.74	1.238	82.12	40.54	BDL	**34.49**
Site 4 H 4	155	702	26.19	1.251	74.51	33.82	BDL	**28.53**
Site 4 H 5	143.2	613	24.88	1.824	67.26	33.84	BDL	**25.44**
Site 4 H 6	132.4	555.5	22.62	1.372	59.98	28.56	BDL	**21.13**
Site 7 L 6	2.888	78.67	BDL	BDL	13.56	5.687	BDL	**41.73**
Site 7 L 7	3.022	79.31	BDL	BDL	10.33	2.099	BDL	**47.63**
Site 7 L 8	2.949	83.33	BDL	BDL	9.339	BDL	BDL	**25.77**
Site 8 L 5	2.177	329.5	2.82	BDL	1.507	BDL	BDL	**22.54**
Site 9 L 5	3.13	110.6	1.565	BDL	6.74	3.305	BDL	**45.97**
Site 10 H 1	2.467	61.57	1.412	BDL	16.92	59.96	1.963	**23.86**
Site 11 L 6	2.114	18.76	BDL	BDL	6.204	6.509	BDL	**25.93**
Site 11 H 1	7.142	92.97	2.252	1.888	14.16	669.2	BDL	**19.84**
Site 12 L 5	8.721	63.34	BDL	BDL	BDL	BDL	BDL	**19.3**
Site 12 M 2	8.48	370.5	6.282	BDL	3.892	BDL	BDL	**17.83**
Site 12 M 4	8.334	408	6.276	BDL	1.751	BDL	BDL	**25.84**
Site 12 M 5	8.712	433.4	6.792	BDL	BDL	BDL	BDL	**25.22**
Site 12 M 6	9.533	620.3	9.261	BDL	BDL	BDL	BDL	**28.5**

Sample ID	Al (µg/L)	Fe (µg/L)	Mn (µg/L)	Ni (µg/L)	Cu (µg/L)	Zn (µg/L)	Sn (µg/L)	**Pb (µg/L)**
Site 12 M 7	9.535	733.9	9.597	BDL	BDL	BDL	BDL	**32.01**
Site 12 M 8	10.95	1364	15.01	BDL	1.552	BDL	BDL	**51.09**
Site 12 M 9	14.57	3060	28.11	BDL	2.958	BDL	BDL	**80.22**
Site 12 H 1	38.73	189.8	3.02	1.597	44.46	407.2	9.849	**154.3**
Site 12 H 2	12.45	155.5	2.438	BDL	42.29	17.09	2.119	**63.65**
Site 12 H 3	11.28	145.7	2.312	BDL	33.53	8.195	BDL	**47.8**
Site 12 H 4	9.001	145.9	2.347	BDL	25.47	13.05	1.088	**35.82**
Site 12 H 5	8.123	128.9	2.108	1.661	23.73	22.95	BDL	**30.98**
Site 12 H 6	9.357	126.6	2.061	2.49	28.22	55.11	1.532	**33.35**
Site 12 H 7	6.916	129.6	1.967	BDL	19.93	13.8	BDL	**26.05**
Site 12 H 8	5.366	152.5	1.987	BDL	18.04	1.953	BDL	**45.22**
Site 12 H 9	5.457	219.7	2.287	BDL	17.17	2.216	BDL	**39.01**
Site 13 L 1	2.964	159.6	1.834	BDL	4.431	26	2.201	**155.8**
Site 13 L 3	2.663	141.8	1.765	BDL	1.884	BDL	BDL	**92.97**
Site 13 L 5	2.952	482.6	7.361	BDL	BDL	BDL	BDL	**54.07**
Site 13 L 6	2.854	426.2	6.884	BDL	BDL	BDL	1.023	**21.7**
Site 13 L 7	2.927	394.9	6.469	BDL	BDL	BDL	BDL	**15.86**
Site 13 M 1	2.582	360.6	5.874	BDL	4.781	5.404	BDL	**23**
Site 13 M 2	2.624	440.3	6.837	BDL	BDL	BDL	BDL	**49.06**
Site 13 M 3	2.656	398.4	6.232	BDL	BDL	BDL	BDL	**24.59**
Site 13 M 4	2.756	406.3	6.48	BDL	BDL	BDL	BDL	**20.91**
Site 13 M 5	2.693	389.5	6.119	BDL	BDL	BDL	BDL	**19.23**
Site 13 H 1	4.052	324.8	4.806	1.109	7.272	5.997	BDL	**16.67**
Site 13 H 2	2.579	333.4	4.815	BDL	BDL	BDL	BDL	**29.46**
Site 13 H 3	2.646	342.3	4.934	BDL	BDL	BDL	BDL	**32.12**
Site 13 H 4	2.734	337.3	4.907	1.041	4.106	5.515	BDL	**28.97**
Site 13 H 5	2.85	389.6	5.16	2.465	BDL	BDL	BDL	**28**
Site 13 H 6	2.626	330.8	4.879	BDL	BDL	BDL	BDL	**24.26**
Site 13 H 7	2.642	332.7	4.936	BDL	BDL	BDL	BDL	**22.55**
Site 13 H 8	2.609	333.3	4.882	BDL	BDL	BDL	BDL	**21.91**
Site 13 H 9	2.845	318.2	4.801	1.252	10.8	2.03	BDL	**21.44**
Site 16 L 1	1.486	165.8	2.232	BDL	16.78	303.3	BDL	**27.94**
Site 16 M 1	2.774	640.1	8.569	BDL	17.09	314.9	BDL	**53.11**
Site 16 M 2	3.156	731.6	10.09	BDL	21.22	438.8	12.04	**76.69**
Site 16 M 3	3.241	677.1	8.771	BDL	14.65	304.7	BDL	**79.09**
Site 16 M 4	2.575	610.9	8.346	BDL	12.52	293.9	3.963	**49.61**
Site 16 M 5	2.856	541.7	7.637	BDL	10.05	235.6	BDL	**47.28**
Site 16 M 6	2.521	503.9	7.126	BDL	9.002	212.1	1.972	**38.86**
Site 16 M 7	2.569	578.9	8.771	BDL	9.209	206.1	BDL	**29.99**

Sample ID	Al (µg/L)	Fe (µg/L)	Mn (µg/L)	Ni (µg/L)	Cu (µg/L)	Zn (µg/L)	Sn (µg/L)	**Pb (µg/L)**
Site 16 M 8	2.493	530	7.685	BDL	8.08	178.4	BDL	**28.36**
Site 16 M 9	2.49	439.2	6.214	1.893	6.398	173	BDL	**25.6**
Site 16 H 1	4.587	808.1	12.36	BDL	27.44	2680	BDL	**96.15**
Site 16 H 2	3.999	773.1	11.73	BDL	23.9	1474	1.263	**105.4**
Site 16 H 3	3.142	560.3	7.855	BDL	14.43	900.2	BDL	**57.81**
Site 16 H 4	2.752	487.5	7.061	BDL	12.38	661.6	BDL	**48.61**
Site 16 H 5	2.986	464.9	6.597	BDL	10.38	577	BDL	**44.15**
Site 16 H 6	2.5	423.2	6.127	BDL	9.173	516.2	BDL	**37.47**
Site 16 H 7	2.784	452	6.809	BDL	9.184	428.9	BDL	**30.18**
Site 16 H 8	2.482	420.8	6.197	BDL	8.278	525.7	BDL	**30.56**
Site 16 H 9	3.033	389	5.744	BDL	8.132	595	BDL	**31.92**
Site 17 M 5	2.448	356	4.108	BDL	2.454	1.238	BDL	**18.39**
Site 18 H 1	68.94	837	7.164	2.009	85.47	246	BDL	**31.38**
Site 18 H 2	152	2161	10.58	1.885	247.3	396.3	BDL	**100.1**
Site 18 H 3	123.4	1411	7.575	2.259	206.7	264	BDL	**70.78**
Site 18 H 4	89.22	872.2	5.592	3.895	142.1	189.8	BDL	**42.86**
Site 18 H 5	75.16	641.5	4.743	1.852	100.6	138.5	BDL	**31.69**
Site 18 H 6	65.79	516.4	4.358	1.066	82.69	117.7	BDL	**25.44**
Site 18 H 7	62.11	447.1	4.175	1.01	72.43	98.81	BDL	**21.08**
Site 18 H 8	57.8	380.5	3.993	BDL	62.5	86.44	BDL	**17.88**
Site 18 H 9	60.65	428.3	4.159	1.554	67.43	106.8	BDL	**18.81**
Site 19 H 1	222	4139	13.37	1.768	71.42	1225	BDL	**165.8**
Site 19 H 2	383.3	6417	24.61	1.878	65.45	1945	BDL	**277.5**
Site 19 H 3	359	5290	20.77	6.856	54.18	1697	BDL	**269.1**
Site 19 H 4	224.7	3059	13.89	1.432	34.92	871.7	BDL	**165.4**
Site 19 H 5	161.1	1740	9.588	1.427	26.22	690.8	BDL	**98.26**
Site 19 H 6	124.4	1374	7.292	1.158	20.96	509.7	BDL	**78.73**
Site 19 H 7	113.1	1094	6.494	1.553	21.4	439.3	BDL	**63.42**
Site 19 H 8	94.37	923.6	5.462	1.038	17.13	364.9	BDL	**54.22**
Site 20 H 1	270.2	1286	9.373	4.252	326.2	240.7	78.17	**1801**
Site 20 H 2	213.7	1038	7.582	1.099	248.7	60.33	157.5	**276.5**
Site 20 H 3	276.5	834.4	6.497	1.298	211.5	1357	19.86	**208.1**
Site 20 H 4	151	654.3	5.47	1.105	146.5	33.31	16.54	**157.3**
Site 20 H 5	142.5	580.4	4.739	1.292	131.3	26.92	6.909	**139.6**
Site 20 H 6	133.1	506.3	4.415	1.066	117.4	24.21	9.975	**123.3**
Site 20 H 7	111.3	411.8	3.768	1.01	103.1	21.2	7.313	**104.3**
Site 20 H 8	96.7	342.8	3.362	1.064	80.18	20.76	5.755	**84.22**
Site 20 H 9	85.25	291.1	2.947	1.075	70.22	15.28	4.417	**71.52**
Site 20 H 10	40.73	90.04	1.504	BDL	22.79	5.404	3.337	**17.36**

Sample ID	Al (µg/L)	Fe (µg/L)	Mn (µg/L)	Ni (µg/L)	Cu (µg/L)	Zn (µg/L)	Sn (µg/L)	**Pb (µg/L)**
Site 21 H 1	82.92	717.5	5.644	1.502	125.5	136.2	18.55	**123**
Site 21 H 2	66.86	527.5	4.243	1.217	102.2	81.8	3.593	**81.97**
Site 21 H 3	55.98	380.7	3.334	1.194	76.19	59.14	BDL	**55.56**
Site 21 H 4	49.48	290.1	2.907	1.142	62.67	47.19	BDL	**42.42**
Site 21 H 5	45.14	253.6	2.621	1.126	53.99	39.49	1.622	**34.98**
Site 21 H 6	42.02	214	2.43	1.102	48.79	33.24	BDL	**29.57**
Site 21 H 7	40.26	178.1	2.252	1.006	44.2	28.88	BDL	**25.6**
Site 21 H 8	38.69	170.8	2.232	1.121	44.23	31.43	BDL	**28.19**
Site 21 H 9	37.71	162.2	2.167	1.034	41.89	26.03	BDL	**30.87**
Site 22 L 4	28.54	134.7	1.476	30.1	46.31	4.099	BDL	**177.6**
Site 22 L 5	16.68	115.9	8.765	BDL	8.306	14.63	BDL	**15.8**
Site 22 L 6	16.31	76.93	8.405	BDL	6.851	12.37	BDL	**15.62**